

**Field Investigations and SWMM Modeling of an Undeveloped Headwaters
Catchment Located in the Lower Coastal Plain Region of the Southeast USA**

by

Kyle Patrick Moynihan

A thesis submitted to the Graduate Faculty of
Auburn University
in partial fulfillment of the
requirements for the Degree of
Master of Science

Auburn, Alabama
December 14, 2013

Keywords: Headwaters, Field Investigations, SWMM

Copyright 2013 by Kyle Patrick Moynihan

Approved by

Jose Goes Vasconcelos Neto, Chair, Professor of Civil Engineering
T. Prabhakar Clement, Professor of Civil Engineering
Xing Fang, Associate Professor of Civil Engineering

Abstract

The southeastern region of the United States is host to a diverse variety of geophysical regions including the Blue Ridge, Piedmont, Inland Basins and Coastal Plains. Each region shows its own distinctive set of hydrological characteristics and understanding the connections between these processes is key to developing responsible watershed management practices. This thesis presents a study performed in the undeveloped headwaters of an intermittent watershed. Containing an area of 2.9 km^2 the study site, referred to as WS-AGC, is located in the Coastal Plains region of Alabama. With collaboration between Auburn University and the Alabama chapter of the Associated General Contractors of America (AGC), this work intended to perform a water budget study and to assess the feasibility of sustaining a pond at WS-AGC. To achieve this goal, two separate tasks were performed. The first was the construction, deployment, monitoring and maintenance of various field monitoring facilities and equipment. These included rain gauges, weirs, groundwater observation wells and a portable weather station. The second objective focused on the development and calibration/verification of a *SWMM* model with respect to various hydrological conditions.

Field monitoring studied offered a glimpse on the hydrological processes related to water motion in the watershed. Such monitoring supported the development of hypotheses on the interactions between these processes at WS-AGC. These dynamics processes included; 1) the observed effects of the forested land cover on the water table level due to evapotranspiration; 2) stream flows that were either connected or not to the groundwater; 3) variations of runoff responses over seasonal fluctuations. Also, results from *SWMM* simulations were generally able to represent the dynamic nature of WS-AGC with regards to mean flow and total volume runoff characteristics. However, this could only be achieved with the use of groundwater compartment in the model.

Acknowledgments

I would like to start out by thanking my good friend and adviser Professor Jose Neto Vasconcelos for the support and knowledge he has provided me over the past few years. It has truly been an honor to work with such a dedicated and hard working individual. From the short planned meetings, which never ended under an hour or two, to the blood and sweat that was put into field studies, I will never forget all the great memories we have created during this research.

I would also like to thank everyone that assisted me with my field work. To Paul Simmons, Cameroun Thomas, George Merriam and Will Brown thank you for all your hard work and strength, without you guys I could have never accomplished all that I did these past two years. To Carmen Chosie and Thomas Weems thanks for all good times in class and during the many hours spent down in the dungeon debugging VBA codes.

Lastly I want to thank my friends and family for all the support and encouragement these past two years. To Austin Millwood thank you for all the great times we shared during my brief periods of free time. It really helped having such a great friend around during these challenging times. To my parents, Tim and Sue Moynihan, thank you both for being so incredible as you have done nothing but support and encourage me since I can remember. Without all your love and support I would not be who I am today.

Table of Contents

Abstract	ii
Acknowledgments	iii
List of Figures	vi
List of Tables	xi
1 Introduction and Literature Review	1
1.1 Literature Review	2
1.1.1 Water Budget Analysis Techniques	2
1.1.2 Undeveloped Watershed Modeling Using SWMM	4
1.2 Knowledge Gaps	8
2 Scope and Objectives	9
3 Methodology	11
3.1 Site Description	11
3.2 Field Investigations	15
3.2.1 Precipitation Collection	15
3.2.2 Meterological Data	18
3.2.3 Evapotranspiration Calculations	18
3.2.4 Runoff Monitoring	21
3.2.5 Weir Discharge Equations	32
3.2.6 Groundwater Observation Wells	37
3.2.7 Infiltration Testing	38
3.2.8 Soil Sampling	40
3.3 Fundamentals of Operating SWMM	43
3.3.1 Introduction	43

3.3.2	Internal Mechanisms	45
3.3.3	Interface Objects	52
3.4	SWMM Model Development	53
3.5	Model Calibration	58
4	Results and Discussion	62
4.1	Collected Field Data	62
4.1.1	Precipitation	62
4.1.2	Temperature	68
4.1.3	Potential Evapotranspiration (PET)	70
4.1.4	Runoff	72
4.1.5	Groundwater	79
4.2	SWMM Simulation Comparisons	85
4.2.1	Hydrographs Comparison	85
4.2.2	Flow Duration Exceedance curves	90
4.2.3	Simulation Error Analysis	92
4.2.4	Statistical Summary	99
5	Summary of Findings and Suggestions for Future Studies	103
5.1	Summary	103
5.2	Suggested Future Studies	106
	Bibliography	107
	Appendices	111
A	Soil Analysis	112

List of Figures

3.1	Left: Areal view of the WS-AGC with the network of intermittent streams. Right: Respective contours lines	12
3.2	Watershed <i>AGC</i> soil composition, provided from (NRCS/USDA web soil survey)	14
3.3	Rain gauge locations	16
3.4	Rain gauge post and meteorological station	17
3.5	Construction of Cipolletti weir	22
3.6	Roots causing issues on the lateral walls of the weir	23
3.7	Support post for the Cipolletti weir	23
3.8	Upstream view of the Cipolletti weir	24
3.9	Downstream view of the Cipolletti weir	24
3.10	Riprap placed at the downstream side of the Cipolletti weir	25
3.11	Finished Cipolletti weir looking upstream: completed (June 1st 2012)	26
3.12	Cipolletti weir dimensions	26
3.13	Support post for the rectangular weir	27
3.14	Upstream view of rectangular weir	28

3.15	Rectangular weir dimensions	28
3.16	HOBO pressure sensor installed upstream at each weir	29
3.17	Erosion damage at the Cipolletti weir to the right	30
3.18	Upstream view of broad crested weir	31
3.19	Broad crested weir dimensions	31
3.20	Modified rectangular weir dimensions	32
3.21	Values of width-adjustment factor, taken from (Dodge, 2001)	34
3.22	Effective coefficient of discharge, C_e , as a function of L/B and H/P , taken from (Dodge, 2001)	34
3.23	Shallow groundwater wells	37
3.24	Locations of Infiltration Testing	39
3.25	Bore sites at WS-AGC indicated by black markers	40
3.26	Drill rig entering WS-AGC	41
3.27	Setting up to drill boring	41
3.28	Soil exiting the bore hole from approximately 4.6 m below the surface	42
3.29	Samples taken from the SPT	42
3.30	Shelby tubes being prepared to take out of the site	43
3.31	Conceptual view of <i>SWMM</i> 's runoff mechanism, (Rossman and Supply, 2005) .	45

3.32	Conceptual view of Horton’s infiltration capacity recovery mechanism used in <i>SWMM</i> ’s computational code, (Viessman et al., 2003)	48
3.33	Conceptual view of <i>SWMM</i> ’s groundwater mechanism, (Rossman and Supply, 2005)	49
3.34	Discretized Sub-Catchments based on topography and soil types for WS-AGC .	53
3.35	Surveying a downstream cross section	54
3.36	Shallow ground water level relative to the surface for the out of stream observation well	57
4.1	Rainfall recorded at WS-AGC (February 4th - August 14th, 2012-2013)	63
4.2	Off-site rain gauges used as quality control)	64
4.3	Onsite vs off-site monthly rainfall totals (February 4th - August 14th, 2012-2013)	65
4.4	Temperature recorded at Columbus, GA Airport (January 1st - August 14th, 2012-2013)	69
4.5	PET calculations using Hamon’s and Hargreaves Methods	71
4.6	Rainfall runoff events at Cipolletti weir used during calibration efforts	72
4.7	Rainfall runoff events at broad-crested weir used during verification efforts . . .	73
4.8	Rainfall runoff events at rectangular weir	74
4.9	Comparision between runoff at Cipolletti weir and rectangular weir (Pre-Construction February 8th-14th, 2013)	75
4.10	Comparision between runoff at broad-crested weir and rectangular weir (Post-Construction February 23rd-26th, 2013)	75

4.11 Representation of the dynamic groundwater processes of a gaining/losing stream such as the one at WS-AGC, (Winter, 2007)	80
4.12 Instream ground water level vs rainfall intensity	81
4.13 Instream ground water level vs cumulative rainfall	81
4.14 Out of stream ground water level vs rainfall intensity	82
4.15 Out of stream ground water level vs cumulative rainfall	82
4.16 Rainfall event without runoff event during August 6th, 2012 at Cipolletti/Broad- Crested weir	83
4.17 Smaller rainfall event yielding runoff during July 20th, 2013 at Cipolletti/Broad- Crested weir	84
4.18 Signs of ET from the out of stream ground water well	85
4.19 Output hydrographs produced with multiple aquifer configuration	87
4.20 Output hydrographs produced with single aquifer configuration	88
4.21 Output hydrographs produced with no aquifer configuration	89
4.22 Verification Flow duration exceedance curves produced with multiple aquifer con- figuration	91
4.23 Verification flow duration exceedance curves produced with single aquifer config- uration	91
4.24 Verification flow duration exceedance curves produced with no aquifer configuration	92
4.25 Verification error analysis for max flow during multiple aquifer simulation . . .	93

4.26	Verification error analysis for max flow during single aquifer simulation	94
4.27	Verification error analysis for max flow during no aquifer simulation	94
4.28	Verification error analysis for mean flow during multiple aquifer simulation . . .	95
4.29	Verification error analysis for mean flow during single aquifer simulation	96
4.30	Verification error analysis for mean flow during no aquifer simulation	96
4.31	Verification error analysis for total flow during multiple aquifer simulation . . .	97
4.32	Verification error analysis for total flow during single aquifer simulation	98
4.33	Verification error analysis for total flow during no aquifer simulation	98

List of Tables

1.1	Comparison of annually measured precipitation and evapotranspiration for forested ecosystems in the Southeastern USA, (Sun et al., 2010)	4
3.1	USGS web soil survey results for WS-AGC study site	13
3.2	Kestrel 4500 meteorological station measurements and accuracy	18
3.3	Coefficient and constants used when determining the effective coefficient of discharge, taken from (Dodge, 2001)	35
3.4	Coefficient, C , values used for broad crested weirs, taken from (Brater et al., 1996)	36
3.5	Literature values of maximum and minimum infiltration rates for Horton Equation, (Akan, 1993)	55
3.6	Minimum and maximum ranges used for Horton's infiltration input parameter,(Akan, 1993) and (Rossman and Supply, 2005)	59
3.7	Aquifer properties for various soil types, taken from (Rossman and Supply, 2005)	60
3.8	Minimum and maximum ranges used for aquifer component input parameter, (Rossman and Supply, 2005)	61
4.1	Rainfall statistics for (February 4th - December 31st, 2012)	66
4.2	Rainfall statistics for (January 1st - August 14th, 2013)	66

4.3	Normal Monthly Rainfall Totals (Period of Record 1981-2010)-Location: Columbus, GA (Airport)	67
4.4	Monthly rainfall average and yearly totals for (February 4th - July 31st, 2012-2013)	67
4.5	Percent differences between monthly rainfall average (February 4th - July 31st, 2012-2013)	68
4.6	Monthly Recorded Temperatures vs Normal Monthly Temperatures (Period of Record 1981-2010)-Location: Columbus, GA Airport	69
4.7	Yearly PET totals calculated from Hamon and Hargreaves Methods	71
4.8	Descriptive rainfall runoff statistics	76
4.9	Descriptive rainfall runoff statistics and R/P ratios for wet season events 2012-2013	77
4.10	Rainfall runoff statistics and R/P ratios for dry season events 2012	78
4.11	Rainfall runoff statistics and R/P ratios for dry season events 2013	78
4.12	Performance ratings for NSE, (Moriassi et al., 2007)	100
4.13	Calibration error analysis for all simulations performed	101
4.14	Verification error analysis for all simulations performed	102

Chapter 1

Introduction and Literature Review

Developing regions of the United States face a tight balancing act between sustaining city growth and protecting the quality of surrounding natural resources. Growing populations and cities create large strains on local resources and increase potential pollution hazards throughout the watershed. The southeastern region in particular has become a major concern with an increase in timber production, poor timber management practices and urban development (Harder et al., 2007). Forests play a great role in regulating the regional hydrologic patterns of the southern United States where 55% of the region is covered by forest (Sun et al., 2002). According with Wear and Greis (2002) the timber production has more than doubled from 1953 to 1997 in the southeastern United States. However, timber production is not the only factor affecting this region. The southeastern U.S. is expected to lose about 4.9 million forest hectares (ha) to urbanization between 1992 and 2020, with a substantial part of the loss concentrated in the Atlantic Coastal Plains (Harder et al., 2007). Despite such growth tendencies, maintaining the natural ecology and resources is critical for creating a healthy sustainable environment.

In order to promote better industry practices, hydrological processes across the diverse geological regions of the Blue Ridge, Piedmont, Inland Basins and Coastal Plains must be better understood. Field investigations have been conducted for several decades providing sites across these regions with long term hydrological data. These studies have helped describe the hydrology of dynamic forested watershed while providing evidence of the diverse geophysical regions in the southeastern USA (Sun et al. (2002); Amatya et al. (2007); Davis et al. (2007); Harder et al. (2007); Sun et al. (2010); La Torre Torres et al. (2011)). Inter-site eco-hydrological comparison studies have the potential to predict more accurately the

hydrologic effects of headwater forest management under different environments (Sun et al., 2002).

However, further research is needed to understand the natural dynamics of water balance components in such forested systems along the Coastal Plains to accurately assess impacts of anthropogenic disturbances and for improving forest management strategies related to water quality (Harder et al., 2007). Long-term hydrologic data is essential for understanding the hydrologic processes as base line data for assessment of impacts and conservation of regional ecosystems as well as for developing and testing eco-hydrological models (Amatya et al., 2007). The need for continued research efforts focusing on forested watersheds of the southeastern USA has led to investigations described in this thesis.

1.1 Literature Review

This section provides discussions and a summary of current watershed analysis techniques found in literature. Initial discussions focus on the water budget approach that incorporates a simple mass balance technique to identify key hydrological characteristics. Then a summary of case studies utilizing and testing the Storm Water Management Model *SWMM* ability to simulate natural undeveloped watershed dynamics are presented.

1.1.1 Water Budget Analysis Techniques

The water budget method was a major breakthrough in qualitatively depicting natural undeveloped watersheds. One of the pioneers into this development was Thornthwaite (1948), who provided detailed descriptions of the driving forces behind watershed dynamics. Seven years later, in 1955, Thornthwaite and Mather (1955, 1957) presented two contributions that laid the foundation for the standards in water budget studies. With its origins predating the computer age, this technique allows for the researcher to simplify and visually track the propagation of water through separated mechanisms.

Some components within the watershed dynamics pose a great challenge for researcher to quantify. These challenges mainly lie within the groundwater component of a water budget analysis. Generally, in long term site studies, most researchers ignore influences from the groundwater inflow and outflow. This is assumed to have a very small net fluctuation throughout the year (Harder et al., 2007). After all simplifications are made, main driving forces are typically compartmentalized into the following mass balance formula Equation (1.1) (Harder et al., 2007).

$$\Delta S = P - ET - Q \quad (1.1)$$

Where ΔS is the change in the water storage within the soil column, P is the amount of rainfall, ET is the actual evapotranspiration (AET) and finally Q is the amount of runoff. All of the prior are normalized with the study regions area and measured in terms of millimeters or inches. In order to conduct an effective investigation using this technique, study areas must have long term local data. Having local data reduces any bias effects from drastic weather changes over temporal and spacial variations. Typically a water budget analysis is performed with hydrological data ranging between (2 to 30⁺) years (Sun et al., 2002; Amatya et al., 2007; Sun et al., 2010; La Torre Torres et al., 2011). Studies including Sun et al. (2002), Harder et al. (2007) and Sun et al. (2010) have used this simple approach to investigate the connections between rainfall runoff, AET and potential evapotranspiration (PET) as well as ΔS through headwaters undeveloped watersheds.

One of the most difficult variables to determine from Equation 1.1 is AET . Several methods have been developed to calculate PET . PET calculations can be performed using various input parameters and they are one valid way to estimate AET . Some of the most common methods rely on temperature based inputs. The interested reader can find in-depth descriptions from Federer and Lash (1978), Vörösmarty et al. (1998) and Hargreaves and Allen (2003). Sun et al. (2010) summarized the average precipitation (P), ET and ET/P values for 18 separate watershed studies around the southeastern region of the USA. This summary is presented in Table 1.1 where the importance of ET can be seen. The range of

ET/P ratios vary from 0.41 to 0.93 providing evidence that ET is one of the most influential loss components in the watershed system.

Table 1.1: Comparison of annually measured precipitation and evapotranspiration for forested ecosystems in the Southeastern USA, (Sun et al., 2010)

Ecosystems	Evapotranspiration (mm/year)	Precipitation (P)	ET/P	References
Loblolly pine plantation (LP) 16 years old, North Carolina	1087 (1011–1226)	1238	0.88	Sun et al. (2010)
Loblolly pine plantation (CC), 4 years old, coastal North Carolina	838 (755–885)	1274	0.66	
Loblolly pine plantation, 4 years old, Parker Track, North Carolina	895 (702–1078)	1152	0.78 (0.73–0.94)	Diggs (2004)
Loblolly pine plantation, 15 years old, Parker Track, North Carolina	988, 938 (after thinning 1/3 of basal area)	1098	0.9	Grace et al. (2006a,b)
Loblolly pine plantation, 14–30 years old, Parker Track, North Carolina	997 (763–1792)	1538 (947–1346)	0.65	Amatya et al. (2006)
Loblolly pine plantation (PP), 25 years old, Piedmont North Carolina	658 (560–740)	1092 (930–1350)	0.60	Stoy et al. (2006)
Mature deciduous hardwoods (HW), Duke Forest, Piedmont North Carolina	573 (460–640)		0.52	Stoy et al. (2006)
Grass-cover old field (OL), Duke Forest, Piedmont North Carolina	508 (360–650)		0.46	Stoy et al. (2006)
Slash pine (<i>Pinus taeda</i> L.) plantation, clearcut, Florida	958 (869–1048)	959 (869–1048)	0.85 (0.84–0.86)	Gholz and Clark (2002)
Slash pine (<i>Pinus taeda</i> L.) plantation, 10 years old, Florida	1058 (994–1122)	1062 (877–1247)	1.0 (0.9–1.1)	
Slash pine (<i>Pinus taeda</i> L.) plantation, full-rotation, Florida	1193 (1102–1284)	1289 (887–1014)	0.93 (0.92–0.93)	Gholz and Clark (2002)
Slash pine (<i>Pinus taeda</i> L.) plantation, full-rotation, Florida (extreme drought years)	754 (676–832)	883 (811–956)	0.85	Powell et al. (2005)
Pine flatwoods, Bradford Forest, Florida	1077	1261	0.87	Sun et al. (2002)
Deciduous hardwoods, Coweeta, North Carolina	779	1730	0.47	Sun et al. (2002)
Mixed Pine and hardwoods, Santee Exp. Forest, South Carolina	1133	1382	0.82	Lu et al. (2003)
White pine (<i>Pinus strobus</i> L.), Coweeta, North Carolina	1291	2241	0.58	Ford et al. (2007)
Deciduous hardwoods, Oak Ridge, Tennessee	567 (537–611)	1372 (1245–1682)	0.41	Wilson and Baldocchi (2000)
Deciduous hardwoods, Oak Ridge, Walker Branch watershed, Tennessee	575	1244	0.45	Updated data from Lu et al. (2003); Hanson et al. (2003)

Other methods are based on more sophisticated techniques that make use of local solar radiation inputs. These methods are difficult to employ in most areas since the availability of long term localized solar radiation data is very limited. The sensitivity analysis performed by Bormann (2011) provides a detailed in-depth description into the uses of 18 different *PET* model strategies. Bormann (2011) concluded that selecting a *PET* model depends solely on the type of data available and the climate on the region of interest.

1.1.2 Undeveloped Watershed Modeling Using SWMM

Many numerical models exist for simulating hydrological processes of a watershed. Most of which incorporate mechanisms that simplify observed processes such as runoff, infiltration,

interflow, and groundwater. The simplified structure is typically a collection of subsystems each representing individual hydrologic processes (Axworthy and Karney, 1999). Numerical models range from custom-built algorithms to government supported user interface software packages. Distinguishing which model is the best fit for a specific project can be a challenging task. Work performed by Borah et al. (2009) provides detail descriptions into capabilities and limitations of 14 currently offered watershed modeling packages. However, the focus in this section is a review of studies which have analyzed the ability of the Storm Water Management Model (*SWMM*) to model undeveloped watersheds. Also included is a review of algorithms incorporated into *SWMM* to make the calibration processes more efficient.

Davis et al. (2007) analyzed *SWMM*'s capability to model four rural watersheds with areas ranging from 3.22 to 8.94 mi^2 located in the Piedmont ecoregion of North Carolina. In order to develop physical properties of the catchments, many sophisticated techniques were utilized. Using Geographical Information Systems (*GIS*) software, a 10 m Digital Elevation Map (*DEM*) and aerial photos, the local catchment characteristics such as area, slope, runoff length and imperiousness were determined. Channel dimensions were found from field surveys and soil hydrologic groups provided estimations of infiltration rates. Finally, Horton's infiltration equations were utilized within all catchments.

Once each model was constructed, calibration efforts were initiated. Results indicated that calibration by flow duration curves cannot be achieved for all events of record through the adjustment of watershed parameters like percent imperiousness, infiltration, overland roughness, and conduit roughness alone (Davis et al., 2007). This led to development of a single aquifer component with one receiving node. During this effort default aquifer parameters were initially used. Then soil texture classes properties inputs were altered to create the best calibration results.

The best fit calibration results were seen when incorporating the sandy clay aquifer properties. Flow duration exceedance curves were unable to match peak flow rates but did provide good results in the mid to low range flow rates. However, during the study no

comparisons between local soil data were used to confirm the sandy clay conditions. The study also relied only on flow duration exceedance curves and single event hydrographs to determine the accuracy of simulations. Statistical analysis between calibration and observed data was not performed during the calibration efforts. In order to perform a comprehensive analysis Legates and McCabe (1999), Krause et al. (2005) and Moriasi et al. (2007) suggest that not only should graphical methods be used to evaluate a models performance but a compilation of statistics as well. This suggest that results from (Davis et al., 2007) were not analyzed sufficiently. To truly suggest that *SWMM* can be used for undeveloped watersheds, a more in-depth statistical study must be performed.

Work performed by Jang et al. (2007) focused on developing *SWMM* simulations for pre- and post-development conditions. Models were created for three natural watersheds and four disaster stricken areas in Korea, where impact assessments have already been conducted. Studies were split into two phases of *SWMM* modeling, the first phase of testing focused on the three undeveloped headwaters watersheds and the second phase examined the four separate disaster stricken watersheds. Since the proposed approach was to use *SWMM* both for pre- and post- development condition, it is necessary to verify the applicability of *SWMM* to natural watershed condition (Jang et al., 2007)

During the first stage, research sites at the Seolmacheon, Weecheon and Pyungchang River watersheds provided observed rainfall runoff data to compare *SWMM* simulation results against. The catchment areas ranged from 8.51 to 55.93 km^2 with slopes between 5.45 to 36.96 %. When constructing the model a single sub-catchment compartment was selected as this produced the closest results to observed data. Along with *SWMM* modeling of the researched watersheds other methods of runoff estimation were applied to the natural catchments. The Soil Conservation Service (*SCS*) or Clark method is the standard method for runoff estimations in Korea (Jang et al., 2007). Comparisons were then made between the Clark method and *SWMM* model outputs.

Each *SWMM* model created for the three study catchments were only tested with three rainfall runoff events. Parameters were estimated from either physical information available or the suggested values from the tables in the *SWMM* manual or existing literature (Jang et al., 2007). The models were left uncalibrated in order to simulate the typical process that would be encountered with an ungauged pre-development site. Maximum flow rate and time to peak results from the *SWMM* simulations during the three separate rainfall runoff events showed close results to observed data. The Clark method also produced good agreement but underestimated peak runoff for most rainfall runoff events analyzed.

Evidence presented from this study shows that *SWMM* was able to represent the behavior of the undeveloped watershed. However, to provide a stronger case for the ability of *SWMM* to handle these conditions more events must be analyzed. Also Jang et al. (2007) did not incorporate any sophisticated error analysis techniques. The determination of the models performance was based purely on hydrographs, peak flow rates and time to peak flow rates. Although these results have shown good agreement more analysis is needed to truly deem modeling results as acceptable.

Davis et al. (2007) used manual techniques to calibrate four watersheds and Jang et al. (2007) did not incorporate calibration in their modeling efforts. Manual or no calibration efforts severely limit the ability of a user to achieve an optimal set of defensible parameters. A poorly calibrated model might lead to poor designs resulting in four serious impacts: flooding, stream erosion, water quality violations and habitat destruction (James et al., 2002). In order to improve future studies involving *SWMM*, James et al. (2002) has developed a computing evolution-strategy called a genetic algorithm (*GA*). Generally, the evolution-strategy is an optimization method based on strategies encountered in biological evolution (James et al., 2002). The strategy also incorporates a limit or range of uncertainty for the calibration parameters of interest. This allows for parameters to remain within meaningful ranges.

Using a related theory, *PCSWMM* software developed a variation of SWMM which incorporates an automated calibration tool called the Sensitivity-based Radio Tuning Calibration (*SRTC*) function. Simulations are run from the upper to lower limits and users are able to tune each parameter. With the assistance of a hydrograph interface, effects from calibration tuning can be seen in real time. This advancement brings a significant contribution for current and future modeling efforts. If watershed models are better accurately depicted then results from simulations can be more representative of actual observed conditions.

1.2 Knowledge Gaps

As presented in the literature review current knowledge is limited in regards to *SWMM*'s ability to simulate the undeveloped watershed. Studies including Davis et al. (2007) and Jang et al. (2007) have developed *SWMM* models to simulate undeveloped watersheds but were unable to comprehensively examine simulation results. Presented in this section are the current knowledge gaps that exist among the ability of *SWMM* to effectively simulate the undeveloped watershed.

The identified knowledge gaps may be summarized as following:

1. How do processes such as rainfall, infiltration, evapotranspiration affect the behavior of surface water and groundwater in the headwaters of an intermittent watershed?
2. What is the ability of SWMM to simulate the hydrology of an undeveloped, intermittent watershed, over a hydrological year?
3. Which runoff characteristic is SWMM able to simulate best (e.g. maximum flow, mean flow or total volumes)?

Chapter 2

Scope and Objectives

Beginning in early 2012, the Alabama chapter of the Associated General Contractors of America (*AGC*) partnered with Auburn University. *AGC*'s goal was to engage students at Auburn University and provide an unique opportunity of working on a real-life land development project. This involved students developing new ideas to improve the value and quality of land owned by *AGC* . Several disciplines were involved in this study including: building science; landscape architecture; biosystems engineering and civil engineering. Each discipline was tasked with different objectives but all worked simultaneously to achieve *AGC*'s goals. The civil engineering team was given the task of developing a water budget study and providing a feasibility assessment of a pond to be sustained on site. This task offered an opportunity to provide the needs of *AGC* while also allowing to study and model local hydrological processes.

To study watershed behavior and provide a feasibility assessment several different hydrological monitoring devices were installed. During this initial phase of the field monitoring program two in-stream weirs, two shallow groundwater wells, three automated rain gauges and a Kestrel 4500 micro meteorological station were installed. Data collected from these devices was used to analyze and develop relationships between various hydrologic components.

After 15 months of data collection a *SWMM* model was developed and calibrated to replicate the watersheds behavior. Geographic Information Systems (*GIS*) remote sensing data and local survey information was obtained and used to provide input parameters for the *SWMM* model. Locally recorded rainfall, temperature, atmospheric pressure and runoff

were used as input data sets. Then during calibration and verification efforts, runoff hydrographs from installed weirs were used to verify simulation output. Finally, several graphical and statistical methods were utilized to determine the models capabilities to replicate watersheds behavior.

The specific objectives of this research can be outlined as follows:

1. Begin initial phase of the field monitoring program
2. Analyze data and develop hypotheses in regards to local hydrological relationships
3. Develop a *SWMM* model for WS-AGC with the use of detailed local survey and remote sensing GIS data
4. Calibrate and validate the *SWMM* model with respect to observed hydrograph data sets over various hydrological conditions
5. Assess the capabilities of *SWMM* to model a undeveloped, intermittent watershed using graphical and statistical techniques

Chapter 3

Methodology

3.1 Site Description

The study watershed referred to as (WS-AGC), is located in Pittsview, AL ($32^{\circ} 9' 29.30''$ N, and $85^{\circ} 10' 8.09''$ W). Covering an area of 2.90 km^2 in Russell County, WS-AGC drains a first order intermittent stream positioned at the headwaters of a complex series of tributaries that connect and discharge into Hatchechubbee Creek. The Hatchechubbee Creek then continues south and eventually discharges in the Chattahoochee River just north of Eufaula, AL. Figure 3.1 provides an aerial imagine of the WS-AGC, its stream development predicted from GIS and topographic lines. This area has been used as a hunting preserve over the past decades and remains relatively untouched except for a few trails and green fields. The effects of these areas were assumed to have a negligible effect on the hydrology of WS-AGC.

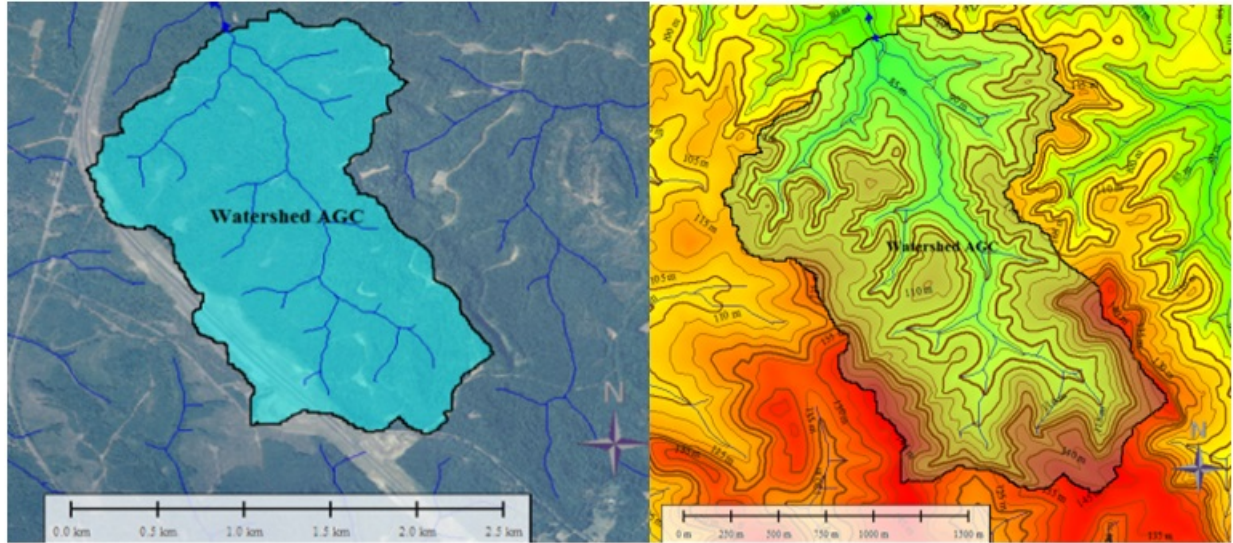


Figure 3.1: Left: Areal view of the WS-AGC with the network of intermittent streams. Right: Respective contours lines

Since WS-AGC's location is at the transition zone between the Piedmont and Lower Coastal Plains (LCP) regions, the study site possesses characteristics that are particular to both regions. With respect to the Piedmont region, the watershed is in an area of many low rolling foothills and contains various patches of clay-like soils. However the area also reflects the LCP region at its low laying central areas. Composition in the LCP environments plays a major role in runoff responses due to the presence of very well to poorly drained soils in low- topographic relief areas (La Torre Torres et al., 2011). Similarly to other LCP watersheds, groundwater field measurements have indicated that WS-AGC hydrological responses are influenced by evapotranspiration. Observations of this phenomenon show distinct differences between the dry (May-November) and wet (December-April) seasons. These seasonal separations were selected based on the study conducted by La Torre Torres et al. (2011) on a LCP watershed in the southeastern USA.

Finally, the site also displays some hydrological characteristics of uplands regions. Hydrologic processes in upland areas are mainly influenced by steep gradient profiles and hill-slope processes (i.e. interflow, sheetflow and overland flow) and less influenced by soil composition (La Torre Torres et al., 2011). These characteristics provide an opportunity to study a distinct watershed type that to our knowledge has not been examined in literature (Sun et al., 2002; Czikowsky and Fitzjarrald, 2004; Harder et al., 2007; Sun et al., 2010; La Torre Torres et al., 2011; Davis et al., 2007).

WS-AGC has an average slope of approximately 12.4% and is comprised of several soil types. After applying the NRCS/USDA web soil survey tool (<http://websoilsurvey.nrcs.usda.gov>), the site was determined to consist of mostly Hannon Clay and Trout-Springhill-Luverne (33 and 36% of the watershed respectively) as shown in Table 3.1. The drainage classes are classified as moderately well drained (Hannon clay) and well to excessively drained (Trout-Springhill-Luverne) soils. Toward the lower portion of the catchment the soils transition to Kinston Mantachie and Luka (KMA), see Figure 3.2. This soil type only makes up around 4.6% of the area of interest (AOI).

Table 3.1: USGS web soil survey results for WS-AGC study site

Russell County, Alabama (AL113)			
Map Unit Symbol	Map Unit Name	Acres in AOI	Percent of AOI
CnB	Conecuh fine sandy loam, 1 to 3 percent slopes	45.4	7.7%
CoC2	Conecuh loam, 3 to 8 percent slopes, eroded	2.2	0.4%
HnD2	Hannon clay, 5 to 8 percent slopes, eroded	196.6	33.3%
KMA	Kinston, Mantachie, and luka soils, 0 to 1 percent slopes, frequently flooded	27.0	4.6%
LnB	Luverne sandy loam, 2 to 5 percent slopes	52.4	8.9%
LsE	Luverne-Springhill complex, 15 to 25 percent slopes	51.9	8.8%
TsE	Troup-Springhill-Luverne complex, 10 to 30 percent slopes	214.9	36.4%
Totals for Area of Interest		590.5	100.0%

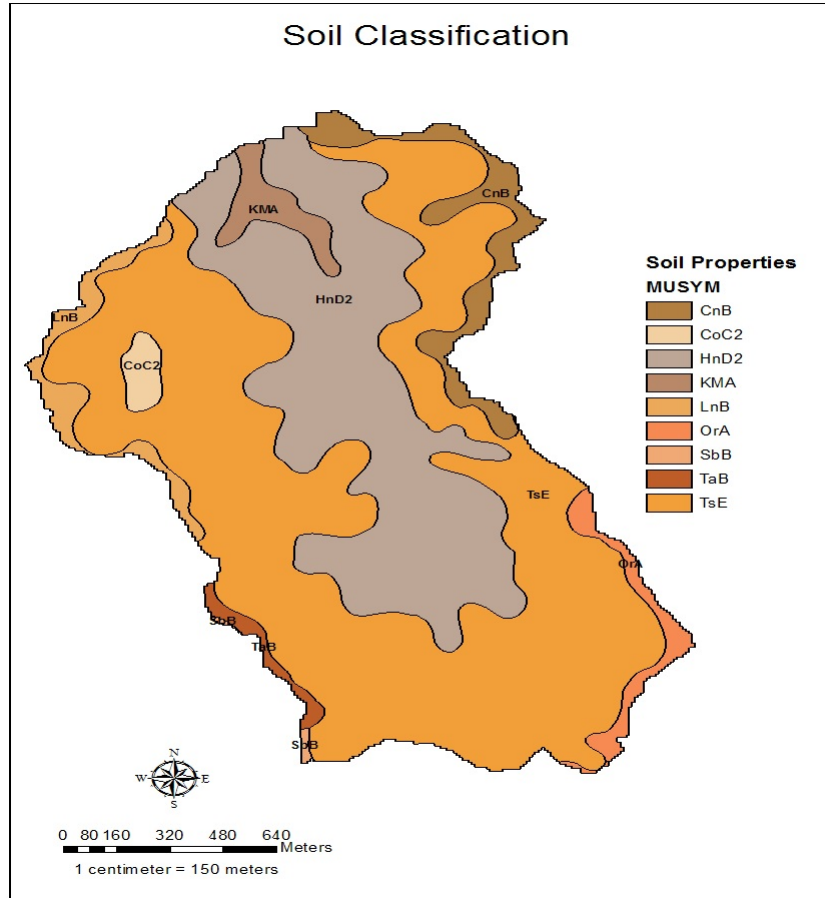


Figure 3.2: Watershed *AGC* soil composition, provided from (NRCS/USDA web soil survey)

Near the southern end, which constitute in the upstream portion of the watershed, a swamp-like collection area exists. Water during the rainy season collects here and discharges into the stream through a series of natural weir-like outlets. As the stream progresses northward from this point. Downstream the channel cross section begins to dramatically increase in size. Originating with channel dimensions of 0.5 m deep and 1 m wide, erosive processes have caused the farther downstream channel segment to reach dimensions of 3.5 m deep and 3 m wide at the base, each with side slopes of approximately 4:1 (V:H). The highly erodible sandy stream bed soil has also formed many abstraction diversions throughout the channels length. For instance, at one location the stream channel completely disappears into a large mound of sandy soil and then reappears about 20 m downstream. Abstractions

have also been created throughout the channel. Large amounts of tree branches and debris that have been conveyed downstream from large runoff events have caused natural dam like structures to form. Beavers also have created dams within the watershed.

Vegetative cover in WS-AGC consists of a mixture between Slash (*Pinus elliotii*) and Loblolly Pine (*Pinus taeda*) throughout, similar to the study site of Harder et al. (2007). The density of trees begins to increase closer to the stream bed and into the riparian-zone. The riparian-zone also contains a bamboo, and vines which are mixed with the pines and becomes very dense in many areas. This area is where evidence of a shallow water table has been found which is supported throughout most of the year depending on the rainfall totals experienced.

3.2 Field Investigations

The investigation began in early February 2012 with the installation of three rain gauges and a portable meteorological station. As the year progressed the field monitoring program grew to incorporate an entire system of monitoring equipment that collects data on local runoff, groundwater levels, rainfall, temperature and pressure. Data from this equipment is provided at a high resolution, ranging from 15-30 minute sampling intervals. This section incorporates details into the construction processes and placement of the hydrological monitoring equipment.

3.2.1 Precipitation Collection

Precipitation at WS-AGC was collected using three automated recording Onset RG3-M rain gauges. Before deployment, calibration of each gauge was performed. This calibration was completed in the Harbert Engineering Center Hydraulics Laboratory following guidelines provided from the User's Manual, (Onset, 2011). The calibration test used a known volume of water, 473 ml, that was dripped upon the top of each gauge. Water funneled down into a two bucket tipping mechanism, where each bucket represented 0.2 mm of rainfall. The number

of tips were recorded with a goal of reaching 100 ± 2 tips. Screws located at the bottom of the gauge were then adjusted either clockwise or counter clockwise to increase/decrease the number of tips recorded. Once the test provided consistent results for each gauge it was considered fully calibrated.

After the calibration period the gauges were installed on February 2012 in the open grass fields located throughout the property, see Figure 3.3. Data at each location was recorded at regular 30 minute intervals with a capability of a finer resolution as an event is occurring. These gauges provide data that is accurate to $\pm 1.0\%$ of the readings and can record maximum rainfall rates of $12.7 \frac{cm}{hr}$. In order to capture rainfall for the entire watershed, gauges were strategically placed in such a way to divide the watershed into three nearly equal areas. The Thiessen polygon method was then used to average each rainfall collection area into a single precipitation time series file, later to be used in numerical modeling investigations.

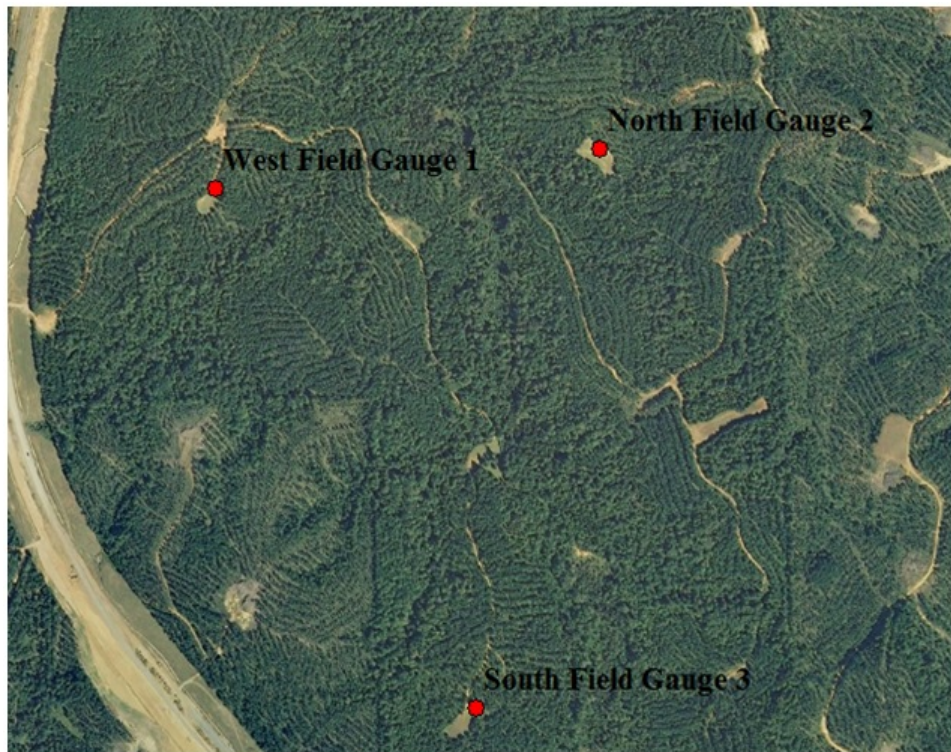


Figure 3.3: Rain gauge locations

Rain gauges were installed using (10cmx10cmx5m) pressure-treated wooden posts anchored with concrete. The bases of the posts were placed approximately 1.5 meters below the surface and supported with vertical stabilizing arms during the drying process. The posts were extended 3.4 meters off the ground to limit interference from the surrounding tree cover as well as human and animal interaction. Figure 3.4 shows the two posts installed at the west gauge location. On the left is a rain gauge and on the right is the Kestrel 4500 pocket weather tracker.

To promote Quality Assurance/Quality Control (QA/QC), collected data was compared with two off-site gauges managed by (Community Collaborative Rain, Hail Snow Network-CoCoRaHS) that are located within a 10 mile radius of the site. CoCoRaHS involves many trained volunteers across the country and is supported by the National Oceanic and Atmospheric Association (NOAA). Recorded rainfall at these locations were compared with field data for each month during research efforts.



Figure 3.4: Rain gauge post and meteorological station

3.2.2 Meteorological Data

Located along side of the west rain gauge is a Kestrel 4500 portable weather station, see Figure 3.4. Recording continuously at 30 minute intervals, measurements of various climate information including temperature, barometric pressure, wind speed and humidity are captured. In Table 3.2 the accuracy of each measurement recorded is shown. One of the most influential measurements taken with this device was the barometric pressure. It provided critical local barometric pressure that was used in calibrating the other pressure transducers placed throughout the site. Temperature data was also a critical measurement. It provided the input data for calculating potential evapotranspiration rates through different methods which are discussed later in this chapter.

Table 3.2: Kestrel 4500 meteorological station measurements and accuracy

Measurement	Maximum	Minimum	Accuracy (+/-)	Units
Temperature	125	-45	1.00	°C
Pressure	1100	10	1.50	hPa
Wind Speed	60	0.4	3%	m/s
Relative Humidity (RH)	0	100	3.00	%RH
Altitude	9000	-2000	15.00	m
Wind Chill	125	-45	1.00	°C
Heat Index	125	-45	2.00	°C
Dewpoint	125	-45	2.00	°C
Wet Bulb Temperature	125	-45	2.00	°C

3.2.3 Evapotranspiration Calculations

Evapotranspiration (ET) is one of the major components of the hydrologic cycle (Trajkovic, 2005). ET accounts for the catchments water losses through plant transpiration, ponded water and upper soil zone evaporation. This study incorporated estimates of ET with assistance from two temperature based methods for predicting potential evapotranspiration (PET). Temperature based PET methods may over or under estimate ET but when

local pan evaporation or solar radiation data is unavailable these methods provide the closest estimate possible.

The first temperature based PET method used in this study was the Hamon method, (Hamon, 1963). This empirical method incorporates the following equations to calculate the daily PET (mm).

$$PET = 0.1651 * L_d * RHOSAT * KPEC \quad (3.1)$$

$$RHOSAT = 216.7 * ESAT / (T + 273.3) \quad (3.2)$$

$$ESAT = 6.108 * e^{17.26939 * T / (T + 237.3)} \quad (3.3)$$

Where:

- PET is the daily PET (mm)
- L_d is the daytime length from sunrise to sunset in multiples of 12
- RHOSAT is the saturated vapor density ($\frac{g}{m^3}$)
- T is the daily mean air temperature
- ESAT is the saturated vapor pressure (mb)
- KPEC is the calibration Coefficient, set to 1 in this study

Values of L_d in Equation 3.1 were found at (<http://www.orchidculture.com/COD/daylength.html>). The site is versatile and can be applied to any where in the world by selecting the closest line of latitude nearest the study region. Temperature data for Equations 3.2 and 3.3 was provided by the local Kestrel 4500 meteorological station.

The second temperature based PET method applied was the Hargreaves-Samani approach. This empirical method involves the use of a more complex series of equations. These include equations to solve for parameters including temperature reduction coefficient, relative distance between the earth and sun, solar declination, sunset hour angle, extraterrestrial solar radiation and finally PET.

$$PET = 0.0075 * R_a * C_t * \delta^{\frac{1}{2}} * T_{avg} \quad (3.4)$$

In order to calculate daily PET from Equation 3.4 the series of equations below must be evaluated.

$$d_r = 1 + 0.033 * \cos\left(\frac{2\pi J}{365}\right) \quad (3.5)$$

Equation 3.5 is the first step in this process. It uses the Julian date (J) to solve for the relative distance between the earth and the sun, d_r .

$$\delta = 0.4093 * \sin(d_r - 1.405) \quad (3.6)$$

Then the solar declination δ is calculated with Equation 3.6. This again uses J to solve for δ (radians).

$$w_s = \arccos(-\tan(\phi) * \tan(\delta)) \quad (3.7)$$

Next Equation 3.7 is used to determine the sunset hour angle w_s (radians). This involves inputting the previously solved variable δ and the latitude of the study site ϕ .

$$R_a = 15.392 * d_r (w_s * \sin(\phi) * \sin(\delta) + \cos(\phi) * \cos(\delta) * \sin(w_s)) \quad (3.8)$$

Now all prior solutions of Equations 3.5-3.7 can be incorporated into Equation 3.8. This value of extraterrestrial solar radiation R_a ($MJ/m^2/day$) can then be used in Equation 3.4 to solve for daily PET.

$$C_t = 0.035 * (100 - wa)^{\frac{1}{3}} (wa \geq 54\%) \quad (3.9)$$

$$C_t = 0.125 (wa < 54\%) \quad (3.10)$$

Lastly Equations 3.9 and 3.10 must be solved. These two equations are dependent upon the value of relative humidity w_a . If values of w_a are greater or equal to 54% then Equation 3.9 is used and if w_a is less than 54% then Equation 3.10 must be used.

3.2.4 Runoff Monitoring

Several options exist when attempting to monitor a streams flow rate. The United States Department of Agriculture (USDA) Water Measurement Manual (Dodge, 2001) provides numerous options. Such as available include weirs, flumes, orifices and venturi meters. The choice of flow monitoring structures is site dependent and not every type may be right for the situation. Runoff monitoring in this study was completed with the use of weirs due to the simplicity of the construction and their conformity to the cross sections faced at the site. The interested reader should examine Dodge (2001) for more detailed descriptions into the other options listed above.

The first weir installed was a Cipolletti type that was constructed instream at the lower downstream portion of WS-AGC. It was selected because it conformed the best with natural vertical slopes of the channel. The weir also provided data that has been proven to be within $\pm 5\%$, Dodge (2001). Construction did not begin until late Spring 2012 since the streams were still flowing. Wet season conditions had supported high water table levels and it was not until several consecutive weeks of dry weather that construction efforts could begin. Figure 3.5 shows the conditions faced during the construction process. Even with a few weeks of dry conditions the high water table levels caused the base of the weirs foundation to become flooded as the trench was dug. This slowed the construction down considerably.

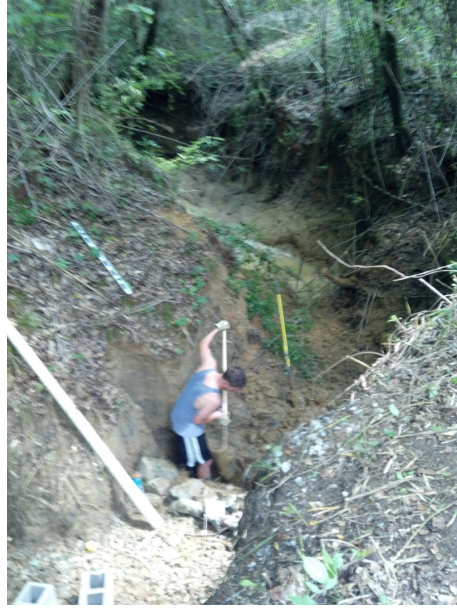


Figure 3.5: Construction of Cipolletti weir

The dense and thriving forest root systems surrounding the construction area became a major issue to excavate through by with shovels. Figure 3.6 shows the dense root systems in the vicinity. This issue is revisited later in this section as it also became a major issue with erosion control around the laterals of the weir.

In order to support the weir during the potential five-to-six feet backwater water elevations, five ($10\text{cm} \times 10\text{cm} \times 5\text{m}$) post were placed at a depth of 1.5 meters below the streams bed elevation, Figure 3.7. The voids around the post were then back filled with concrete and allowed to set. The walls were prefabricated in a workshop with guidance from Dodge (2001) for Cipolletti dimension requirements. They were brought out to the field and installed across the stream bed.



Figure 3.6: Roots causing issues on the lateral walls of the weir



Figure 3.7: Support post for the Cipolletti weir

Shown in Figures 3.8 and 3.9 are the walls installed against the post. The trench was first lined with a thin layer of limestone gravel to create a solid base. Then it was over topped with twenty centimeters of concrete all the way across. The rest of the trench was back filled with soil from the construction process.



Figure 3.8: Upstream view of the Cipolletti weir



Figure 3.9: Downstream view of the Cipolletti weir



Figure 3.10: Riprap placed at the downstream side of the Cipolletti weir

Continuing the finishing process, plastic lining was placed along the upstream portion to help prevent the seepage beneath and along the sides of the weir. Lastly, large rip-rap was placed to provide energy dissipation on the downstream channel side, see Figure 3.10. Figure 3.11 shows the finished Cipolletti weir at the downstream location.



Figure 3.11: Finished Cipolletti weir looking upstream: completed (June 1st 2012)

The stream bed at this location is approximately 4.6 m deep and 3 m wide with irregular side slopes of roughly 4:1 (V:H). Stretching across the channel at 3.0 m, the Cipolletti weir has a crest length of 1.1 m and two 1.8 m vertical sides, cut at the 4:1 slopes, conforming to the natural slopes. Figure 3.12 provides a schematic of the Cipolletti weirs dimensions, where (H) represents the height of water flowing over the crest.

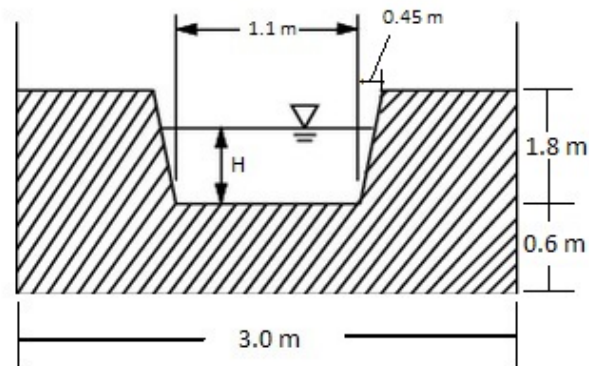


Figure 3.12: Cipolletti weir dimensions

Further upstream, the second runoff measurement device a fully contracted rectangular weir was constructed. Completed in September 2012, it measures flows from approximately 60% of the contributing watershed area. The construction process followed the same procedure as the Cipolletti weir discussed previously. However, this fully contracted rectangular weir provides runoff data that is accurate between $\pm 1.5\%$ to $\pm 2.5\%$ according with the Water Measurement Manual, (Dodge, 2001).

Figure 3.13 shows the (10cmx10cmx5m) post placed in the stream to support the weir walls. Stream cross-section dimensions here are smaller, measuring approximately 3.4 m across and 1.2 m deep, with irregular side slopes. The finished weir has crest length of 0.67 m and height of 1.5 m, see Figure 3.15.



Figure 3.13: Support post for the rectangular weir



Figure 3.14: Upstream view of rectangular weir

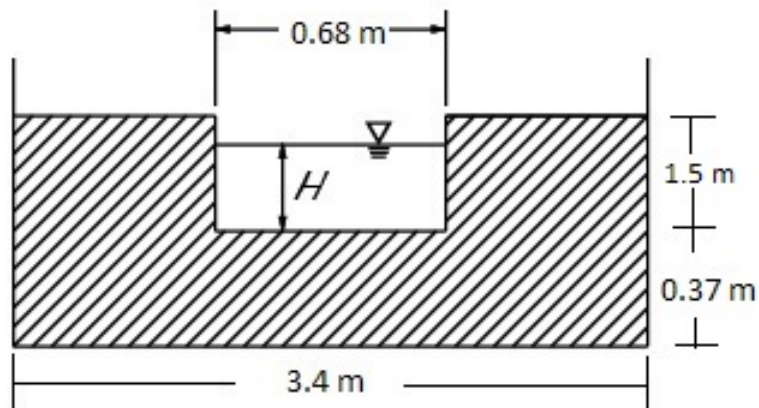


Figure 3.15: Rectangular weir dimensions

At both locations, wooden posts with level loggers (HOBO U20, pressure head range 4 m H₂O, accuracy ± 0.014 m H₂O) have been positioned at a distance of four times the weirs maximum measured head upstream from the crest of the weirs, following the recommendations of Dodge (2001). This was determined to be approximately 2.44 m upstream from both weirs. The large distance ensures that the readings are not affected by draw down associated

with the discharge over the weirs. Sensors were placed on the lateral of the posts parallel to the flow, see Figure 3.16. To mark the start of an event, 6.1 cm of head is required to consider the flow fully-developed over each weir, Dodge (2001). Level logger data collection was continuously measured at 15-minute intervals throughout the study period.



Figure 3.16: HOBOT pressure sensor installed upstream at each weir

As mentioned, the stream bed is mostly comprised of a highly erodible soil that has caused many challenges in maintaining the integrity of weirs. Throughout the first year of service, the Cipolletti weir experienced a few large peak discharges which caused erosion around the side walls. One example of this can be seen in Figure 3.17, where the right side wall experienced large amounts of erosion after a runoff event.



Figure 3.17: Erosion damage at the Cipolletti weir to the right

After several attempts to repair this weir, the decision to convert it to a broad crested weir was made in February 2013. This involved cutting across the level of the crest, creating a weir with a length of 3.7 m and adding a width of 45 cm, see Figure 3.19. Figure 3.18 depicts the changes made to the Cipolletti weir. The remodeling has significantly decreased the erosion seen from large runoff events insuring it will be able to withstand a longer period of recording.



Figure 3.18: Upstream view of broad crested weir

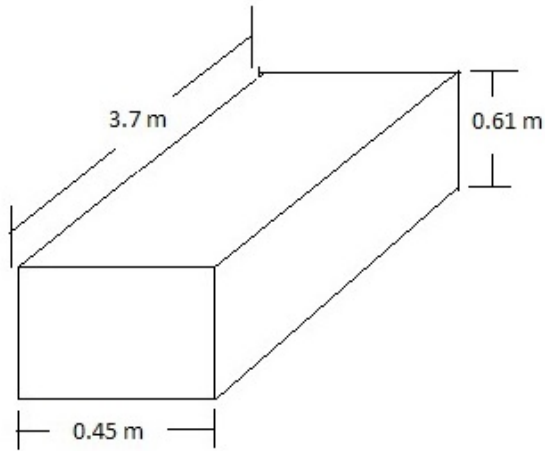


Figure 3.19: Broad crested weir dimensions

The upstream rectangular weir experienced some minor damages during the monitoring time. Lateral seepage resulting from animal interference began to erode soils out and cause the channel walls to expand. This was repaired by extending the side wall of the weir and expanding the crest length from 0.67 m to 1.2 m. Figure 3.20 shows the modified crest dimension and (H) which represents the height of water measured over the weir. Along with

the remodeling of both weirs the governing flow equations associated with each were adjusted accordingly.

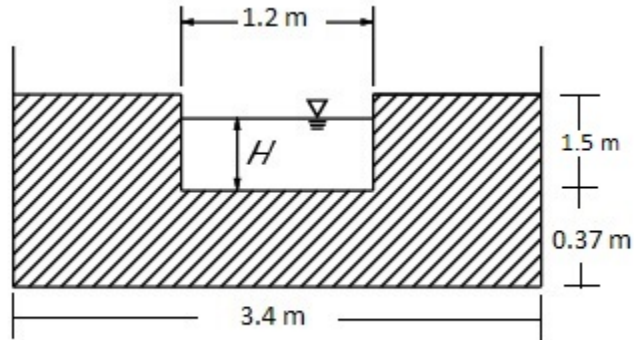


Figure 3.20: Modified rectangular weir dimensions

3.2.5 Weir Discharge Equations

Both the Cipolletti and fully contracted rectangular weirs were calibrated by referencing methods provided in Chapter 7 of the Water Measurement Manual, Dodge (2001). The modified broad crested weir was calibrated with assistances from the Handbook of Hydraulics, Brater et al. (1996). Each calibration process is presented below.

The Cipolletti weirs discharge calibration was similar to the suppressed weir since the side walls contract the flow over the crest. Dodge (2001) has developed the governing flow equation ignoring the effects of the approach velocity. Equation 3.11 shows the generic formula available to calculate flowrate Q over the Cipolletti weir.

$$Q = 3.367LH^{\frac{3}{2}} \quad (3.11)$$

Cipolletti calibration method limitations:

- Crest length must be at least 0.152 meters (L)
- Crest Height must be at least 0.102 meters (P)
- Head measurements must be taken at least four times the maximum head upstream

- Head measurement must be at least 0.061 meters (H)
- Ratios of (H/P) must be less than 2.4
- Downstream water elevation must be at least 0.051 meters below crest elevations
- Accuracy is within $\pm 5\%$ of determined value, Dodge (2001).

Calibration of the fully contracted rectangular weir was completed by applying the Kindsvater-Cater method for determining the head discharge relationship. This method allows for the calibration of weirs that may not meet the crest height limits of traditional rectangular weirs. However, this method has limitations, a few of which are listed below. More detailed discusses can be found in Dodge (2001).

Kindsvater-Carter calibration method limitations:

- Crest length must be at least 0.152 meters (L)
- Crest Height must be at least 0.102 meters (P)
- Head measurements must be taken at least four times the maximum head upstream
- Head measurement must be at least 0.061 meters (H)
- Ratios of (H/P) must be less than 2.4
- Downstream water elevation must be at least 0.051 meters below crest elevations
- Accuracy is between $\pm 1.5\%$ and $\pm 2.5\%$ of determined value, Dodge (2001)

The Kindsvater-Carter calibration method begins with the use of the basic weir formula, Equation 3.12. Note: Inputs for this method are in U.S. units, but for this study all values were converted into SI units.

$$Q = C_e L_e H_e^{\frac{3}{2}} \quad (3.12)$$

Where:

- Q is discharge ($\frac{ft^3}{s}$)
- C_e is the effective coefficient of discharge ($\frac{ft^{\frac{1}{2}}}{s}$)
- B is the average width of the approach channel
- $L_e = L + k_b$

- $H_e = H + k_h$

In order to determine the value of k_b specific to the weir of interest, Figure 3.21 must be used. Using the ratio of L/B and following from the x-axis up to the plotted line, a value of k_b can be obtained.

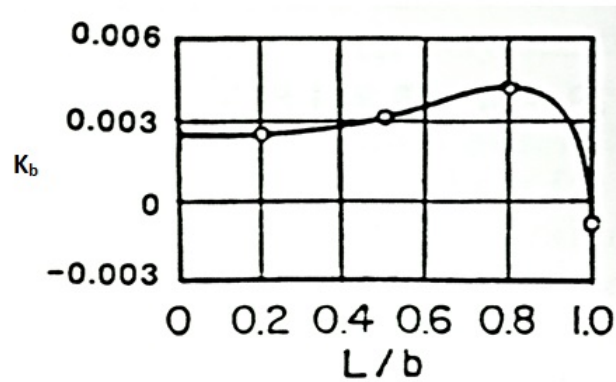


Figure 3.21: Values of width-adjustment factor, taken from (Dodge, 2001)

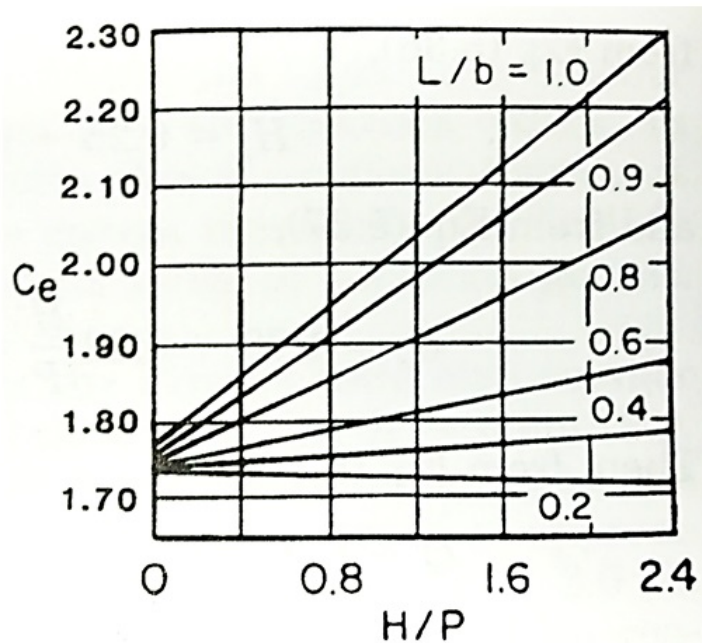


Figure 3.22: Effective coefficient of discharge, C_e , as a function of L/B and H/P , taken from (Dodge, 2001)

Then, from Table 3.3, the ratio of L/B is used to determine C_1 and C_2 found in Equation 3.13. Linear interpolation may be used if necessary.

Table 3.3: Coefficient and constants used when determining the effective coefficient of discharge, taken from (Dodge, 2001)

L/B	C_1	C_2
0.2	-0.0087	3.152
0.4	0.0317	3.164
0.5	0.0612	3.173
0.6	0.0995	3.178
0.7	0.1602	3.182
0.8	0.2376	3.189
0.9	0.3447	3.205
1.0	0.4000	3.220

$$C_e = C_1 \left(\frac{H}{P} \right) + C_2 \quad (3.13)$$

Once the coefficients are determined then Equation 3.13 can be updated with varying values of H and Equation 3.12 is continuously calibrated. Since the weir was modified due to erosion factors, this process was followed twice to provide a new head discharge relationship. Provided below are the final calibrated head discharge equations used in this study. Equation 3.14 represents the calibrated equation at original geometry and Equation 3.15 represents the calibrated equation after expansion.

$$Q = \left(0.0115 \left(\frac{H}{1.21} \right) + 3.158 \right) 2.216(H^{\frac{3}{2}}) \quad (3.14)$$

$$Q = \left(0.02059 \left(\frac{H}{1.21} \right) + 3.161 \right) 3.791(H^{\frac{3}{2}}) \quad (3.15)$$

Finally, the broad crested weir was calibrated with reference to the Handbook of Hydraulics, Brater et al. (1996). Experiments on broad crested weirs have been performed by Blackwell, Bazin, Woodburn, the U.S. Deep Waterways Board, and the U.S. Geological

Survey (Brater et al., 1996). Equation 3.16 provides the basic equation used to determine discharge over a broad crested weir.

$$Q = CLH^{\frac{3}{2}} \quad (3.16)$$

Where:

- C is the calibration coefficient
- L is the length of the crest
- H is the head measured over the crest

The previously mentioned experimental results were combined into Table 3.4 which has been made available by Brater et al. (1996). Using this table, values of C can be determined based on the weirs breadth (B) and the measured head. The broad crested weir in this study had a breadth of 0.45 m so the C values in this column were used to continuously update the flow formula, Equation 3.16. By incorporating a Visual Basic code in a Excel spreadsheet, C values were found using linear interpolation in Table 3.4.

Table 3.4: Coefficient, C , values used for broad crested weirs, taken from (Brater et al., 1996)

Measured head, m	Breadth of crest of weir, m										
	0.15	0.20	0.30	0.45	0.60	0.75	0.90	1.20	1.50	3.00	4.50
0.10	1.61	1.55	1.50	1.46	1.44	1.44	1.43	1.40	1.38	1.41	1.49
0.20	1.70	1.60	1.52	1.46	1.44	1.44	1.48	1.49	1.49	1.49	1.49
0.30	1.83	1.73	1.65	1.52	1.47	1.46	1.46	1.48	1.48	1.48	1.45
0.40	1.83	1.80	1.77	1.61	1.53	1.48	1.46	1.46	1.46	1.48	1.46
0.50	1.83	1.82	1.81	1.70	1.60	1.52	1.48	1.47	1.46	1.46	1.45
0.60	1.83	1.83	1.82	1.67	1.57	1.52	1.50	1.48	1.46	1.46	1.45
0.80	1.83	1.83	1.83	1.81	1.70	1.60	1.55	1.50	1.48	1.46	1.45
0.90	1.83	1.83	1.83	1.83	1.77	1.69	1.61	1.51	1.47	1.46	1.45
1.0	1.83	1.83	1.83	1.83	1.83	1.76	1.64	1.52	1.48	1.46	1.45
1.2	1.83	1.83	1.83	1.83	1.83	1.83	1.70	1.54	1.49	1.46	1.45
1.4	1.83	1.83	1.83	1.83	1.83	1.83	1.83	1.59	1.51	1.46	1.45
1.5	1.83	1.83	1.83	1.83	1.83	1.83	1.83	1.70	1.54	1.46	1.45
1.7	1.83	1.83	1.83	1.83	1.83	1.83	1.83	1.83	1.59	1.46	1.45

Broad crested calibration method limitations:

- Crest length must be at least 0.152 meters (L)
- Crest Height must be at least 0.102 meters (P)

- Head measurements must be taken at least four times the maximum head upstream
- Head measurement must be at least 0.061 meters (H)
- Ratios of (H/P) must be less than 2.4
- Downstream water elevation must be at least 0.051 meters below crest elevations
- Accuracy is between $\pm 1.5\%$ and $\pm 2.5\%$ of determined value, Dodge (2001)

3.2.6 Groundwater Observation Wells

Two shallow groundwater wells were installed, in October 2012, next to the upstream rectangular weir. The first well is located approximately one meter outside of the stream and reaches a depth of three meters below the surface. Five meters away and located in the center of the stream is the second well which has been drilled at the same depth, see Figure 3.23.



Figure 3.23: Shallow groundwater wells

Both wells were drilled with an 8.25 cm diameter hand auger. This allowed for the installation of 3.8 cm diameter PVC with screens lengths of 61 cm attached at the ends. A sand pack was placed up to one meter to act as a filter and keep fines from entering. Finally, each well was back filled and capped with a layer of sodium bentonite. Doing so prevented any water flowing on the surface to interfere with the shallow groundwater levels. Pressure transducers or level loggers (HOBO U20, range 9 m, accuracy ± 0.021 m H₂O) have subsequently been deployed at these wells. These devices provide fine resolution water level data at 15 minute intervals.

During the dates between December 19th, 2012 and January 25th, 2013, various large rainfall runoff events hit WS-AGC. Consistent rainfall along with the largest intensity event $45 \frac{mm}{hr}$ occurred in a short period of time and caused large amounts of debris from the surrounding areas to enter the stream. The two groundwater wells suffered major damage as the PVC pipes, which extend about two feet above the surface, were broken. Forces within the stream were so strong that the sensor 3 meters below the surface was lifted out and brought downstream approximately 61 meters. This event is represented by the missing data in Figure 3.36.

3.2.7 Infiltration Testing

Several locations were chosen throughout WS-AGC to conduct infiltration tests using a AMS 24-inch double-ring infiltrometer. These locations were selected based on topology and soil characteristics provided from the web soil survey (<http://websoilsurvey.nrcs.usda.gov>). Figure 3.24 shows the location at four separate sub-catchments. At each sub-catchment 4-7 tests were run. The average of each sub-catchment was made and the values were used as comparison to the *SWMM* models maximum infiltration rate ($\frac{mm}{hr}$) input.

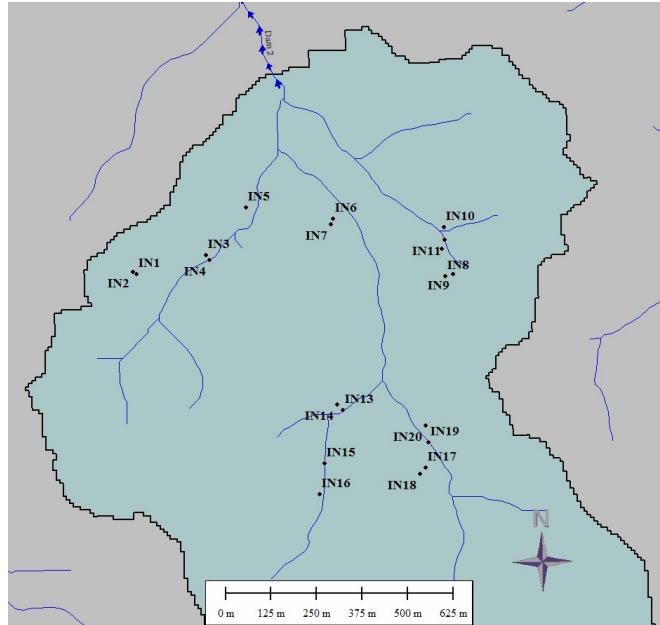


Figure 3.24: Locations of Infiltration Testing

The procedure followed to run these tests are as follows:

- Insert double ring into the soil at the test area by pushing handles and rotating back and forth
- After the double ring has reached at least two inches, fill both inner and outer rings with clean water until they start to overflow
- Using a ruler or a pre-installed tape measure, record the initial water level within the inner ring and start the timer
- Note the water level and time of sample as the water begins to drop
- Continue this test and fill ring as needed until 15 minutes has passed
- Take the amount of infiltrated water by 4 to obtain the infiltration rate per hour
- Depending on the soil types in the area this test may be shorted due to large amounts of water that would be needed to run a 15 minute test
- Note: Be sure to mind the amount of time the test was run since this will affect your infiltration rate multiplier

3.2.8 Soil Sampling

On July 10th and 11th, 2013, soil sampling was conducted across the potential earth embankment location. Collaborating with *AGC*, a subcontractor from TERRACON Inc was hired to consult and perform the soil sampling and analysis. The site of interest was first clear cut across the approximate 137 m-long embankment centerline. Then four locations on the centerline and two others approximately 30 m upstream and downstream of the line were chosen for soil sampling, see Figure 3.25.

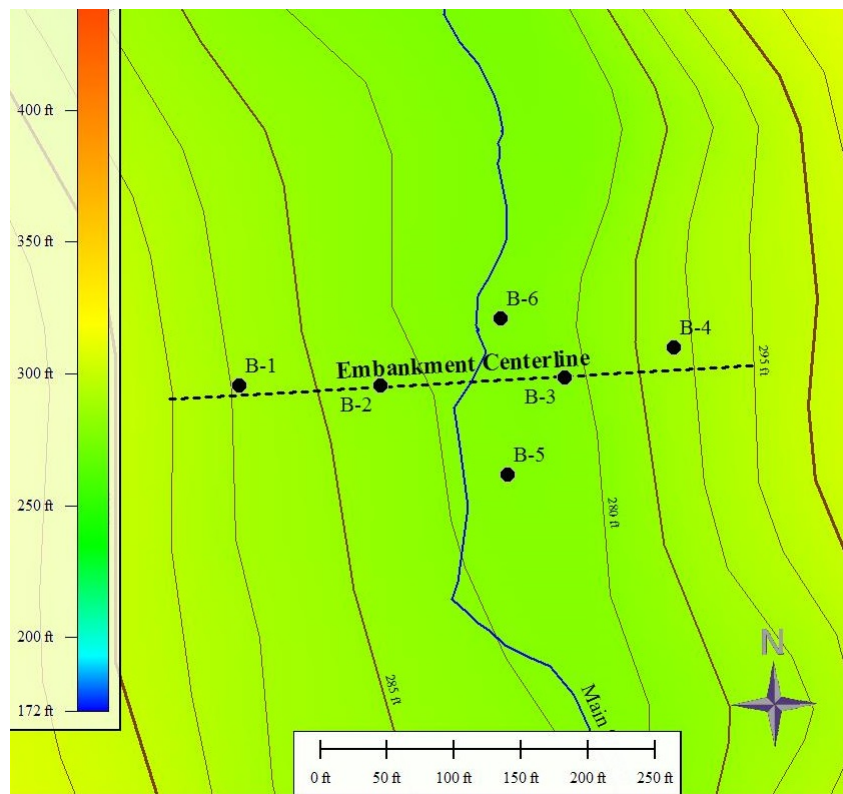


Figure 3.25: Bore sites at WS-AGC indicated by black markers

On the trip into the site the 25 thousand pound CME-550 rotary drill rig faced some challenges with steep grades and narrow cut firebreak paths. The weather conditions also provided a saturated upper layer of soil which increased the difficulty of the trip, Figure 3.26.



Figure 3.26: Drill rig entering WS-AGC

Once the rig made it to the sampling location, drilling was commenced. The sampling was conducted using a 15.2 cm diameter hollowed stem auger. Figure 3.27 shows the drill crew setting up the rig to begin drilling and sampling.



Figure 3.27: Setting up to drill boring



Figure 3.28: Soil exiting the bore hole from approximately 4.6 m below the surface

At each drill site standard penetration tests (SPT) were performed at specified depths as the auger progressed downward. All samples were collected with accordance to ASTM D1586. Samples taken from these tests were then used for soil analysis, Figure 3.29. At drill site B-1 two bulk samples were taken to conduct grain size distributions, compaction and Atterburg limits.



Figure 3.29: Samples taken from the SPT

Along with the SPT test and bulk samples taken across the centerline, three Shelby tubes were used in this analysis. At location B-2 just offset from the creek, samples were

taken at approximately 1.5, 3.0 and 4.6 m intervals with accordance to ASTM D4220. Figure 3.30 shows one of the Shelby tube samples that was taken to the professional laboratories operated by TERRACON Inc. There the samples were analyzed with a Mercury Permeometer test to determine permeability rates. Results from these sampling efforts can be found in the appendix of this document.



Figure 3.30: Shelby tubes being prepared to take out of the site

3.3 Fundamentals of Operating SWMM

3.3.1 Introduction

The storm water management model (*SWMM*) was developed in 1971. Since then it has evolved into the current version, *SWMM* 5.0. Completely rewritten from the previous

version, it incorporates a user-friendly interface and new visual effects to assist with analysis. This version has been used for numerous water-related projects and analysis throughout its operational history, the majority of which has been focused on urban storm water system modeling. It has the capability to simulate single and long-term (continuous) rainfall runoff events, and its intuitive user interface has opened the door for less experienced modelers due to its shallower learning curve.

Driving the hydrological processes in the program is a computational engine that routes excess runoff through a series of sub-catchments, links, nodes, weirs, storage devices and pumps. The engine tracks water quality as well as quantity throughout the constructed model. More details of the internal components of the program are discussed in the following sections below.

SWMM is capable of modeling system networks of very large complexities. Channels can be modeled as either opened or closed systems with a variety of size and shapes that the user may input manually or select from predefined list. Generally a system is comprised of various orifices, weirs, storage/treatment units, flow dividers and pumps. The program is able to handle all of prior network components using an array of predefined objects located in the interface.

Flow can be routed with three separate user defined methods. These include steady-state, kinematic wave and full dynamic wave. The user must select a routing method based on the system and outcomes they wish to achieve. For example, if the user selects the full dynamic routing method, the program will take in consideration effects from backwater, surcharging and reverse flow in the model. Each routing method provides its own unique advantages and are discussed in more detail later in this section.

3.3.2 Internal Mechanisms

The underlying computational engine of *SWMM* uses physically-based information to simulate the hydrological processes discussed in the following pages. Principles of conservation of mass, energy and momentum are used to account for the transport of water, contaminants or sediments through the model. This allows the model to accurately and effectively simulate runoff quantity and storm water quality through the system. Presented in this subsection is background into the algorithms and theory which *SWMM* uses to simulate the hydrological processes.

Surface Runoff

Figure 3.31 presents a conceptual view of the surface runoff process used by the computational engine of *SWMM*. It illustrates the various components, treated as non-linear reservoirs, that water contaminants or sediments travel through once they have been delivered to the sub-catchment by rainfall or another upstream catchment. These components include infiltration, evaporation and surface runoff. No matter how water is delivered to the sub-catchment it is first collected as maximum depression storage. This includes the catchments abstractions such as ponding, surface wetting and interception.

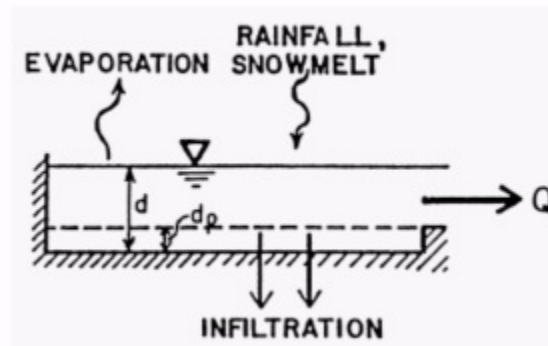


Figure 3.31: Conceptual view of *SWMM*'s runoff mechanism, (Rossman and Supply, 2005)

Then once this component has reach full capacity, surface runoff begins. Runoff is routed according with Manning’s equation, Equation 3.17. The depth of surface runoff is updated with time by use of a water balance equation.

$$Q = \frac{1}{n}AR^{\frac{2}{3}}\sqrt{S} \quad (3.17)$$

Where:

- n is the Manning’s roughness
- A is the area of channel cross section
- R is the hydraulic radius
- S is the slope of channel from one node to the next

Infiltration

Water that is lost from the sub-catchment components of *SWMM* is generally in the form of infiltration. As the precipitation begins to fall into the sub-catchment, it is percolated through the unsaturated soil zone of the pervious area. To model this phenomena *SWMM* offers three choices from which the user can select from. These include the Horton’s, Green-Ampt’s and Curve Number methods. However, Horton’s method was selected for use in this investigation and is descried in detail below. Further details on the other methods can be found in Rossman and Supply (2005).

Horton’s Equation:

The Horton’s infiltration method is simply based on empirical observations which show that infiltration decreases as an exponential function from the maximum to minimum rate over a rainfall event, see Equation 3.18. The most difficult inputs for this type of infiltration are initial infiltration or maximum infiltration f_o and the decay constant k . They dictate the initial infiltration or maximum rate and the rate at which the infiltration will decay over

the rainfall period. It is critical to get the closest estimates as possible. Values are usually found in literature defined by soil characteristics or derived from experimental test.

$$f_p = f_c + (f_o - f_c)e^{-kt} \quad (3.18)$$

Where:

- f_t is the infiltration rate at time (t)
- f_o is the initial maximum infiltration rate
- f_c is the final or constant infiltration rate once the soil column has become fully saturated
- k is the decay constant specific to each soil type

SWMM applies a modified version of Equation 3.18 that is represented below in Equation 3.19. The modifications help to account for the recovery of infiltration capacity during dry or no surface ponding time periods within a continuous simulation. These modifications were created by *SWMM* developers and Figure 3.32 shows the approach they followed. Values of k_d are assumed constant or a scaled value of k from Equation 3.18.

$$f_p = f_o - (f_o - f_c)e^{-k_d(t-t_w)} \quad (3.19)$$

Where:

- k_d is a decay coefficient for the recovery curve
- t_w is a hypothetical projected time at which $f_p = f_c$ on the recovery curve

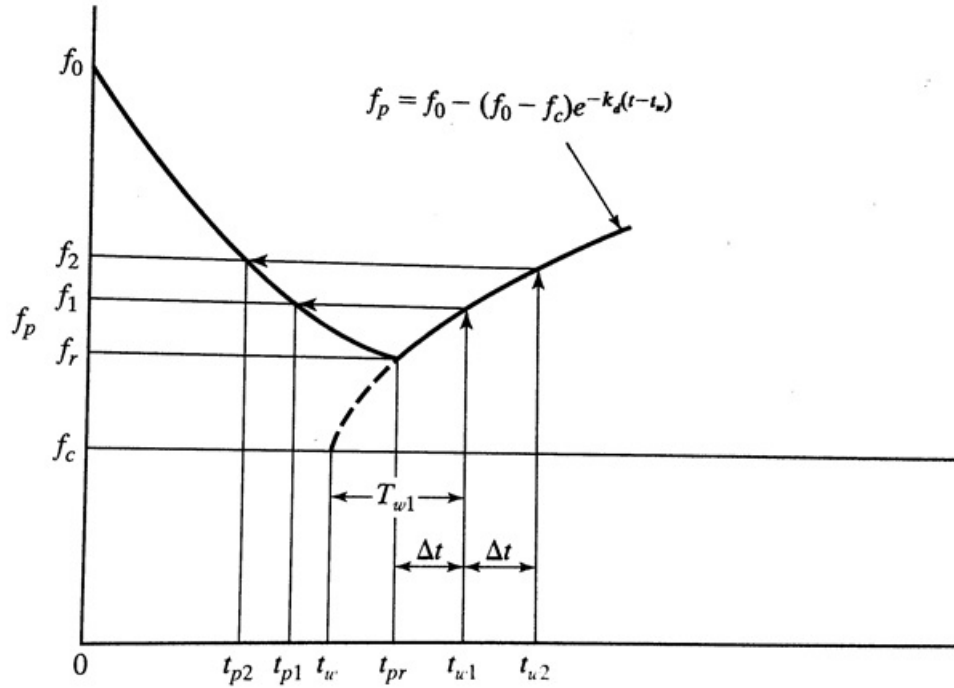


Figure 3.32: Conceptual view of Horton's infiltration capacity recovery mechanism used in *SWMM*'s computational code, (Viessman et al., 2003)

Groundwater

SWMM uses a two-zone groundwater component to model subsurface flows. These two compartments consist of the upper unsaturated and the lower fully-saturated zone. The main difference between the two being that the saturated zone is assumed to have a constant moisture content and is equal to the soil porosity ϕ . However, the upper zone has a variable moisture content of θ . Each area shown in Figure 3.33 is representing the flux per unit area and each one is described below.

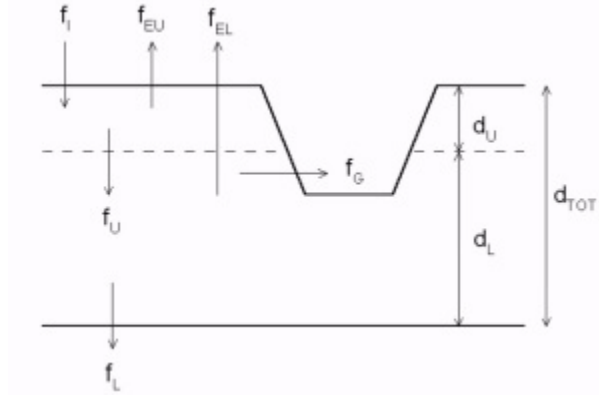


Figure 3.33: Conceptual view of *SWMM*'s groundwater mechanism, (Rossman and Supply, 2005)

Where:

- f_I is the infiltration from the surface
- f_{EU} is the evapotranspiration from the upper zone, defined as a fixed fraction of the un-used surface evaporation
- f_U is the percolation between the upper and lower zones, dependent on the upper zone θ and the depth d_U .
- f_{EL} is the evapotranspiration from the lower zone, function of the depth d_U
- f_L is the percolation from the lower zone to deep groundwater, function of lower zone depth d_L
- f_G is the lateral groundwater interflow to the drainage system, function of d_L and channel/node water depth
- d_{TOT} is the total distance of the upper zone d_U depth and lower zone depth d_L

In order to link the sub-catchment and aquifer component of *SWMM* Equation 3.20 is implemented. Using the coefficients (A1, A2, B1, B2 and A3) the user is able to defined the rate of groundwater flow between the aquifer and receiving node. If the user wishes to model the surface groundwater interaction as a simple proportional relationship then exponents (B1 and B2) should be set to 1. Also, the coefficients (A2 and A1) should be equal and A3

should be set to zero.

$$Q_{gw} = A1(H_{gw} - E)^{B1} - A2(H_{sw} - E)^{B2} + A3H_{gw}H_{sw} \quad (3.20)$$

Where:

- Q_{gw} is the groundwater flow
- H_{gw} is the elevation of groundwater table
- H_{sw} is the elevation of the surface water at receiving node
- E is the elevation of receiving node invert

Flow Routing

Flow routing takes place within the conduits of the *SWMM* model and between nodes. It is governed by the conservation of mass and momentum equations for gradually varied, unsteady flow. The user is given three choices with which to run their models, including the steady flow, kinematic wave and dynamic wave routing methods.

Steady flow routing represents a uniform and steady assumption within each computation time step. The flow hydrograph inputted into each upstream node is assumed to route with no delay or change in shape. Using the Manning equation a relationship between flow rate and flow is formed. There are many limitations with this routing selection including channel storage, backwater effects, entrance/exit losses, flow reversal or pressurized flow. Using this method is only advised for preliminary analysis for long-term simulations and it is only valid for networks where each node has only one outflow link. More detail is provided in Rossman and Supply (2005).

Kinematic wave routing solves the continuity equation as well as a simplified form of the momentum equation between each node through the conduits. This simplification of the momentum equation includes an assumption that the flowing waters surface is equal with the conduits bed slope. Under these assumptions the maximum flow that can be routed is

constrained to the full-flow Manning equation value. If the water surface level is above this, then it is either lost or ponded atop of the inlet node. The latter allows water to re-enter the system once surface levels have subsided and reducing the amount of water lost in the system. Under this selection, the model is limited to a system that is represented by nodes that only have a single outlet conduit.

This method allows for the modeling of a flow that varies both spatially and temporally which can depict delays in outflow hydrographs from inflow hydrographs. However, it is not able to simulate the effects from backwater, entrance/exit losses, flow reversal or pressurized flow. One great feature of this method is relative stability of the code. Users can apply this method to long-term simulations with a temporal scale in the range of 5-15 minutes. More detail is provided in Rossman and Supply (2005).

The dynamic wave routing method within *SWMM* solves the 1-D depth averaged momentum and continuity equations referred to as the complete 1-D Saint Venant equations, see Equations 3.21 - 3.22. The Saint Venant terms are solved along each component of a computational cell, over a network of junctions and conduits that represents the physical characteristics.

$$\frac{\partial A}{\partial t} + \frac{\partial Q}{\partial x} = 0 \quad (3.21)$$

$$\frac{\partial Q}{\partial t} + \frac{\partial(\frac{Q^2}{A})}{\partial x} + gA \frac{\partial H}{\partial x} + gA(S_f + h_L) = 0 \quad (3.22)$$

Where:

- Q is the flow rate through the conduit
- x is the length of the conduit
- H is the hydraulic head of water in the conduit
- A is the cross sectional conduit area
- t is the simulation time

- S_f is the friction slope
- h_L is the local energy loss per unit length of conduit
- g is the acceleration of gravity

This method allows the user to represent more interesting and realistic scenarios which may occur within the system. For example, if a closed pipe system is the subject of modeling, then pressurized flows which can exceed predictions from the full flow Manning equation value are able to be simulated. Another key feature with the dynamic wave routing method is its ability to simulate channel storage, backwater, entrance/exit losses and flow reversal. This is particularly important when the system includes various orifices or weirs that may cause significant constrictions on the flow. Finally, this method allows the user to simulate systems with any configuration of loops or multiple downstream diversions. However, the drawback of this flexibility comes with the smaller time steps and greater computation effort is needed to maintain numerical stability.

3.3.3 Interface Objects

Within *SWMM* are two types of interface objects that can be implemented into a model. These consist of the visual and non-visual objects. Visual objects of *SWMM* include the components which represent the physical environment experienced at the region of interest. Non-visual objects in *SWMM* include components of the hydrological cycle as well as the inputs time series that drive many of the processes of simulations. They are components that have tremendous impacts in model results; insight and engineering judgment are paramount in their definition. Parameters and data inputs for both types of objects can be sourced directly from local field studies or literature studies on sites of similar description. This subsection does not cover the objects available within *SWMM*'s interface but an in-depth discussions can be found in the *SWMM*'s Users Manual, Rossman and Supply (2005).

3.4 SWMM Model Development

Initially WS-AGC was divided into 7 sub-catchments conforming to the local topography. As the model began developing, the need for additional discretization to depict diverse geophysical characteristics was recognized. To do this the original 7 sub-catchments were broken down into smaller sections, 15 in total. Each new sub-catchment was selected based on soil types predicted from the NRCS/USDA soil survey Figure 3.34.

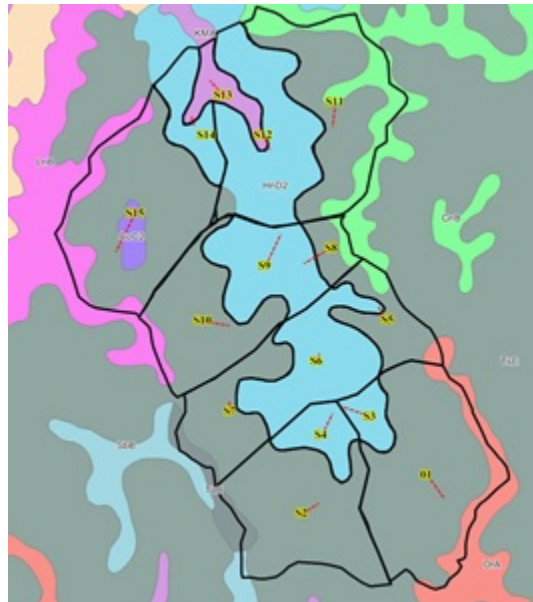


Figure 3.34: Discretized Sub-Catchments based on topography and soil types for WS-AGC

Geographic Information Systems (GIS) were then used to improve the accuracy of physical input parameters such as sub-catchment area, slope, channel lengths and storage reservoirs. Main channel locations and lengths were also established from a 10 m DEM provided by the USGS online data website (<http://ned.usgs.gov/>) and manipulated with ArcGIS software. These terrain features were then confirmed from field investigations. Channel cross sections were input as irregular shapes (transects) determined from field survey measurements, see figure 3.35. The cross sections were chosen while walking the streams at

WS-AGC. A survey was completed to use as model input at locations where major transitions occurred. With such detailed site-specific information, a well-built foundation for the initial stages of modeling was created.



Figure 3.35: Surveying a downstream cross section

As model setup continued, estimations of more subjective parameters became necessary. This included Manning roughness (n) for channel/overland flows, depression storage, minimum/maximum infiltration rates, saturated hydraulic conductivity and field capacity. These were estimated based on published values from literature and insights obtained from several field visits , Table 3.5.

Table 3.5: Literature values of maximum and minimum infiltration rates for Horton Equation, (Akan, 1993)

Soil Type	Maximum (Initial) Infiltration	
	(in/hr)	(mm/hr)
Dry sandy soils with little or no vegetation	5.0	127
Dry loam soils with little or no vegetation	3.0	76.2
Dry clay soils with little or no vegetation	1.0	25.4
Dry sandy soils with dense vegetation	10	254
Dry loam soils with dense vegetation	6.0	152
Dry clay soils with dense vegetation	2.0	51
Moist sandy soils with little or no vegetation	1.7	43
Moist loam soils with little or no vegetation	1.0	25
Moist clay soils with little or no vegetation	0.3	7.6
Moist sandy soils with dense vegetation	3.3	84
Moist loam soils with dense vegetation	2.0	5.1
Moist clay soils with dense or no vegetation	0.7	18

Soil Type	Minimum (Asymptotic) Infiltration Capacity, F_c	
	(in/hr)	(mm/hr)
Clay loam, silty clay loam, sandy clay, silty clay, clay	0.00 - 0.05	0.00-1.3
Sandy clay loam	0.05 - 0.15	1.3 - 3.8
Silt loam, loam	0.15 - 0.30	3.8 - 7.6
Sand, loamy sand, sandy loam	0.30 - 0.45	7.6 - 11.4

Results from the USDA/NRCS web soil survey assisted with determining the range of values for each sub-catchment infiltration parameters, Table 3.6. These ranges provided flexibility when performing the model calibration; more discussion is provided ahead.

Stream beds at the site have many abstractions including vegetal debris, partial obstructions and pooling areas where flow is subjected to large head losses and varying flow conditions. Manning equation within *SWMM* uses n values (roughness) that provide flow frictional losses. Thus a single value of n for each conduit had to be estimated to represent the complex nature of the channels. Mannings n values used for channels simulation ranged from 0.04 to 0.4, following Rossman and Supply (2005). Such values are consistent with natural channels of irregular sections with pools and having a vegetation cover.

Sub-catchments estimates for overland flow roughness, depression storage and sub-catchment width were mostly obtained with published values and further modeling assumptions, (Rossman and Supply, 2005). Mannings n values for overland flow were estimated as 0.8, following McCuen et al. (1996) estimation for dense underbrush in wooded regions. The depression storage value of 7.62 mm (1/4 in) was adopted from the recommended first estimate value in *SWMM 5 Users Manual*, (Rossman and Supply, 2005). To calculate each sub-catchments width an initial assumption is made that the overland sheet flow will not occur more than 150 m before reaching or transitioning to channelized flow.

To distinguish individual runoff events from observed data the minimum inter-event time was selected as six hours and each event's peak discharge must meet a minimum peak flow rate of $0.1 \text{ m}^3/\text{s}$; any event below this was not considered in the study. In addition, various events were extended as needed since water levels in the stream fluctuated during the lower portion of the recession curve. This caused readings of water level to dip above and below the required 6.1 cm of head required for flow to fully develop over the weirs, (Dodge, 2001).

Results from groundwater monitoring in the well positioned in and outside of the stream bed, presented in Figure 3.36, motivated the inclusion of the aquifer component of *SWMM*. Blue bars in the top chart correspond to rainfall intensity, whereas the blue line in the lower chart correspond to the average accumulated rainfall depth measured by the rain gauges deployed in the site. The red lines in both charts correspond to groundwater elevation, and the interruption corresponds to a period of malfunction described earlier on page 35 groundwater observation wells.

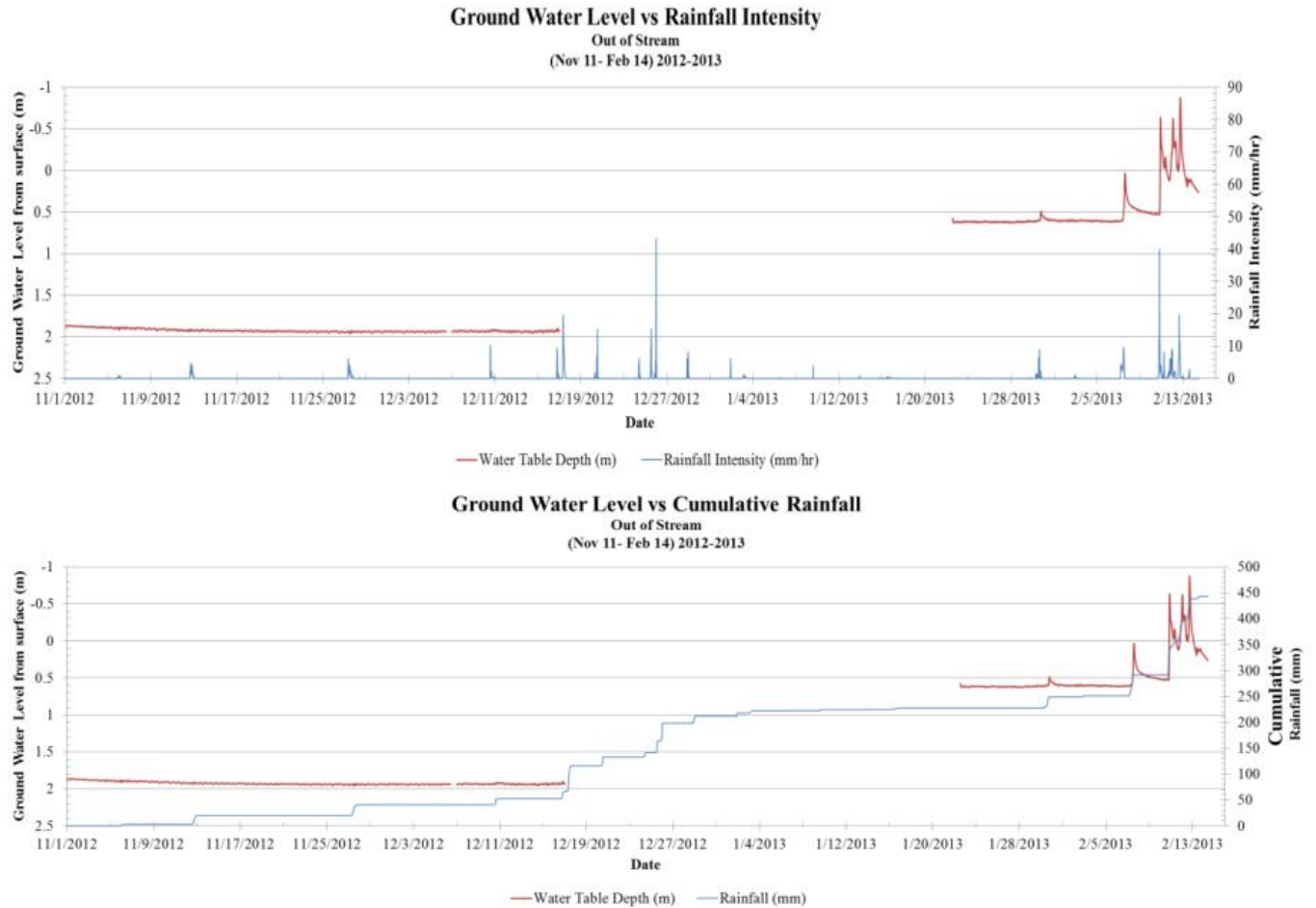


Figure 3.36: Shallow ground water level relative to the surface for the out of stream observation well

Despite of the interruption on the groundwater level measurement, it can be noticed that the initial rain events up to December 19, 2012 have not resulted in any significant changes in the groundwater level. Then after the damage was fixed the groundwater level was much larger, and at that point connected to the stream. As is shown, even small rain events caused measurable and immediate increase in the groundwater level. This dramatically contrasts with the earlier condition, which seems to indicate that the groundwater is disconnected from the stream. Such complexities of interflow and its ability to produce longer recession curves in the wet season made the groundwater module a key addition to *SWMM* modeling.

3.5 Model Calibration

Calibration for the developed *SWMM* models was completed using nine separate recorded rainfall-runoff events from 06/11/2012 to 02/14/2013. This time frame provided data from the below average rainfall year, 2012, and the beginning of the above average wet year, 2013. As mentioned, events were distinguished by inter-event periods of at least six hours and a minimum peak flow rate of $0.1 \text{ m}^3/\text{s}$. The calibration between observed and computed rainfall-runoff events was conducted using the Sensitivity-based Radio Tuning Calibration (SRTC) function of *PCSWMM*. During this process eight parameters were adjusted, limiting their uncertainty rankings to $\pm 40\%$ and below, with nine individual runoff events. The eight calibration parameters can be found in Tables 3.6 and 3.8. Calibration efforts using these guidelines included observed events during the dry season (May-November) and wet season (December-April). Following the work of Davis et al. (2007), peak flow rates were examined in addition to flow duration curves for each model configuration. Both comparisons provided calibrated models with respect to peak flow conditions as well as the more challenging issue of flow volumes.

The SRTC tool works by designating uncertainty percent rankings for each parameter of interest. For efficient calibration, first estimates of the model parameters should be as close as possible to the true value (James et al., 2002). Also, James et al. (2002) suggests that percent rankings should be limited to $\pm 50\%$ as an absolute maximum. This insures that calibration parameters will not become arbitrary values outside of meaningful range for the area of interest, (AOI). Another important aspect to calibration is having a sufficient amount of rainfall-runoff events for the number of parameters of interest. James et al. (2002) points that the amount of calibration parameters must be limited to the amount of individual rainfall-runoff events observed and selected for calibration. Following this rationale a total of nine separate observed rainfall-runoff events were used to calibrate eight parameters. In all events, the hydrograph obtained at the downstream (Cipoletti weir) was used as observed reference data.

Horton’s method was selected to model the infiltration at the site. The four main input parameters include maximum infiltration rate, minimum infiltration rate, decay constant and drying time. The most sensitive of the four infiltration parameters included minimum/maximum infiltration rate and decay constant. Each sub-catchment was assigned an average of the maximum and minimum infiltration rate based on a range found from examining the local soil types. These values were provided from Akan (1993) and are seen in the previous subsection, Table 3.5. Estimates for decay constants and drying times were made from an average of the range provided by the *SWMM* 5.0 Users Manual, (Rossman and Supply, 2005). During the early stage of calibration the drying time was found to have minimal effect on the results so it was fixed at the maximum value of 8 days.

The calibrated infiltration parameters of maximum/minimum infiltration rates and decay constants were limited to $\pm 40\%$ of the original estimate. Large diversity in soil types observed in the field led to the assumption that this approach would provided enough flexibility while keeping infiltration parameter values within a reasonable range. Ranges of values used for Horton’s infiltration method are shown in Table 3.6.

Table 3.6: Minimum and maximum ranges used for Horton’s infiltration input parameter, (Akan, 1993) and (Rossman and Supply, 2005)

Soil Type	f_o		f_c		DC		DT	
	Min.	Max.	Min.	Max.	Min.	Max.	Min.	Max.
KMA	127	254	7.6	11.4	2	7	2	14
TSE	76	254	3.8	7.6	2	7	2	14
HnD2	51	152	0.0	1.3	2	7	2	14

Where:

- f_o is maximum infiltration rate (mm/hr)
- f_c is final/minimum infiltration rate (mm/hr)
- DC is decay constant
- DT is Drying time (days)

Multiple attempts were conducted to calibrate a *SWMM* model without using the aquifer component. However, these calibration efforts did not result good agreement between modeled and observed hydrographs. This became the main justification to implement the aquifer component of *SWMM*. More calibration parameters were introduced with respect to the groundwater component including bottom groundwater elevation, saturated hydraulic conductivity, field capacity and conductivity slope. The range of tested values for calibration parameters were derived from Table 3.7, (Rossman and Supply, 2005). Note that no changes were implemented in the calibrated values for sub-catchment inputs with the introduction of the groundwater components.

Table 3.7: Aquifer properties for various soil types, taken from (Rossman and Supply, 2005)

Soil Texture Class	Hydraulic Conductivity (mm/hr)	Porosity (fraction)	Field Capacity (fraction)	Wilting Point (fraction)
Sand	120.4	0.437	0.062	0.024
Loamy Sand	29.97	0.437	0.105	0.047
Sandy Loam	10.92	0.453	0.19	0.085
Loam	3.30	0.463	0.232	0.116
Silt Loam	6.60	0.501	0.284	0.135
Sandy Clay Loam	1.52	0.398	0.244	0.136
Clay Loam	1.02	0.464	0.31	0.187
Silty Clay Loam	1.02	0.471	0.342	0.21
Sandy Clay	0.508	0.43	0.321	0.221
Silty Clay	0.508	0.479	0.371	0.251
Clay	0.254	0.475	0.378	0.635

During calibration involving aquifer components the SRTC was not able to handle the values of bottom groundwater elevation, so a series of trial and errors had to be performed for each individual aquifer component. The lack of field data with respect to the location of the aquifer's bottom elevation and the variability of site conditions rendered this value somewhat arbitrary. Designer's must use personal judgment to remedy each components bottom depth. *PCSWMM* sets a default value of 10 for the conductivity slope and during

calibration slight tuning of this value provided a better fit between observed and computed hydrograph recession periods.

Lastly, ranges for saturated hydraulic conductivity, porosity, field capacity, and wilting point values were determined based on soil types and texture classes from Table 3.7. These ranges are presented in Table 3.8. First inputs values were based on average values in order to provide a comprehensive description of the AOI. SRTC was then used with percent rankings limited to $\pm 40\%$ and below to insure results would fall within the prescribed ranges. After the fine tuning of input values, results across the entire spectrum became much more satisfactory with the introduction of the aquifer component.

Table 3.8: Minimum and maximum ranges used for aquifer component input parameter, (Rossman and Supply, 2005)

Soil Type	K		ϕ		FC		WP	
	Min	Max	Min	Max	Min	Max	Min	Max
KMA	10.92	120.4	0.437	0.453	0.062	0.19	0.024	0.085
TSE	6.6	29.7	0.453	0.501	0.232	0.284	0.085	0.135
HnD2	0.254	1.52	0.398	0.475	0.244	0.378	0.136	0.635

Where:

- K is hydraulic conductivity (mm/hr)
- ϕ is soil porosity
- FC is field capacity
- WP is wilting point

Chapter 4

Results and Discussion

As previously stated, field data has been collected at WS-AGC since February 4th, 2012, and the following sections present and discuss such data collected until August 2013. Also included are results from temperature based evapotranspiration calculations and soil analysis performed on cores samples taken at the potential embankment centerline. These allowed for calibration/verification of the *SWMM* modeling efforts.

4.1 Collected Field Data

4.1.1 Precipitation

The local precipitation at WS-AGC was collected from February 4th, 2012 until August 14th, 2013. Presented in Figure 4.1 are the rainfall events ($\frac{mm}{hr}$) experienced at the site during this study. Notable rain events include May 14th, July 3rd, September 3rd, December 25th, February 10th, April 11th, July 23rd, July 30th and August 14th, 2012 to 2013 respectively. These events all produced rainfall intensities of at least $40 \frac{mm}{hr}$ and up to a maximum of $78 \frac{mm}{hr}$. Though these events had comparatively short duration, they produced significant volumes of precipitation. For example, the September 3rd, 2012 event produced a rainfall intensity of $80 \frac{mm}{hr}$ lasting 30 minutes. This event alone produced a total volume of approximately $116,000 m^3$ of water over the entire site.

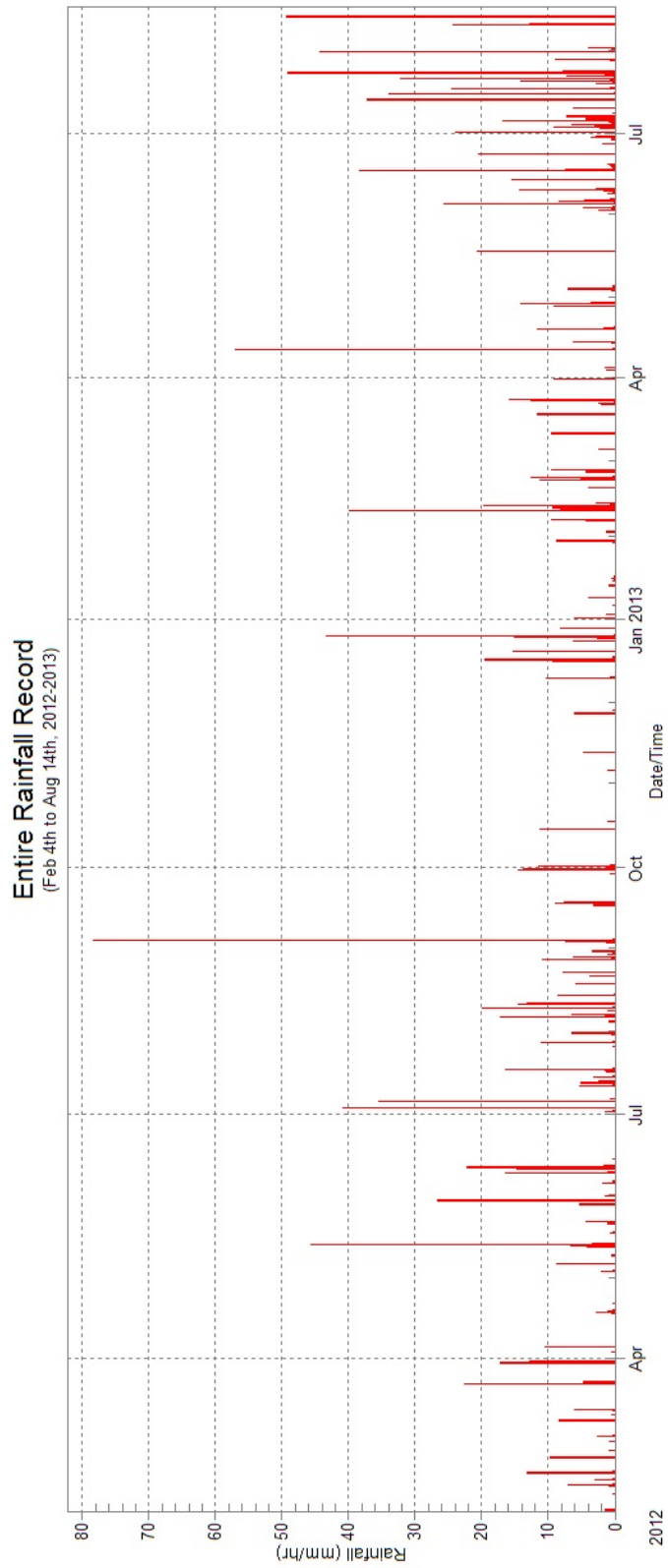


Figure 4.1: Rainfall recorded at WS-AGC (February 4th - August 14th, 2012-2013)

While conducting this study two off-site gauges were used as quality control. Each gauges location relative to WS-AGC is shown in Figure 4.2. Furthest north from WS-AGC was the Seale 1.4 W station and opposite was the Eufaula Wildlife Refuge station. Presented in Figure 4.3 is a comparison between monthly rainfall totals from all gauges used in this study. The three on-site gauges show very close agreement throughout the study as expected. Slight variations in total recorded rainfall were most likely caused by non-uniform rainfall events passing over WS-AGC. Examining the two off-site gauges, a tendency of larger fluctuations is seen through the study period. This difference was most likely caused from the 15.2 and 17.5 km distance each off-site gauge was North and South respectively from WS-AGC. However, these gauges produced rainfall amounts which remained comparable in magnitude with on-site observations.



Figure 4.2: Off-site rain gauges used as quality control)

**February- July 2012-2013
(Onsite vs Offsite Monthly Rainfall Totals)**

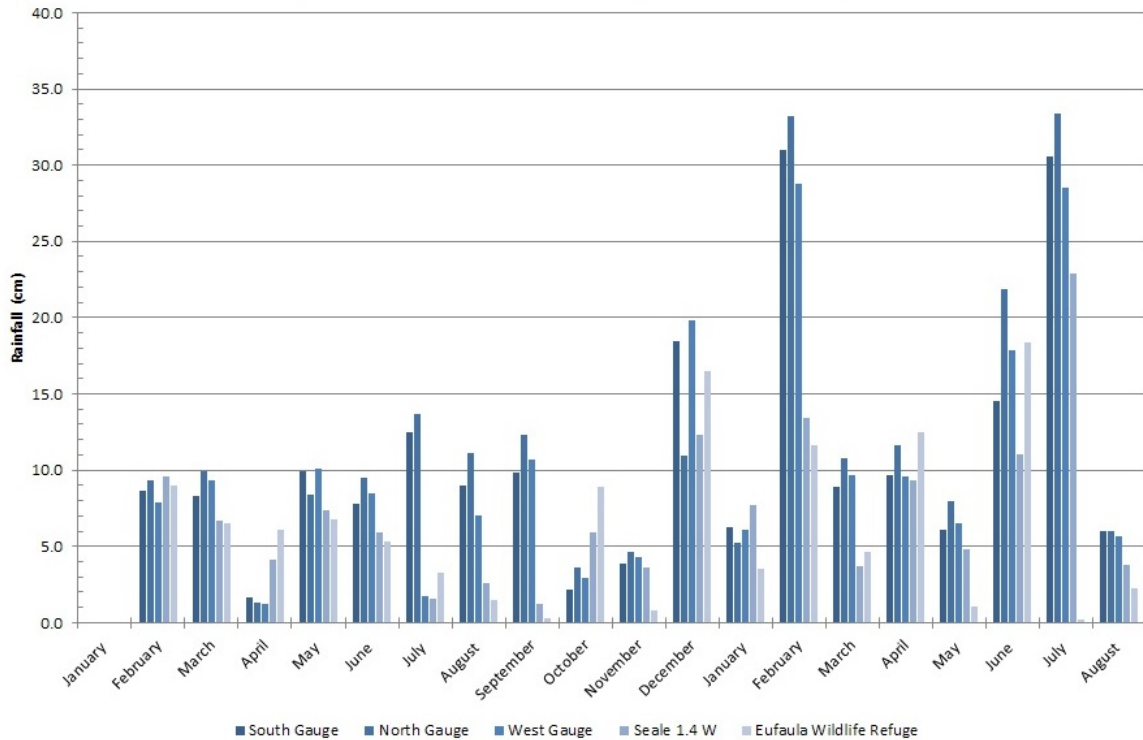


Figure 4.3: Onsite vs off-site monthly rainfall totals (February 4th - August 14th, 2012-2013)

In Table 4.1 statistics for the longest period of locally recorded rainfall during 2012 is presented. With a rainfall total of 924.2 mm over the 11 month period, the amount comes in 263 mm less than the normal yearly total for this area, shown in Table 4.3. If the January normal rainfall from Table 4.3 was added to this total, the yearly precipitation for 2012 would still fall 165 mm below the yearly average for the area. With this observation, 2012 can be considered as a below average rainfall year.

Table 4.1: Rainfall statistics for (February 4th - December 31st, 2012)

	System
Maximum Rainfall (mm/hr)	78.36
Minimum Rainfall (mm/hr)	0
Mean Rainfall (mm/hr)	0.1156
Duration of Exceedances (hrs)	7999
Duration of Deficits (hrs)	7638
Number of Exceedances	1
Number of Deficits	251
Volume of Exceedances (mm)	924.2
Volume of Deficits (mm)	0
Total Rainfall (mm)	924.2

Now examining Table 4.2, total rainfall for the 8.5 month period is 1144 mm. Just 43 mm below the yearly average total with 3.5 months left in the year. If normal rainfall totals from Table 4.3 were added to this current amount, then yearly rainfall for 2013 would be approximately 1548 mm. This results in yearly rainfall exceeding yearly average by 361 mm. However, with 3.5 months of missing data it's impossible to determine what the actual rainfall total will be since there are many other factors to consider. Even with unpredictability of the last few months of precipitation it is likely that 2013 will have rainfall precipitation above an average year.

Table 4.2: Rainfall statistics for (January 1st - August 14th, 2013)

	System
Maximum Rainfall (mm/hr)	56.96
Minimum Rainfall (mm/hr)	0
Mean Rainfall (mm/hr)	0.2109
Duration of Exceedances (hrs)	5426
Duration of Deficits (hrs)	4987
Number of Exceedances	1
Number of Deficits	226
Volume of Exceedances (mm)	1144
Volume of Deficits (mm)	0
Total Rainfall (mm)	1144

Table 4.3: Normal Monthly Rainfall Totals (Period of Record 1981-2010)-Location: Columbus, GA (Airport)

Normal Monthly Rainfall Totals (Period of Record 1981-2010)-Location: Columbus, Ga													
Type	January	February	March	April	May	June	July	August	September	October	November	December	Average Yearly Total
Normal Rainfall (in)	3.9	4.4	5.5	3.6	3.2	3.7	4.8	3.8	3.1	2.6	4.1	4.3	47
Normal Rainfall (mm)	97.8	112.8	138.7	90.2	81.0	94.5	120.9	95.8	77.7	65.5	104.1	108.5	1187

Source: NOAA

Average monthly rainfall data recorded at each rain gauge in WS-AGC is presented in Table 4.4. As mentioned previously local rainfall data was not available for January 2012 and for the full duration of August 2013. These periods are acknowledged as N/A in Table 4.4. Data provided from the west gauge during July and August 2012 was much lower when compared to the other two locations. This was due to a malfunction in the recording device and it was taken offline for repairs for a period of time.

A closer look at this table indicates that in September and December 2012 each gauge has recorded rainfall over the long term averages. On the contrary February to April and October to November 2012 have seen precipitation totals well below long term averages.

Data in 2013 has shown a complete different picture for monthly rainfall totals. August of this year will not be considered in this discussion since data was only recorded through half the month. With this consideration January, March and May are the only months which have seen a significantly lower than long term average rainfall. These three months showed monthly percent difference ranging from 0.9 to 44.4 percent lower than long term averages, Table 4.5. Each of the remaining months have seen rainfalls ranging from 5.3 to 194.6 percent larger monthly rainfall totals, as presented in Table 4.5.

Table 4.4: Monthly rainfall average and yearly totals for (February 4th - July 31st, 2012-2013)

Onsite Rainfall vs Normal Monthly Rainfall														
Type	January	February	March	April	May	June	July	August	September	October	November	December	Average Yearly Total	
2012	North Gauge (mm)	N/A	93.40	99.20	13.20	83.80	94.60	136.60	110.80	123.00	36.00	46.60	109.80	947
	South Gauge (mm)	N/A	86.20	83.40	16.20	99.20	77.60	124.60	89.80	98.80	21.60	38.60	184.80	921
	West Gauge (mm)	N/A	78.60	93.20	12.20	100.60	84.80	17.60	70.60	106.60	29.20	42.80	197.80	834
2013	North Gauge (mm)	52.00	332.20	107.80	116.00	80.00	219.00	334.20	N/A	N/A	N/A	N/A	N/A	1241
	South Gauge (mm)	62.80	310.00	88.60	96.80	61.00	145.20	306.00	N/A	N/A	N/A	N/A	N/A	1070
	West Gauge (mm)	61.00	288.00	96.60	96.20	65.40	178.20	285.60	N/A	N/A	N/A	N/A	N/A	1071
Normal Rainfall (mm)	97.8	112.8	138.7	90.2	81.0	94.5	120.9	95.8	77.7	65.5	104.1	108.5	1187	

Table 4.5: Percent differences between monthly rainfall average (February 4th - July 31st, 2012-2013)

Percent Difference of Onsite Rainfall vs Normal Monthly Rainfall													
Type		January	February	March	April	May	June	July	August	September	October	November	December
2012	North Gauge (mm)	N/A	-17.2	-28.5	-85.4	3.4	0.1	13.0	15.7	58.3	-45.1	-55.3	1.2
	South Gauge (mm)	N/A	-23.6	-39.9	-82.0	22.4	-17.9	3.1	-6.2	27.1	-67.0	-62.9	70.4
	West Gauge (mm)	N/A	-30.3	-32.8	-86.5	24.2	-10.3	-85.4	-26.3	37.2	-55.4	-58.9	82.4
2013	North Gauge (mm)	-40.6	194.6	-22.3	28.6	-1.3	131.8	176.4	148.8	-48.5	N/A	N/A	N/A
	South Gauge (mm)	-31.0	174.9	-36.1	7.4	-24.7	53.7	153.1	116.8	-53.9	N/A	N/A	N/A
	West Gauge (mm)	-32.6	155.4	-30.3	6.7	-19.3	88.6	136.2	140.8	-55.0	N/A	N/A	N/A

4.1.2 Temperature

The local temperature data recorded at WS-AGC has been collected from February 2012 to August 14th 2013. Throughout the period of record there have been several equipment malfunctions. Therefore, off-site records from the Columbus, GA airport (40 km away from WS-AGC) were obtained through the National Oceanic and Atmospheric Administration (NOAA) online data sets. Figure 4.4 depicts that recorded data from Columbus, GA airport which was used in this study. Red bars indicate normal monthly temperatures found from a 29 year period of record (1981-2010) taken at the Columbus, GA airport (NOAA) and gray bars represent daily average temperatures at the same location over the course of this study.

Examining daily temperatures in Figure 4.4 a few instances in which the daily recorded temperature has spiked well above the monthly average are seen. These have occurred during January, February and January, 2012 to 2013 respectively. Where daily temperatures have spiked from 5 to 13 degrees warmer than average.

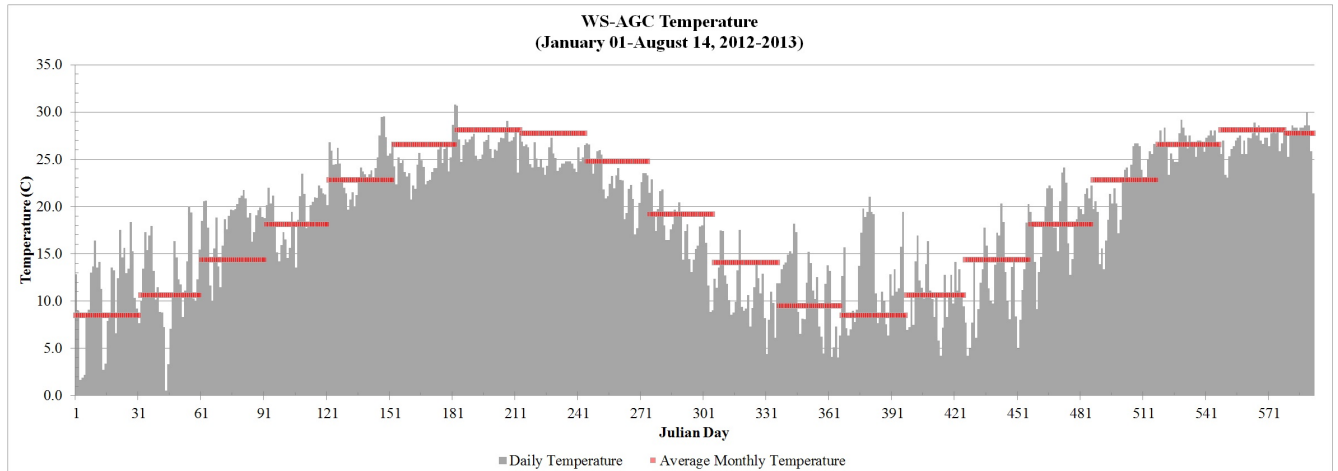


Figure 4.4: Temperature recorded at Columbus, GA Airport (January 1st - August 14th, 2012-2013)

Table 4.6 displays the monthly average temperatures along with the 29 year averages taken at the Columbus, GA airport. Columbus’s monthly temperature averages during the period of study have not shown any major fluctuations from the long term averages. However, an interesting observation occurs during the 2012 records. Temperature stayed slightly above average for the first five months of the study. Besides this slight over average time frame the collection of data shows that the study site did not experience any major outlying points with respect to monthly temperature. In fact, the period of study has indicated that long term normal monthly average temperatures could be applied for short-term studies.

Table 4.6: Monthly Recorded Temperatures vs Normal Monthly Temperatures (Period of Record 1981-2010)-Location: Columbus, GA Airport

Monthly Recorded Temperatures vs Normal Monthly Temperatures												
Location	January	February	March	April	May	June	July	August	September	October	November	December
Columbus, GA-2012 (°C)	11.1	12.7	19.3	19.9	24.5	26.3	29.0	27.0	24.9	19.4	13.2	12.3
Columbus, GA-2013 (°C)	13.1	10.7	12.1	18.7	21.9	26.7	26.7	28.1	-----	-----	-----	-----
Columbus, GA (°C)	8.4	10.6	14.3	18.1	22.8	26.6	28.1	27.7	24.7	19.2	14.1	9.5

Source: NOAA

4.1.3 Potential Evapotranspiration (PET)

As stated in the previous chapter, PET was a parameter that needed to be indirectly computed as an input data for the *SWMM* watershed model. This calculation was developed using two separate well-known, temperature based PET methods. After examining Lu et al. (2005) and Sun et al. (2002) studies on watershed hydrology and PET methods, it was anticipated that Hamon's method would produce accurate PET data.

Lu et al. (2005) showed that when comparing advanced radiation-based PET methods (i.e., Turc (1961), Makkink (1957) and Priestley and Taylor (1972)) to temperature-based methods, Hamon's method produced the highest coefficients of correlation. This study has also shown two temperature based PET methods, Thornthwaite and Hamon, to have the highest correlation coefficient (R) value of 1.0, (Lu et al., 2005). Hargreaves-Samani method produced the lowest correlation with ($R \leq 0.89$) between the three temperature PET strategies, (Lu et al., 2005). The latter was selected as the second calculation alternative for PET.

Figure 4.5 shows daily PET (mm/day) calculations performed using both methods previously discussed. As seen the Hamon method has produced daily PET values which are significantly higher than the those produced from the Hargreaves method. However, both methods have a tendency to follow the same patterns throughout the year. Trends show lower PET values during the colder shorter Winter days and higher PET values during the warmer longer Summer days.

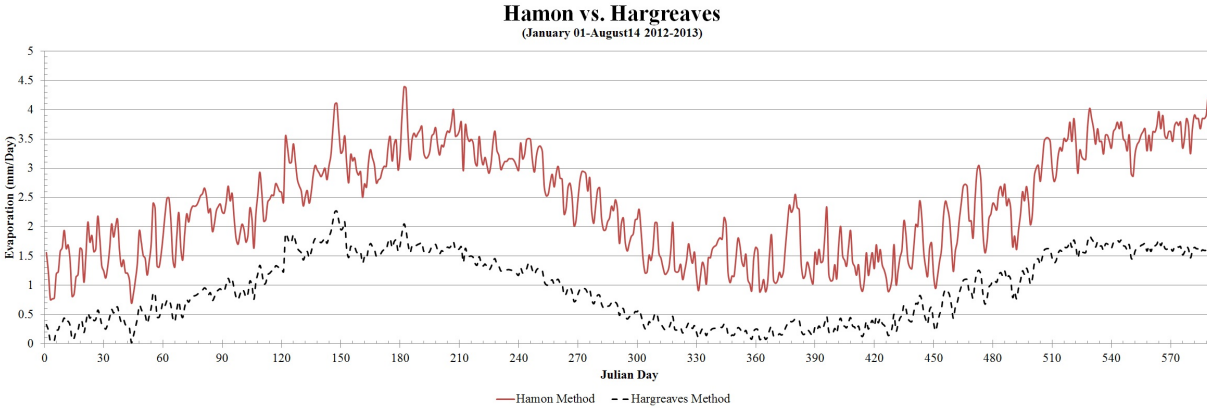


Figure 4.5: PET calculations using Hamon’s and Hargreaves Methods

In Table 4.7 the full yearly 2012 total for PET from both PET methods used in this study are shown. Since 2013 data was only available until August 14th and not an entire year it can’t be included in this table. The Hargreaves method produces approximately 60 % less PET estimates than the Hamon’s method during 2012. Also, yearly Hamon PET totaled to a value that is the most consistent with other watershed studies in literature. Studies including those of Sun et al. (2010) have found PET values in the Southeastern USA LCP regions to be in the range of 575-1792 mm/year.

Table 4.7: Yearly PET totals calculated from Hamon and Hargreaves Methods

Method	Year	PET (mm)
Hamon	2012	857
Hargreaves	2012	340

This once again reinforces the choice in using Hamon’s method to represent the PET at WS-AGC. Continuing research efforts at WS-AGC should provide more confidence in this methods ability to produce reliable results. However, at this point in the study Hamons has proven to be the most reliably temperature based PET method.

4.1.4 Runoff

During the *SWMM* calibration efforts, rainfall runoff data from the first seven months (06/11/2012 to 02/14/2013) of this study were used. This included nine separate rainfall runoff events which fell into the requirements of a six hour inter-event period and a maximum peak flow rate of at least $0.1 \frac{m^3}{s}$. These nine events are represented by the blue lines seen in Figure 4.6. Runoff events were scarce during the first six months of this study as this was the dry season (May-November). Only three events were recorded at the Cipolletti during this period with the highest peak flow recorded at $0.7 \frac{m^3}{s}$. Even with a strong intensity storm of approximately $80 \frac{mm}{hr}$ recorded in September, the dry conditions allowed for the majority of rainfall to be infiltrated.

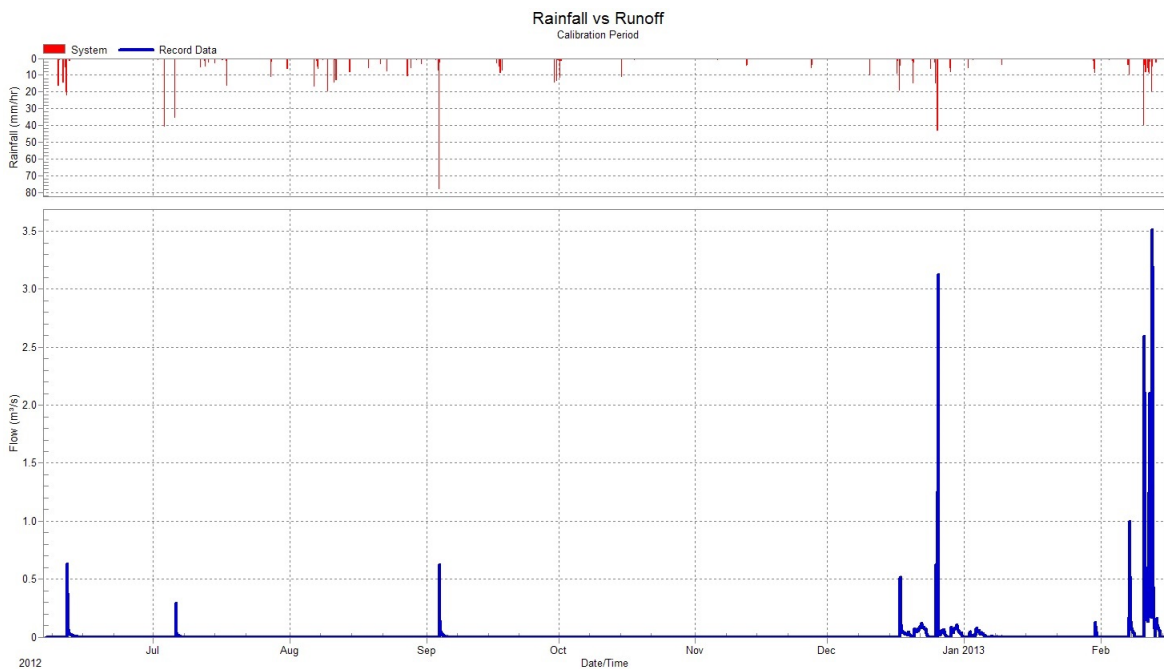


Figure 4.6: Rainfall runoff events at Cipolletti weir used during calibration efforts

Once the wet season (November-April) began, a dramatic increase in the response of runoff was observed. Storms during this period did not show much variation in intensity or duration but runoff responses increased noticeably. In a two month period, six of the nine runoff events used for calibration were obtained. One possible explanation for this increase

in stream flow recorded at WS-AGC is the rise in the local groundwater elevation. Figure 4.14 in the following subsection provides evidence of a water table level increasing from November to December to approximately stream bed elevation. Then during the following seven months groundwater elevations continued to connect and disconnect with the stream bed elevation.

Verification was performed with rainfall runoff data from 02/14/2013 to 08/14/2013. As anticipated runoff over the converted broad crested weir continued to produce frequent flows during the wet season. However, runoff continued strong into the dry season as ten additional runoff events were recorded. Total rainfall from June to July 2012 was 189 mm and rainfall from the same period in 2013 was 443 mm. This large increase in rainfall from the prior year has provided an abnormal dry season. The rainfall runoff events in Figure 4.7 were used during this verification effort. Results of verification are discussed in the following section.

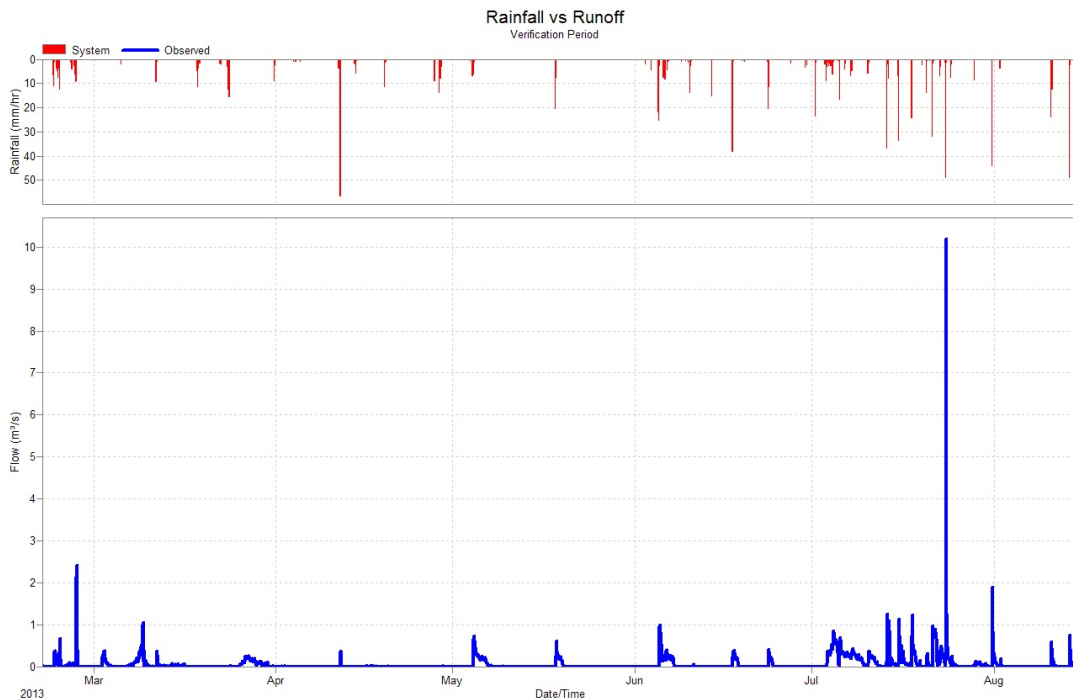


Figure 4.7: Rainfall runoff events at broad-crested weir used during verification efforts

Runoff recorded at the upstream rectangular weir began in September 2012. Data from this weir is shown in Figure 4.8. The rectangular weir was not used for any modeling or watershed analysis in this study. However it was used to verify runoff consistency from the Cipolletti to modified broad crested weir.

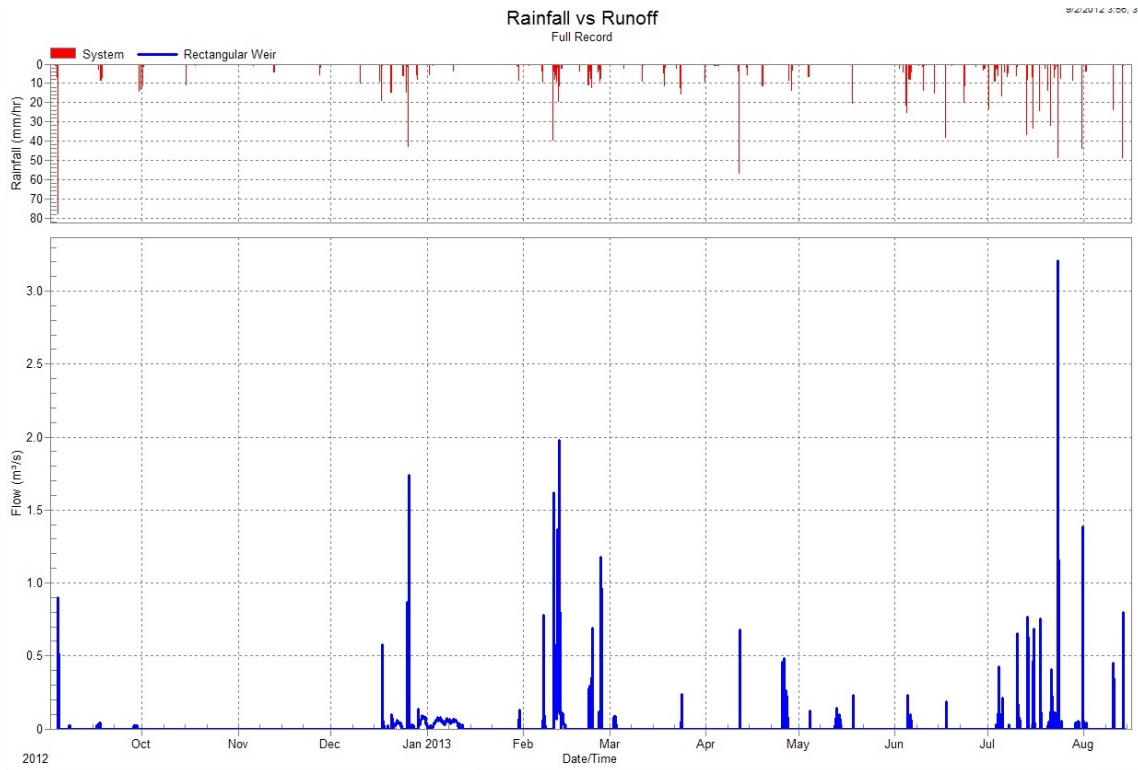


Figure 4.8: Rainfall runoff events at rectangular weir

Similar trends in peaks and recession periods are seen between the upstream rectangular weir and downstream Cipolletti/Broad-crested Weir. Figures 4.9 and 4.10 show recorded runoff comparisons between these two locations prior to the construction performed. In Figure 4.9 an almost identically shaped hydrograph is seen at both locations with differences in peak flow rates and time to peaks. The average lag time between the recorded peaks at the upstream rectangular weir and downstream weir is around 0.5 hours.

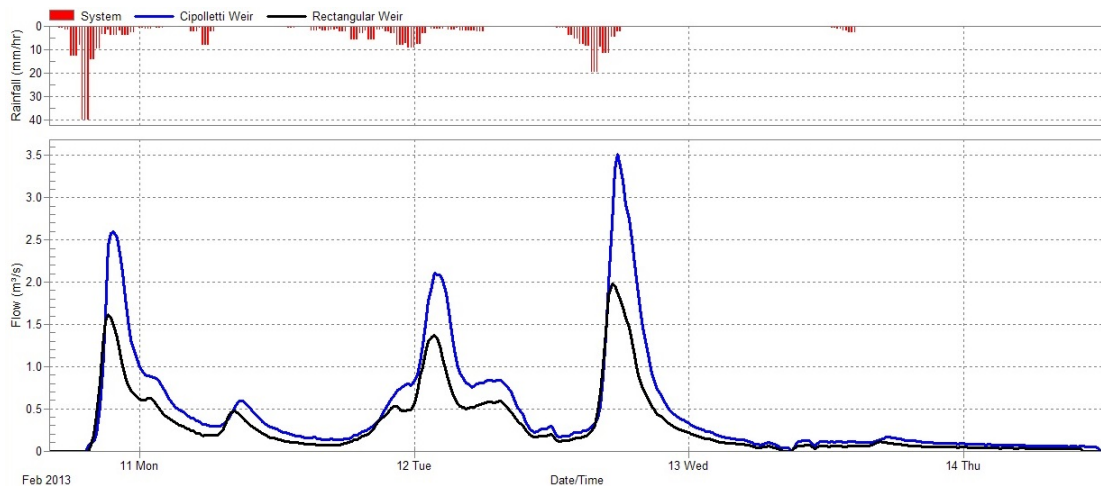


Figure 4.9: Comparison between runoff at Cipolletti weir and rectangular weir (Pre-Construction February 8th-14th, 2013)

The rainfall runoff events in Figure 4.10 represent post construction of Cipolletti to broad crested weir at downstream location records. The runoff recorded at these two location still show similar hydrograph trends and the lag time between weirs is near the same value of 0.5 hours. As mentioned prior rainfall runoff data from this post-construction period was used as verification of the *SWMM* model.

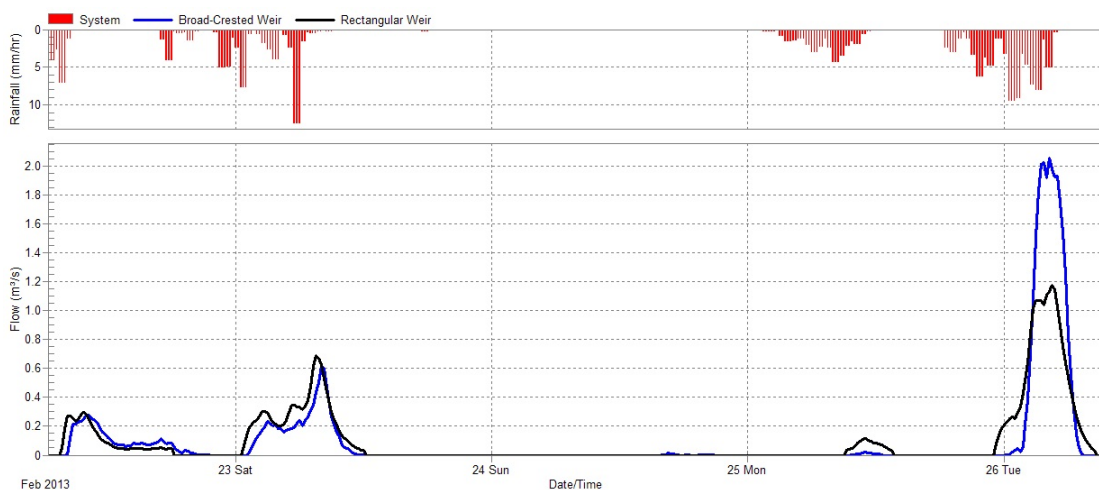


Figure 4.10: Comparison between runoff at broad-crested weir and rectangular weir (Post-Construction February 23rd-26th, 2013)

Presented in Table 4.8 are descriptive statistics for all the rainfall runoff events recorded at the downstream weir. Over the course of the study 31 events matching the requirements of minimum peak flows of $0.1 \frac{m^3}{s}$ and inter-event periods of at least six hours. Data is presented as a whole over the dry and wet seasons 2012 through 2013. Total flow volumes were normalized by watershed area in order to obtain units of mm allowing for the computation of runoff rainfall ration (R/P). Also rainfall totals presented were determined using any rainfall events within 24 hours prior and during the runoff event. This was arbitrarily selected to distinguish between rainfall events which did not directly contribute to runoff.

Table 4.8 also presents the maximum, minimum and average values for rainfall runoff statistics. The longest runoff event recorded at the downstream weir was 218.3 hours or approximately 9 days long while the shortest was only 13.4 hours. Interestingly the longest duration event has not provided the highest flow rate recorded over this weir. This has occurred July 23rd, 2013 with an event lasting 34.9 hours peaking at $10.2 \frac{m^3}{s}$ and a rainfall total of 32 mm. While the longest event July 3rd, 2013 of 218.3 hours produced a peak flow of $0.85 \frac{m^3}{s}$ and rainfall total of 90 mm.

Table 4.8: Descriptive rainfall runoff statistics

Statistics of Rainfall Runoff Events at Downstream Weir										
Event	Date	Start Time	Duration (h)	Maximum Flow (m^3/s)	Minimum Flow (m^3/s)	Mean Flow (m^3/s)	Total Flow (m^3)	Total Flow (mm)	Total Rainfall (mm)	R/P
1	06/11/2012	11:05	35.2	0.64	0	0.07	8707	3.00	53.16	0.06
2	07/06/2012	03:35	23.7	0.29	0	0.04	2988	1.03	25.67	0.04
3	09/03/2012	22:50	25.3	0.62	0	0.07	5949	2.05	60.23	0.03
4	12/17/2012	11:50	61.0	0.52	0	0.05	11340	3.91	49.35	0.08
5	12/25/2012	12:55	26.7	3.12	0	0.26	24730	8.53	56.73	0.15
6	12/29/2012	00:40	69.0	0.11	0	0.05	12150	4.19	13.53	0.31
7	01/30/2013	14:05	136.3	0.28	0	0.06	30290	10.44	21.56	0.48
8	02/07/2013	05:10	32.1	1.26	0	0.28	32780	11.30	40.11	0.28
9	02/10/2013	17:55	115.2	3.88	0	0.54	223500	77.07	151.60	0.51
10	02/22/2013	07:10	53.6	0.67	0	0.11	21590	7.44	52.15	0.14
11	02/25/2013	03:05	30.5	2.42	0	0.29	31880	10.99	40.74	0.27
12	03/02/2013	04:35	44.1	0.37	0	0.11	16790	5.79	0.00	N/A
13	03/11/2013	17:30	41.6	0.37	0	0.04	5295	1.83	25.67	0.07
14	04/11/2013	16:15	180.8	0.38	0	0.00	2353	0.81	33.17	0.02
15	05/04/2013	06:35	127.5	0.74	0	0.12	55790	19.24	33.56	0.57
16	05/18/2013	08:30	39.7	0.62	0	0.16	22730	7.84	32.31	0.24
17	06/04/2013	19:35	69.7	0.98	0	0.25	63820	22.01	73.94	0.30
18	06/17/2013	10:00	41.6	0.39	0	0.12	18660	6.43	26.18	0.25
19	06/23/2013	13:25	22.3	0.41	0	0.16	13030	4.49	27.79	0.16
20	07/03/2013	12:30	218.3	0.85	0	0.26	202400	69.79	89.83	0.78
21	07/13/2013	14:00	43.9	1.26	0	0.28	43490	15.00	38.87	0.39
22	07/15/2013	14:30	39.6	1.13	0	0.27	38580	13.30	21.22	0.63
23	07/17/2013	21:20	39.3	1.23	0	0.22	31630	10.91	23.05	0.47
24	07/20/2013	11:20	21.2	0.30	0	0.06	4482	1.55	10.02	0.15
25	07/21/2013	10:00	21.4	0.97	0	0.70	54100	18.66	21.42	0.87
26	07/22/2013	16:05	21.9	0.49	0	0.26	20260	6.99	10.73	0.65
27	07/23/2013	16:30	34.9	10.20	0	0.64	80030	27.60	32.47	0.85
28	07/31/2013	13:15	25.4	1.89	0	0.27	24540	8.46	32.08	0.26
29	08/02/2013	00:05	13.4	0.19	0	0.03	1246	0.43	3.18	0.13
30	08/10/2013	14:30	21.8	0.59	0	0.11	8588	2.96	24.47	0.12
31	08/13/2013	16:10	16.8	0.75	0	0.14	8711	3.00	30.90	0.10
		Maximum:	218.3	10.20	0	0.70	223500	77.07	151.60	0.87
		Minimum:	13.4	0.11	0	0.00	1246	0.43	0.00	0.02
		Average:	54.6	1.22	0	0.19	36207	12.49	37.28	0.31

Runoff rainfall ratios have shown dramatic fluctuations through the study period. Ranging from 0.02 to 0.87 and having an average value of 0.31. One intriguing event during this record was event 12, which started at 03/02/13. During this event no rain was recorded on any of the rain gauges but the downstream weir experienced a runoff event lasting 25 hours and producing a peak flow of $0.28 \frac{m^3}{s}$. This event seems to only be explained by a very concentrated rainfall event which had to fall in-between or upstream of recording rain gauges. One other explanation could be water released from the small wetland storage area just upstream of the rectangular weir. However, since WS-AGC is at the headwaters this scenario lacks any definitive proof to its origins.

Data presented Tables 4.9 to 4.11 separates the observed rainfall runoff events into wet and dry season events for each year of record. As defined in Chapter 2, wet and dry seasons were specified as (December-April) and (May-November) respectively. One obvious remark from examining these charts is the skewness between events recorded in 2012 to 2013. With this feature acknowledged, there are still some interesting comparisons to be made from this data.

Table 4.9: Descriptive rainfall runoff statistics and R/P ratios for wet season events 2012-2013

Wet Season Rainfall Runoff Events (December-April), 2012-2013										
Event	Date	Start Time	Duration (h)	Maximum Flow (m ³ /s)	Minimum Flow (m ³ /s)	Mean Flow (m ³ /s)	Total Flow (m ³)	Total Flow (mm)	Total Rainfall (mm)	R/P
4	12/17/2012	11:50	61.0	0.52	0	0.05	11340	3.91	49.35	0.08
5	12/25/2012	12:55	26.7	3.12	0	0.26	24730	8.53	56.73	0.15
6	12/29/2012	00:40	69.0	0.11	0	0.05	12150	4.19	13.53	0.31
7	01/30/2013	14:05	136.3	0.28	0	0.06	30290	10.44	21.56	0.48
8	02/07/2013	05:10	32.1	1.26	0	0.28	32780	11.30	40.11	0.28
9	02/10/2013	17:55	115.2	3.88	0	0.54	223500	77.07	151.60	0.51
10	02/22/2013	07:10	53.6	0.67	0	0.11	21590	7.44	52.15	0.14
11	02/25/2013	03:05	30.5	2.42	0	0.29	31880	10.99	40.74	0.27
12	03/02/2013	04:35	44.1	0.37	0	0.11	16790	5.79	0.00	N/A
13	03/11/2013	17:30	41.6	0.37	0	0.04	5295	1.83	25.67	0.07
14	04/11/2013	16:15	180.8	0.38	0	0.00	2353	0.81	33.17	0.02
		Maximum:	180.8	3.88	0	0.54	223500.0	77.07	151.60	0.51
		Minimum:	26.7	0.11	0	0.00	2353.0	0.81	0.00	0.02
		Average:	71.9	1.22	0	0.16	37518.0	12.94	44.06	0.23

Dry season R/P values have shown a much larger fluctuation from year to year. In 2012 the maximum ratio experienced was 0.06 whereas in 2013 a ratio of 0.87 was recorded. These values show the large variability in rainfall seen at the site in 2012 compared to 2013. The number of runoff events recorded has increased by approximately 6 times between the

months of June and July 2012 to 2013. Over the entire dry seasons the average R/P values has also increased by 10.3 times from 2012 to 2013.

Table 4.10: Rainfall runoff statistics and R/P ratios for dry season events 2012

Dry Season Rainfall Runoff Events (May-November), 2012										
Event	Date	Start Time	Duration (h)	Maximum Flow (m ³ /s)	Minimum Flow (m ³ /s)	Mean Flow (m ³ /s)	Total Flow (m ³)	Total Flow (mm)	Total Rainfall (mm)	R/P
1	06/11/2012	10:55	60.6	0.64	0	0.04	9,187	3.17	53.16	0.06
2	07/06/2012	03:35	25.8	0.29	0	0.03	2,986	1.03	25.67	0.04
3	09/03/2012	22:15	26.4	0.62	0	0.06	5,890	2.03	60.23	0.03
		Maximum:	60.6	0.64	0	0.06	9,187	3.17	60.23	0.06
		Minimum:	25.8	0.29	0	0.03	2,986	1.03	25.67	0.03
		Average:	37.6	0.52	0	0.05	6,021	2.08	46.35	0.04

Table 4.11: Rainfall runoff statistics and R/P ratios for dry season events 2013

Dry Season Rainfall Runoff Events (May-November), 2013										
Event	Date	Start Time	Duration (h)	Maximum Flow (m ³ /s)	Minimum Flow (m ³ /s)	Mean Flow (m ³ /s)	Total Flow (m ³)	Total Flow (mm)	Total Rainfall (mm)	R/P
15	05/04/2013	06:35	127.5	0.74	0	0.12	55790	19.24	33.56	0.57
16	05/18/2013	08:30	39.7	0.62	0	0.16	22730	7.84	32.31	0.24
17	06/04/2013	19:35	69.7	0.98	0	0.25	63820	22.01	73.94	0.30
18	06/17/2013	10:00	41.6	0.39	0	0.12	18660	6.43	26.18	0.25
19	06/23/2013	13:25	22.3	0.41	0	0.16	13030	4.49	27.79	0.16
20	07/03/2013	12:30	218.3	0.85	0	0.26	202400	69.79	89.83	0.78
21	07/13/2013	14:00	43.9	1.26	0	0.28	43490	15.00	38.87	0.39
22	07/15/2013	14:30	39.6	1.13	0	0.27	38580	13.30	21.22	0.63
23	07/17/2013	21:20	39.3	1.23	0	0.22	31630	10.91	23.05	0.47
24	07/20/2013	11:20	21.2	0.30	0	0.06	4482	1.55	10.02	0.15
25	07/21/2013	10:00	21.4	0.97	0	0.70	54100	18.66	21.42	0.87
26	07/22/2013	16:05	21.9	0.49	0	0.26	20260	6.99	10.73	0.65
27	07/23/2013	16:30	34.9	10.20	0	0.64	80030	27.60	32.47	0.85
28	07/31/2013	13:15	25.4	1.89	0	0.27	24540	8.46	32.08	0.26
29	08/02/2013	00:05	13.4	0.19	0	0.03	1246	0.43	3.184	0.13
30	08/10/2013	14:30	21.8	0.59	0	0.11	8588	2.96	24.47	0.12
31	08/13/2013	16:10	16.8	0.75	0	0.14	8711	3.00	30.9	0.10
		Maximum:	218.3	10.20	0	0.70	202400	69.79	89.83	0.87
		Minimum:	13.4	0.19	0	0.03	1246	0.43	3.18	0.10
		Average:	48.2	1.35	0	0.24	40711	14.04	31.30	0.41

Comparing Table 4.8 R/P statistics with R/P statistics formulated from a 13 year study by La Torre Torres et al. (2011), similar trends were experienced at WS-AGC. The study site of La Torre Torres et al. (2011) shows very similar physical characteristics of WS-AGC with the major difference being the watersheds area of 72.6 km² compared to the 2.9 km² of WS-AGC. Interestingly, even with the significant catchment area difference between the responses of each watersheds hydrology are very similar.

R/P ratios from La Torre Torres et al. (2011) show ranges during the entire study from (0.01 to 0.80). Similarly WS-AGC has experienced R/P ratios of (0.02 to 0.87) over the course of study. Now when breaking R/P ratios down into wet and dry season tables, similar trends are seen. La Torre Torres et al. (2011) produced R/P ratios from (0.17 to 0.53) and (0.01 to 0.80) during wet and dry seasons respectively. This again is seen when

WS-AGC's R/P ratios are distinguished by wet and dry seasons. Table 4.9 shows R/P values during the wet season from 2012 to 2013, R/P ratios range from (0.02 to 0.51). Now combining Tables 4.10 and 4.11 R/P values range from (0.03 to 0.87), corresponding with results seen from the study presented by La Torre Torres et al. (2011).

4.1.5 Groundwater

Recording the shallow groundwater table at WS-AGC began November 1st, 2012 with two shallow wells. One located outside of the stream and another centered in the stream bed. Data from both of these locations are displayed in Figures 4.12-4.15. Water table elevations are represented as meters from the surface (red lines), where both wells are referenced to the out of stream well ground elevation. Also included within these figure rainfall intensities and cumulative totals, (blue lines). During late December 2012 a major storm hit the area and caused damage to both wells. This is reflected in the missing data between December 2012 and January 2013 in these figures.

In both wells groundwater elevation values were approximately two meters below the surface prior to this damaging large event. However, after the event water table elevations had risen to approximately 0.6 meters below the surface. Then as the record progresses, groundwater elevation begins to fluctuate above and below the grade elevation. This has then resulted in a dynamic groundwater table which became at certain times directly connected with the stream flows. The largest groundwater table elevations recorded during this study period were approximately one meter above surface elevations. These results indicated that the hydrological processes occurring at WS-AGC are typical of losing/gaining of intermittent streams.

Figure 4.11 provides a visual representation of the dynamic water table variation which is likely to be representative of WS-AGC. As the seasons change groundwater elevation vary according to rainfall, evaporation and infiltration processes. As wet season occurs water table levels begin to rise due to larger rainfall events, lower temperatures and decreased PET. This

increase in rainfall and decrease in ET creates larger head potential between groundwater levels and stream surface levels. This is represented in Figure 4.11 (a). On the other hand, during the dry season lack of constant rainfall and higher temperatures cause larger rates of water loss in the watershed system. Represented in Figure 4.11 (b) part or all of the stream flow which may occur during a large intensity or duration rainfall event infiltrates through the channel interface into the aquifers below.

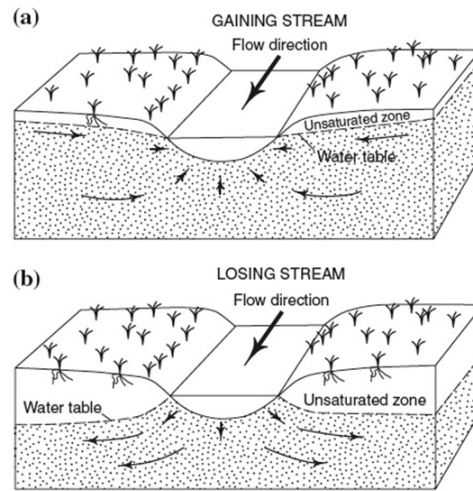


Figure 4.11: Representation of the dynamic groundwater processes of a gaining/losing stream such as the one at WS-AGC, (Winter, 2007)

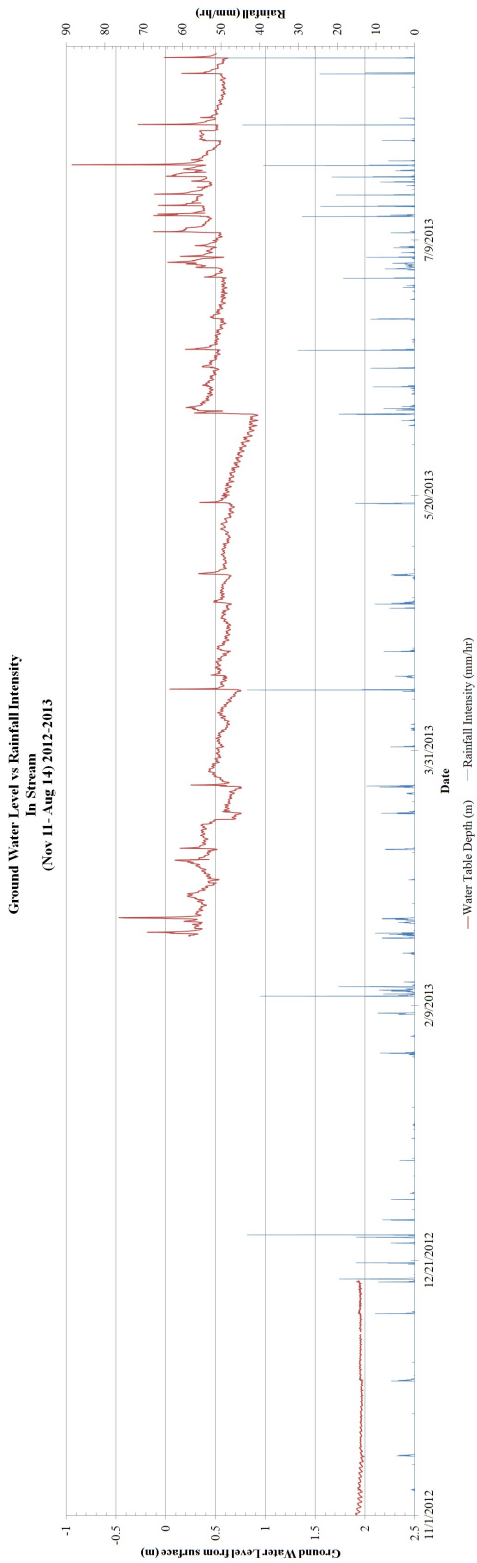


Figure 4.12: Instream ground water level vs rainfall intensity

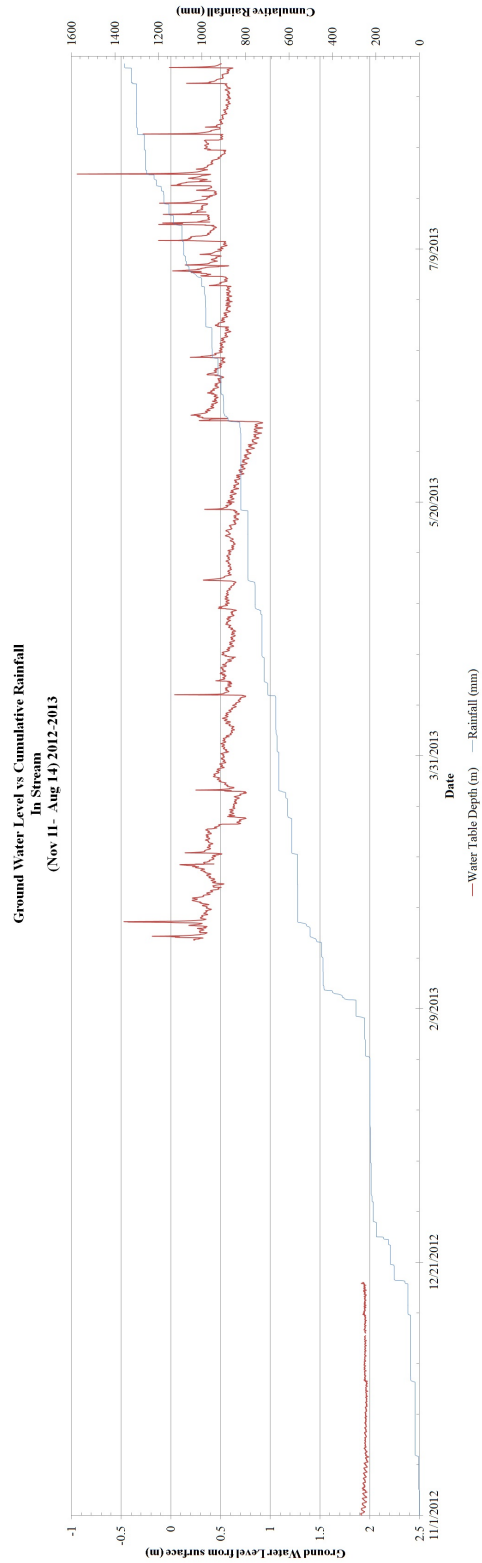


Figure 4.13: Instream ground water level vs cumulative rainfall

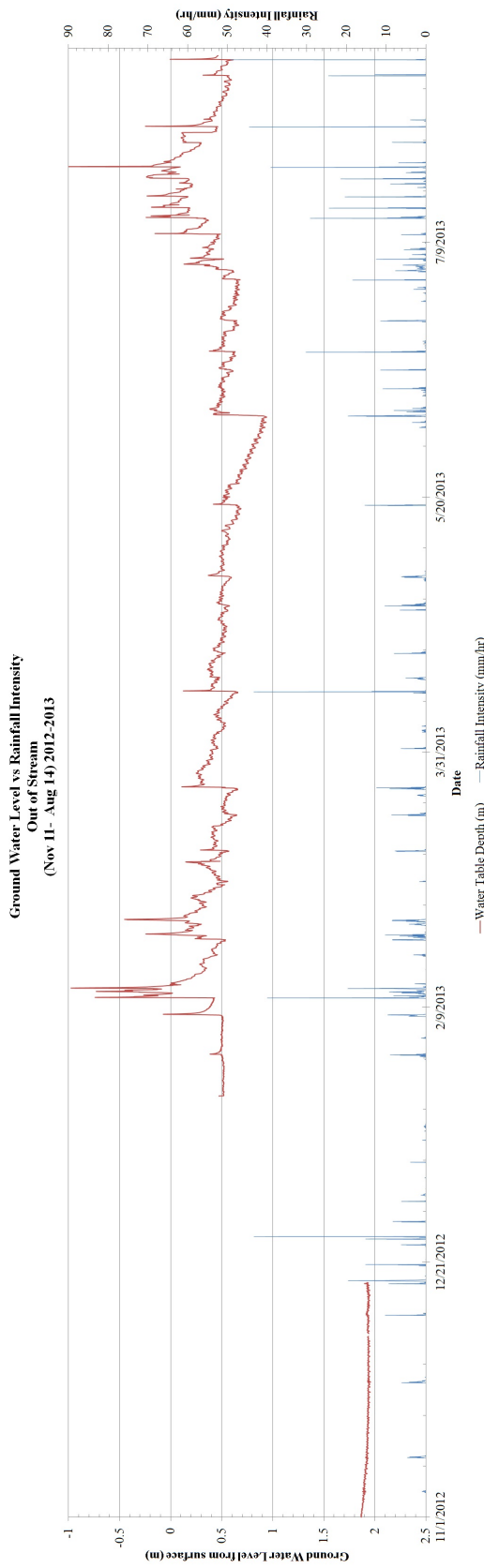


Figure 4.14: Out of stream ground water level vs rainfall intensity

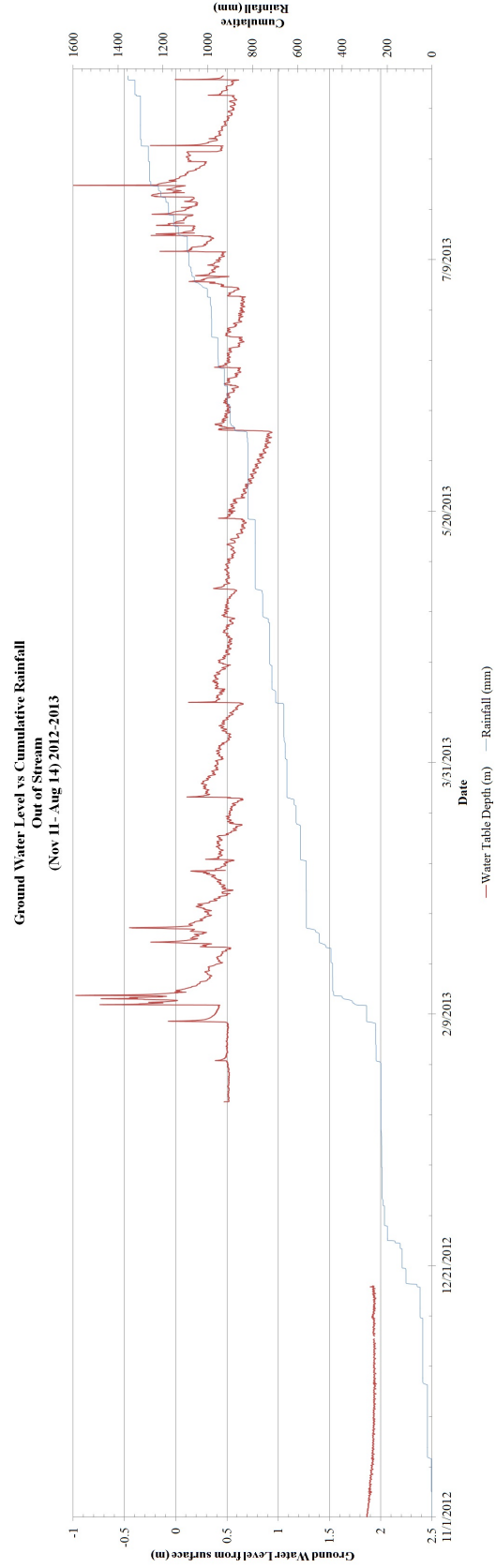


Figure 4.15: Out of stream ground water level vs cumulative rainfall

These observations were significant with regards to the development of the *SWMM* watershed model. Physical evidence that groundwater elevations were gaining to above channel bottom grade levels showed the importance of including the aquifer component in modeling efforts. With the larger number of rainfall events occurring during the 2013 dry season, groundwater elevations have maintained comparatively higher levels. Comparing the levels at the end of the dry season 2012 to 2013 dry season levels, a difference of approximately two meters has been recorded. As stated prior, the higher groundwater elevations in 2013 have been a major factor in the increase of observed runoff events. During the dry season 2012 several storms hit WS-AGC and produced no runoff, see Figure 4.6. Compared with the data of 2013 many other smaller storms with intensities below $30 \frac{mm}{hr}$ have produced runoff, see Figure 4.7. For example, shown in Figures 4.16 and 4.17 are two similar rainfall events during the dry seasons of 2012 and 2013 respectively. This data provides more evidence that higher groundwater levels change the dynamics of the rainfall runoff relationships at WS-AGC.

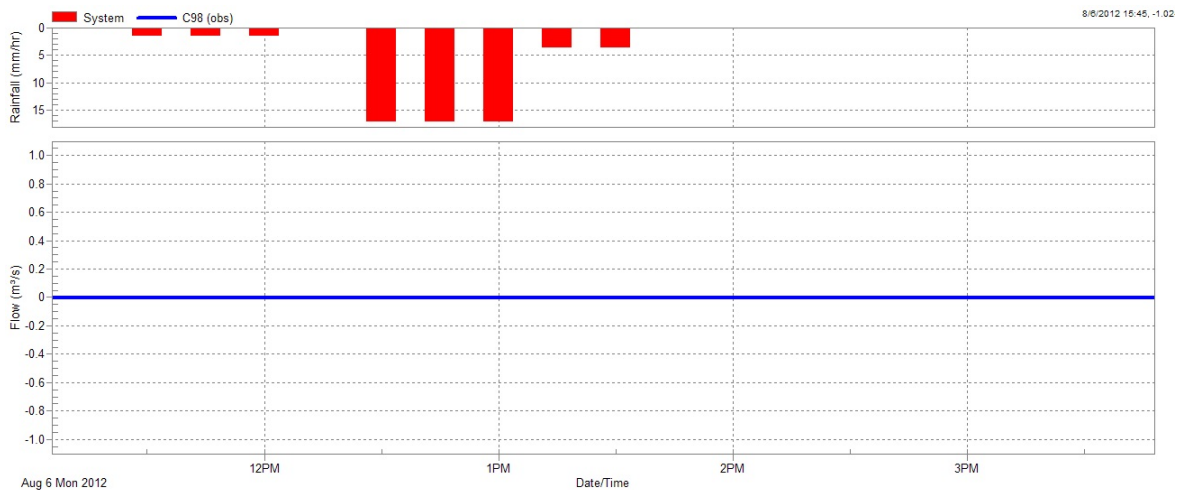


Figure 4.16: Rainfall event without runoff event during August 6th, 2012 at Cipolletti/Broad-Crested weir

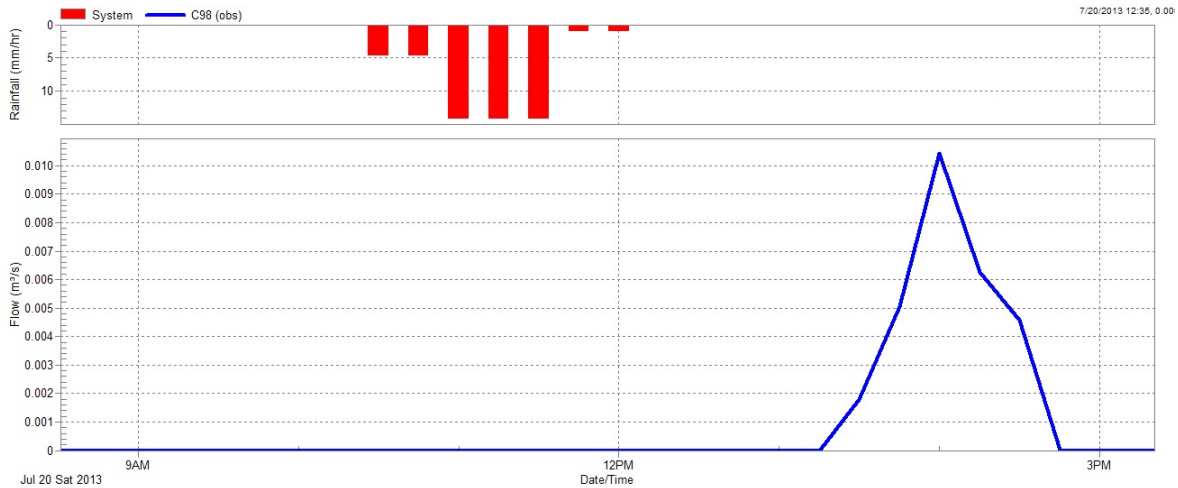


Figure 4.17: Smaller rainfall event yielding runoff during July 20th, 2013 at Cipolletti/Broad-Crested weir

Another interesting phenomenon recorded at WS-AGC was the evidence of diurnal ET. Several studies have recorded this process in the Southeastern region of the USA including Czikowsky and Fitzjarrald (2004), Gribovszki et al. (2008) and Gribovszki et al. (2010). These studies have recorded shallow groundwater elevations with similar patterns of diurnal fluctuations seen at WS-AGC.

Due to the large density of vegetation in the riparian zone, ET has caused groundwater levels to drop diurnally at WS-AGC. For example, Figure 4.18 shows groundwater fluctuations on the magnitude of 2.8 cm over a 12 hour period. The main decreases in water table elevation occur during afternoon hours and recharging periods occur through night time hours. This process also shows the largest rates of loss during long hot days of the dry period. It's during this time that vegetation in WS-AGC is in full bloom and natural evaporation/transpiration processes are occurring. While in Winter when vegetation has gone mainly dormant for the year, signs of ET tend to decrease to smaller amplitudes.

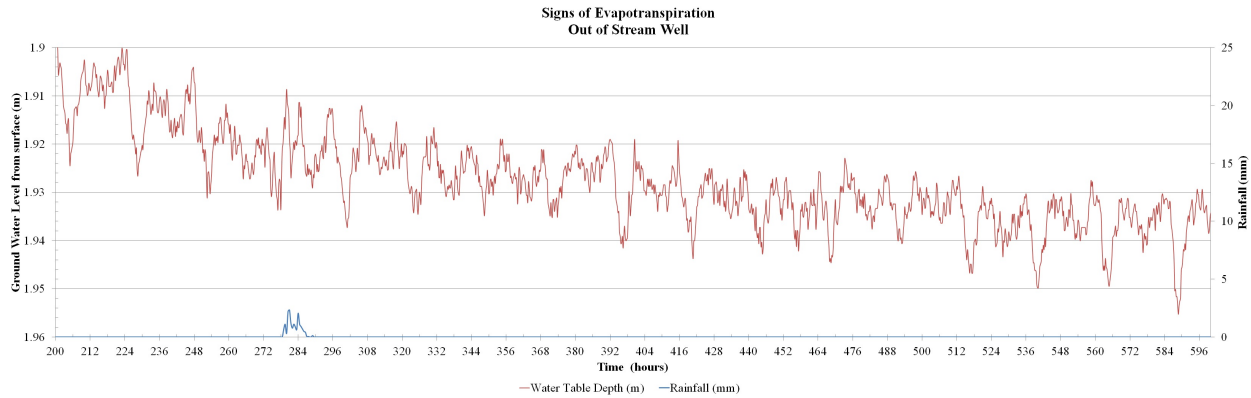


Figure 4.18: Signs of ET from the out of stream ground water well

4.2 SWMM Simulation Comparisons

Presented in this section are results from three *SWMM* models comprised of multiple aquifer, single aquifer and no aquifer configurations developed to simulate watershed behavior at WS-AGC. Comparisons of each models ability to predict various key hydrological behaviors such peak discharges, mean discharge, total volumes and flow duration exceedance are analyzed. Using graphical techniques as well as statistical approaches suggested from Moriasi et al. (2007) each configuration is examined and assessed.

4.2.1 Hydrographs Comparison

Hydrographs allow the modeler to visually inspect simulation result to observed values and help to identify model bias toward timing as well as recession curves (Moriasi et al., 2007). The following subsection provides graphical representation of key rainfall runoff events modeled from each configuration. Each configuration with three separate events ranging from dry to wet periods are displayed in Figures 4.19-4.21.

Output hydrographs across both dry and wet periods from the multiple aquifer verification results have shown responses matching peaks and duration from observed hydrographs. The top chart from Figure 4.19 shows the models ability to handle the initial flow events by matching peak flows and duration. It however is not able to handle the large flow event that

follows with a peak of approximately $2.4 \frac{m^3}{s}$. Proceeding to the second chart from the top in Figure 4.19 a longer duration rainfall runoff event starting July 3rd, 2013 is presented. Recession curves during this event last for several days. This configuration simulates the first portion lasting till July 5th well with respect to peaks and duration. As another rainfall event occurs on WS-AGC during the late afternoon of July 5th a spike in water level occurs. The simulation once again is able to capture this but then begins to recede quickly. This causes a misrepresentation of the slow recession observed in field measurements. Finally the last chart of Figure 4.19 displays three separate rainfall runoff events commencing on July 14th, 2013. Verification simulations here produced results which fit observed data the best from the two latter charts.

Hydrograph results from the single aquifer verification simulation have produced results which have generally under predicted runoff from all three events shown in Figure 4.20. The top chart of Figure 4.20 displays similar results as the multiple aquifer configuration. Early events beginning February 22nd, 2013 are simulated well with peaks flows and duration corresponding to one another. Then just as seen in the multiple aquifer configuration, simulated runoff during February 26th does not agree with observed data. In the second chart from the top of Figure 4.20 simulation runoff agrees well with the initial portion of the July 3rd, 2013. Then is unable to model the second halves of the observed events peak and recession. Following similar trends the simulation results displayed in the bottom chart of Figure 4.20 have under predicted peak flows during these three runoff events. However, this configuration has reproduced recession curve behavior fairly well.

Finally when examining the no aquifer configuration simulation results displayed in Figure 4.21 dramatic differences are noticed. Runoff output from each separate event fell far below observed hydrographs. This was expected since the same outcomes occurred during the calibration period of this analysis. Results were carried through to verification for comparison purposes. They have also provided visual evidence reinforcing the importance of using aquifer components in WS-AGC's model.

Multiple Aquifer Simulation

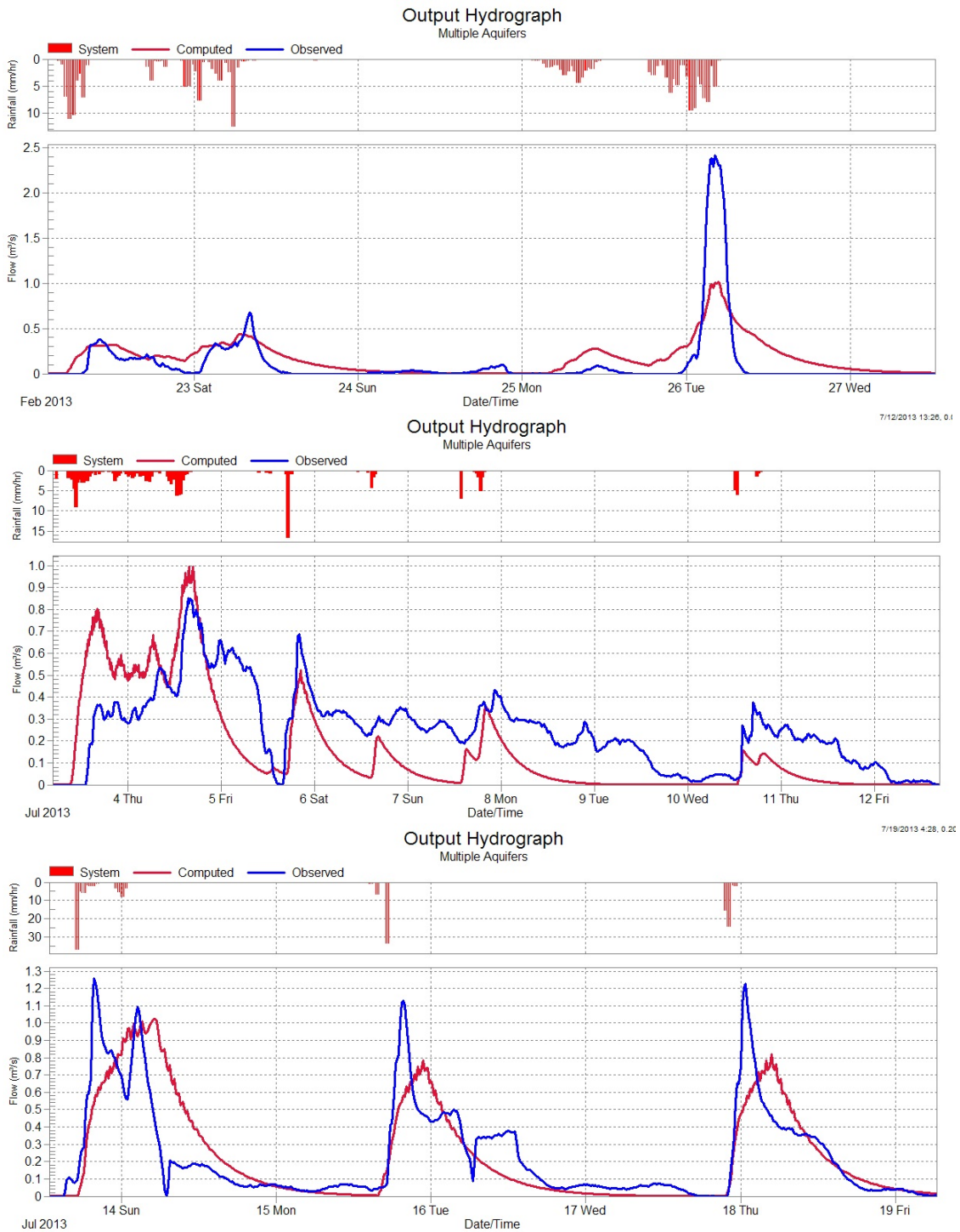


Figure 4.19: Output hydrographs produced with multiple aquifer configuration

Single Aquifer Simulation

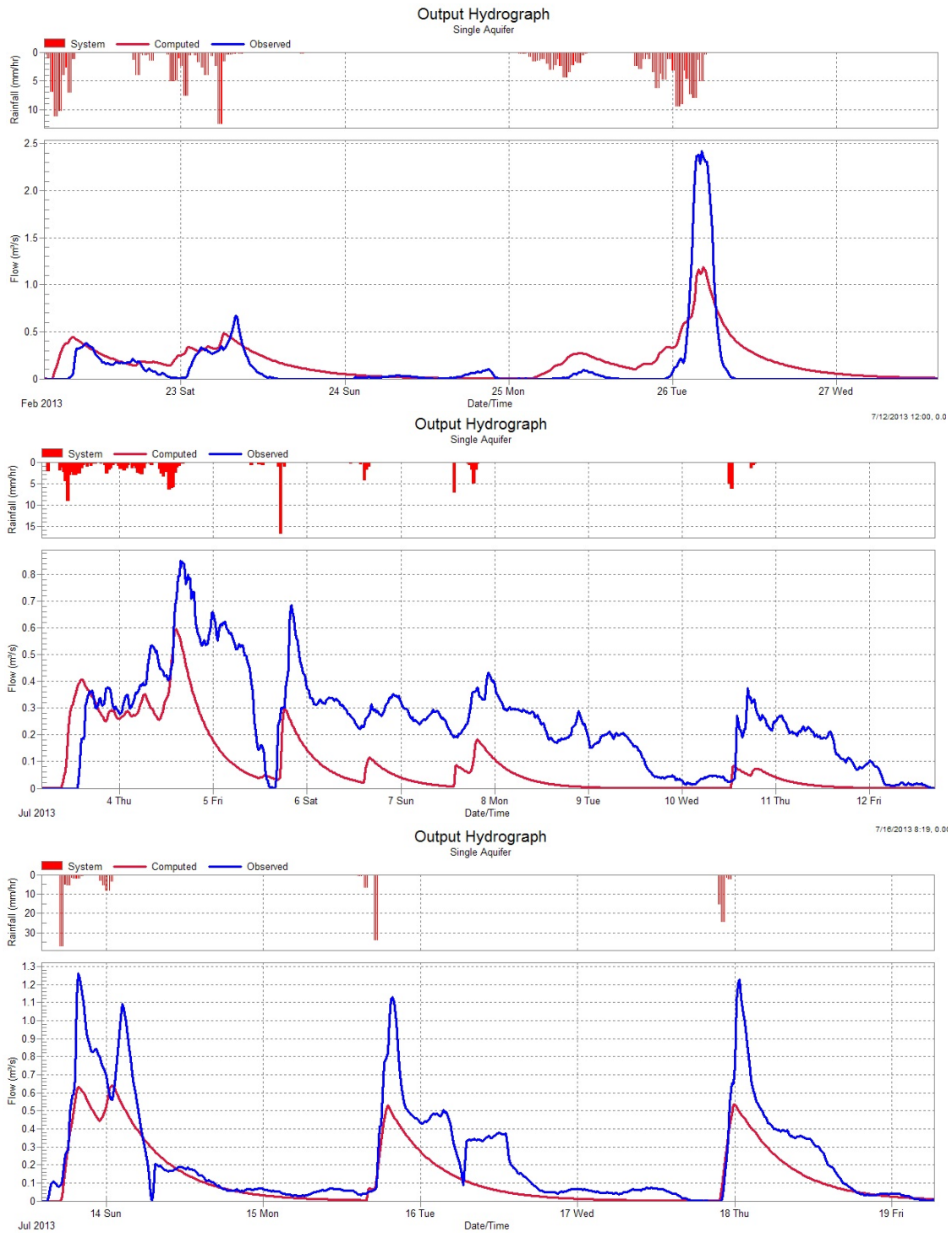


Figure 4.20: Output hydrographs produced with single aquifer configuration

No Aquifer Simulation

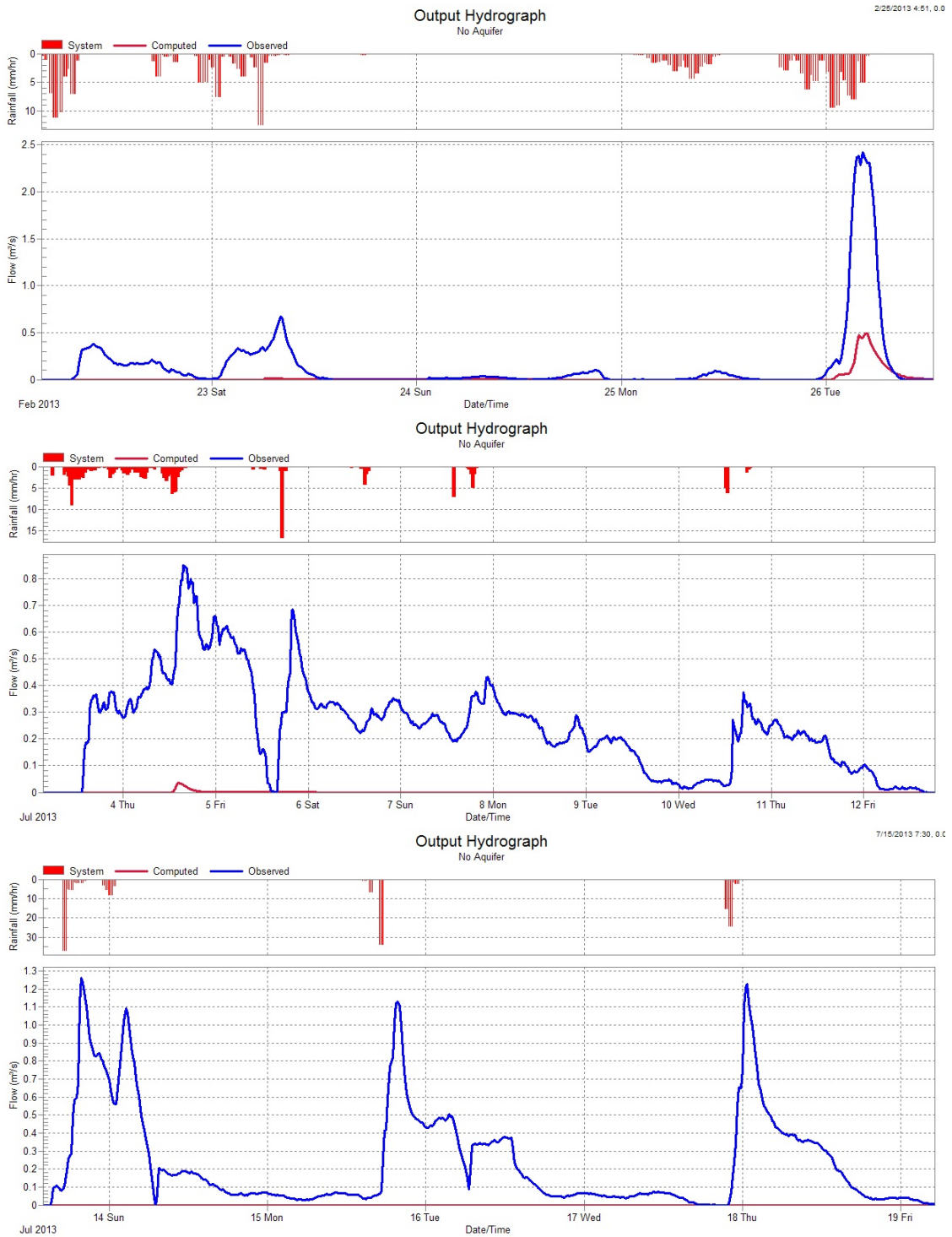


Figure 4.21: Output hydrographs produced with no aquifer configuration

4.2.2 Flow Duration Exceedance curves

Presented in this subsection are flow duration exceedance curves produced from simulated and observed runoff data during the verification period. These figures provide insight into the models ability to capture the range of flow rates recorded in the field. In Figures 4.22-4.24 blue lines represent observed runoff at the downstream weir and red lines represent computed runoff.

Results from Figure 4.22 show the multiple aquifer configurations ability to reproduce runoff recorded at WS-AGC. Flows in the mid range between 0.7 and 10 % of total duration were modeled at a high level of accuracy, whereas the larger peak flow rates, which occurred from 0.09 to 0.7 % of total duration, were not computed by this configuration. The computed flow line also begins to drop at a faster rate as flows begin to drop lower then $0.04 \frac{m^3}{s}$. This is due to under prediction of the recession curves duration at low flow rates during the simulations. This may suggest that parameters in the aquifer component may need further adjustment to allow for a longer recession curve during a rainfall runoff event.

Figure 4.23 shows similar results from the single aquifer configuration to the prior discussion. However, results during the period between 0.7 and 10 % of total duration show a larger difference between computed and observed values. This means that not only were peak discharges somewhat misrepresented but mid range and low flow conditions were also below observed data. The single aquifer configuration was able to produce a curve that followed the observed curves slopes and patterns well. On the contrary this configuration was unable to produce any flows that matched observed data set directly.

The no aquifer configuration produced the least fitting of all the flow duration exceedance curves. Computed flows from highest to lowest were all well under predicted. This result showed the significance of adding in the aquifer component, especially where mid range and low flows occurred. The lack of contribution from a slower releasing groundwater component was one of the major issues in capturing the large amount of low flow events occurring during this verification period.

Multiple Aquifer Simulation

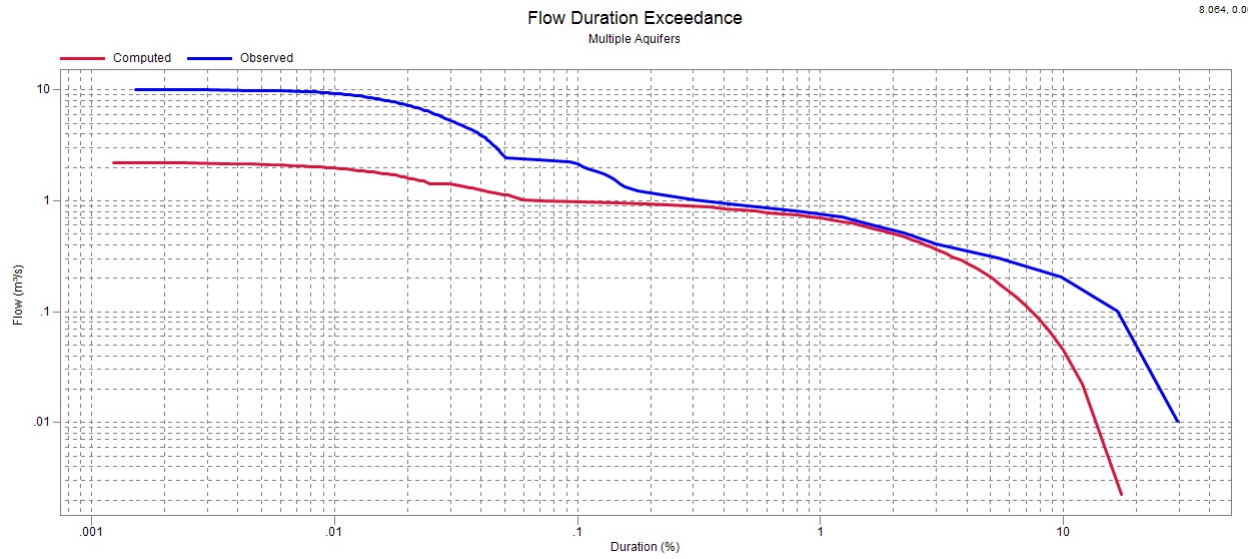


Figure 4.22: Verification Flow duration exceedance curves produced with multiple aquifer configuration

Single Aquifer Simulation

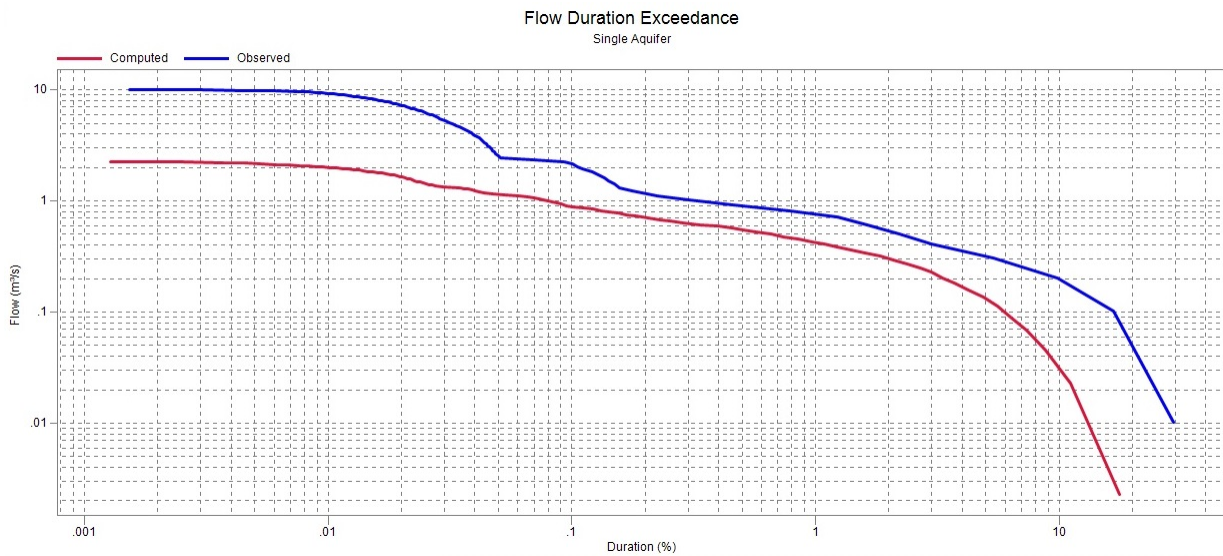


Figure 4.23: Verification flow duration exceedance curves produced with single aquifer configuration

No Aquifer Simulation

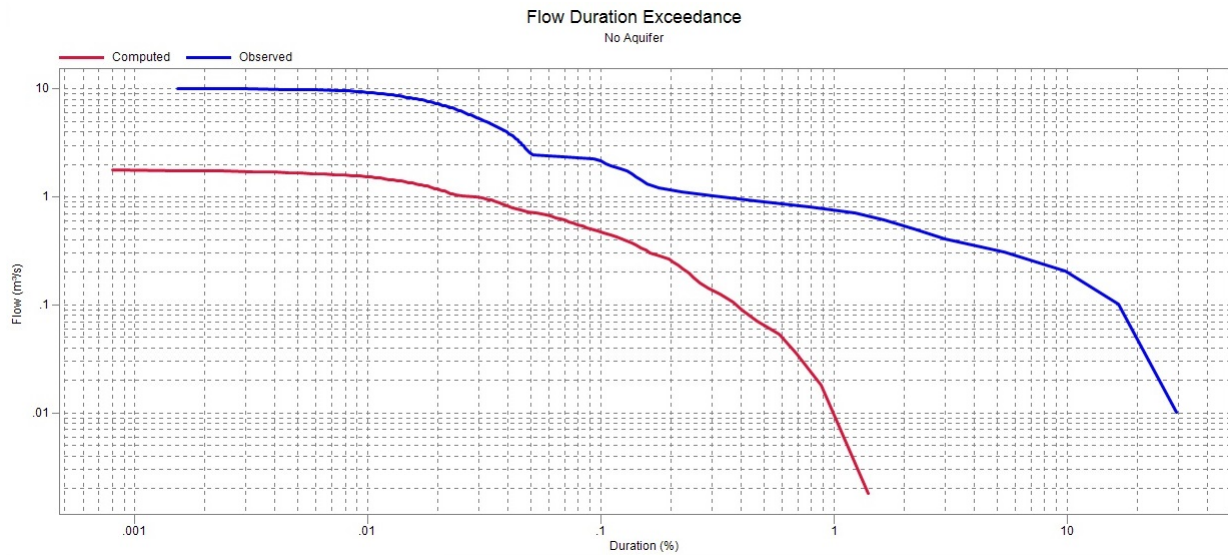


Figure 4.24: Verification flow duration exceedance curves produced with no aquifer configuration

4.2.3 Simulation Error Analysis

The following subsection aims to provide visual displays of observed versus computed data points for three rainfall runoff parameters. Each configuration's performance was analyzed with respect to its ability to simulate peak discharges, mean flows and total volumes observed in the field. Linear regression plots were determined with each simulated runoff event plotted as a black dot with respect to observed values. Percent envelopes were also included to display a 10% and 30% range of values from the 1 : 1 linear regression line. Any data points that fall within 30% of the regression line were considered to be satisfactory. Following this subsection are statistical summaries from both the calibration and simulation periods.

Peak Discharge

Multiple Aquifer Simulation

Peak discharge comparisons from the multiple aquifer configuration are presented in Figure 4.25. Each data point represents a peak discharge value produced from a simulated rainfall runoff event during the verification period. Simulated peak flows agree well with observed values for events up to approximately $1.25 \frac{m^3}{s}$. Any peak flow above this threshold was under predicted by the model. This produced a few outliers especially with a $10 \frac{m^3}{s}$ flow experienced at WS-AGC.

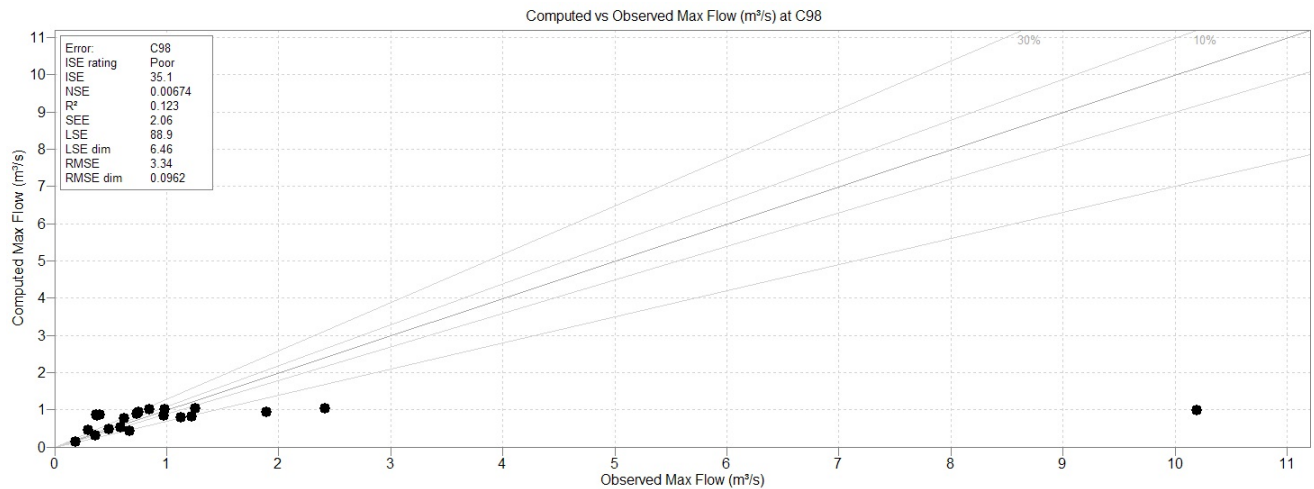


Figure 4.25: Verification error analysis for max flow during multiple aquifer simulation

Single Aquifer Simulation

The single aquifer configuration results presented in Figure 4.26 shows similar trends to those seen in the multiple configuration. Peak flows however were not predicted as well as the prior configuration. Events where maximum flow rate values exceeded $0.8 \frac{m^3}{s}$ simulation results is unable to achieve values within 30 % of observed values. Also outliers begin to show past $2 \frac{m^3}{s}$ with the largest deviation occurring with the $10 \frac{m^3}{s}$ observed event.

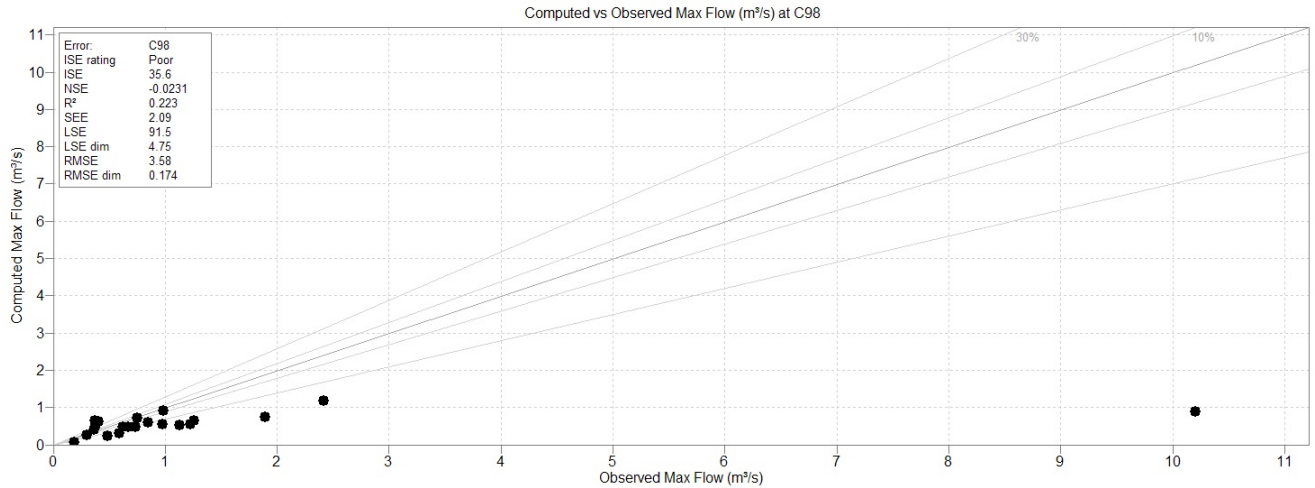


Figure 4.26: Verification error analysis for max flow during single aquifer simulation

No Aquifer Simulation

As expected the no aquifer simulation was unable to predict any peak flows through the entire verification period. Results in Figure 4.27 clearly show this as all events fell well below the 1 : 1 linear regression line.

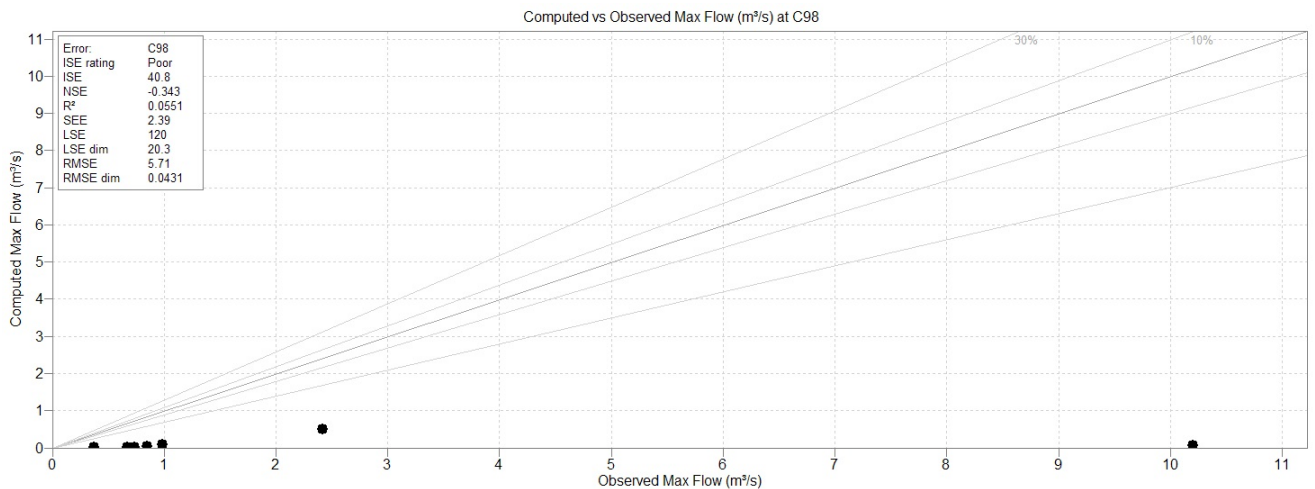


Figure 4.27: Verification error analysis for max flow during no aquifer simulation

Mean Discharge

Multiple Aquifer Simulation

Mean discharges simulated during the multiple aquifer configuration are shown in Figure 4.28. Each event is highly dependent on the characteristics of the rainfall runoff event of interest. Rain events with high intensities may have short duration but large flows thus causing increases in the mean discharge value. It can be seen that computed mean flows tended towards over prediction through the lower portion of flows. Very few events fell within the 30 % envelope from the regression line especially for small mean values. Then during larger computed mean values a generally under prediction trend is seen through the verification events.

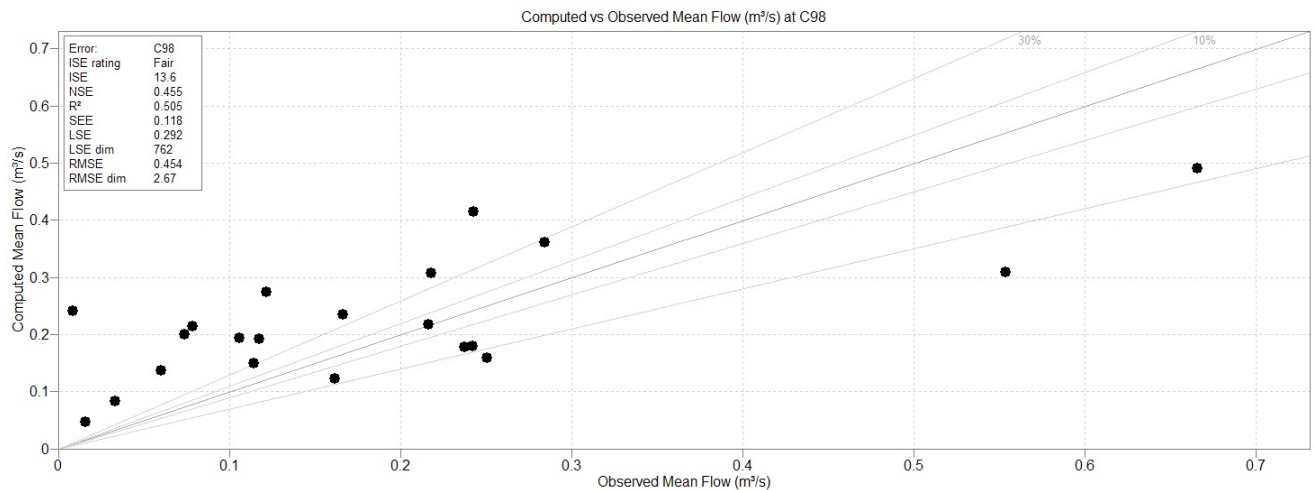


Figure 4.28: Verification error analysis for mean flow during multiple aquifer simulation

Single Aquifer Simulation

The single aquifer configuration has shown computed results with better agreement to observed values for low mean flows. Figure 4.29 shows that once mean flow values reached about $0.2 \frac{m^3}{s}$ computed values began to under predicted observed values. After this threshold the model has under predicted mean flows by as much as 46 %.

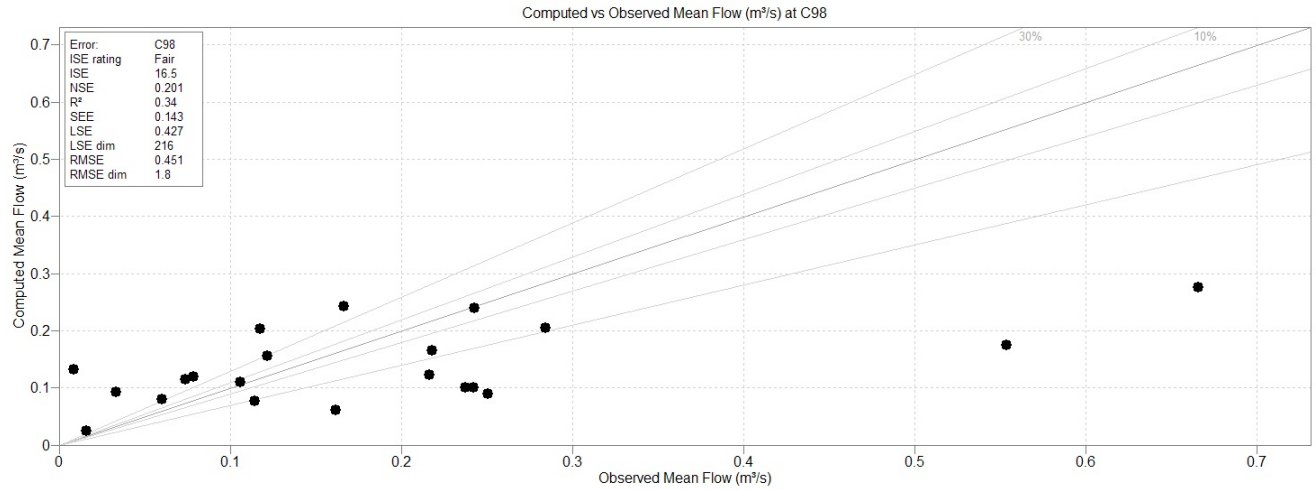


Figure 4.29: Verification error analysis for mean flow during single aquifer simulation

No Aquifer Simulation

Mean flow values were simulated very poorly with the no aquifer configuration. Figure 4.30 displays this clearly without any data points nearing the regression line.

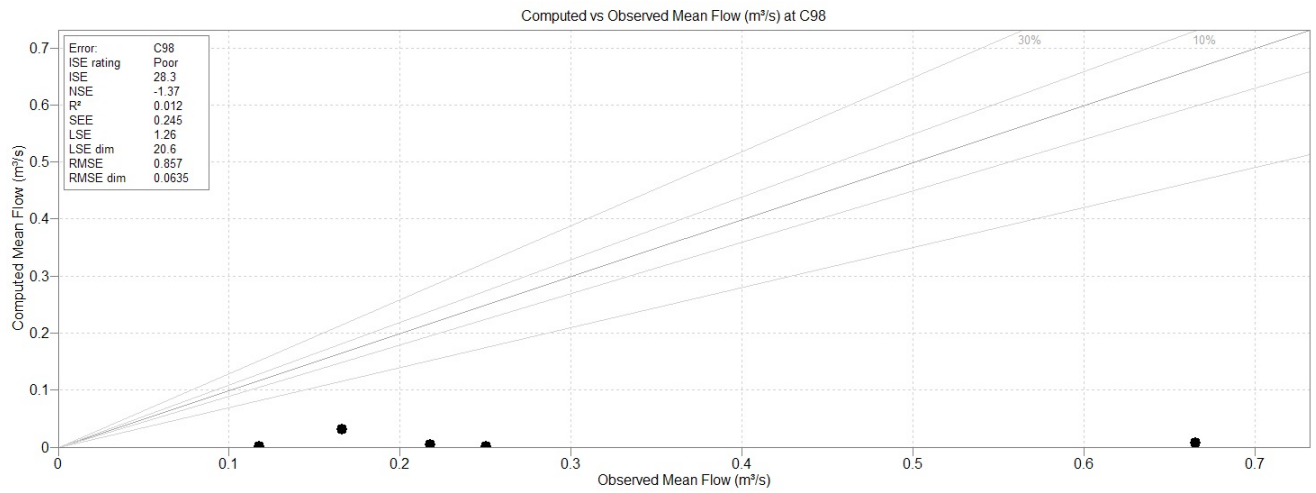


Figure 4.30: Verification error analysis for mean flow during no aquifer simulation

Total Volumes

Multiple Aquifer Simulation

Total volume analysis for the multiple aquifer configuration is shown in Figure 4.31. Computed total volumes have been predicted moderately well during this simulation. With volumes less than 8000 m^3 data points show good agreement between computed and observed with some over-estimation tendency. Larger volumes also showed good agreement. The largest observed total volume event producing approximately 20000 m^3 was only under predicted by approximately 30 %. Which for this study was considered an acceptable predictability range.

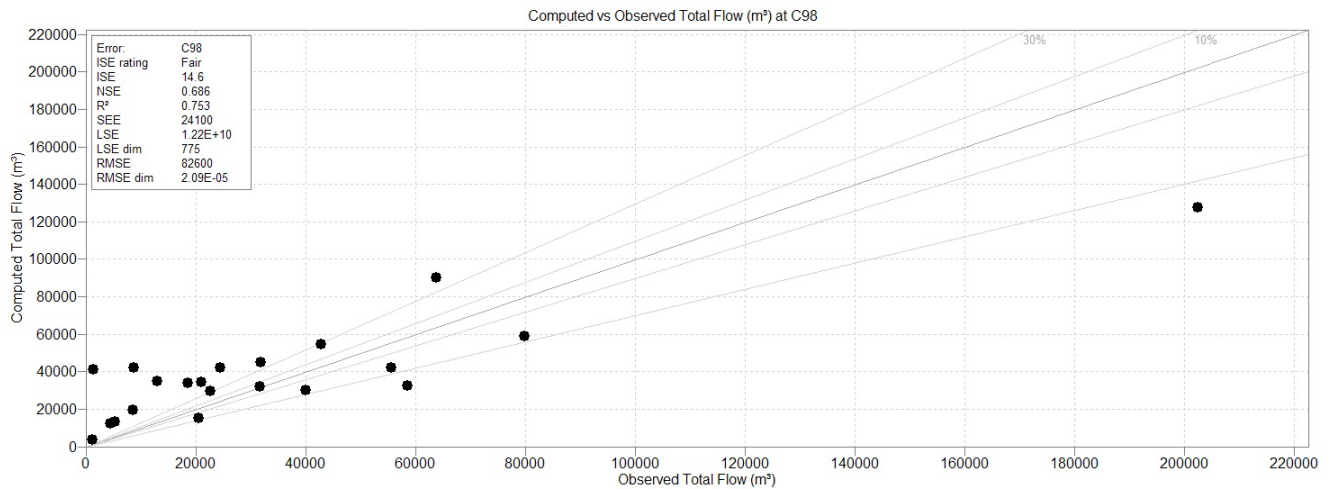


Figure 4.31: Verification error analysis for total flow during multiple aquifer simulation

Single Aquifer Simulation

The single aquifer configuration has shown similar signs to the multiple aquifer configuration during total volume analysis. Some significant differences occurred after the 4000 m^3 mark of observed volumes. At this point simulation output was under predicting the observed field data by more than 30 %. The large event of approximately 20000 m^3 has been under predicted by much less than the acceptable 30 % envelope.

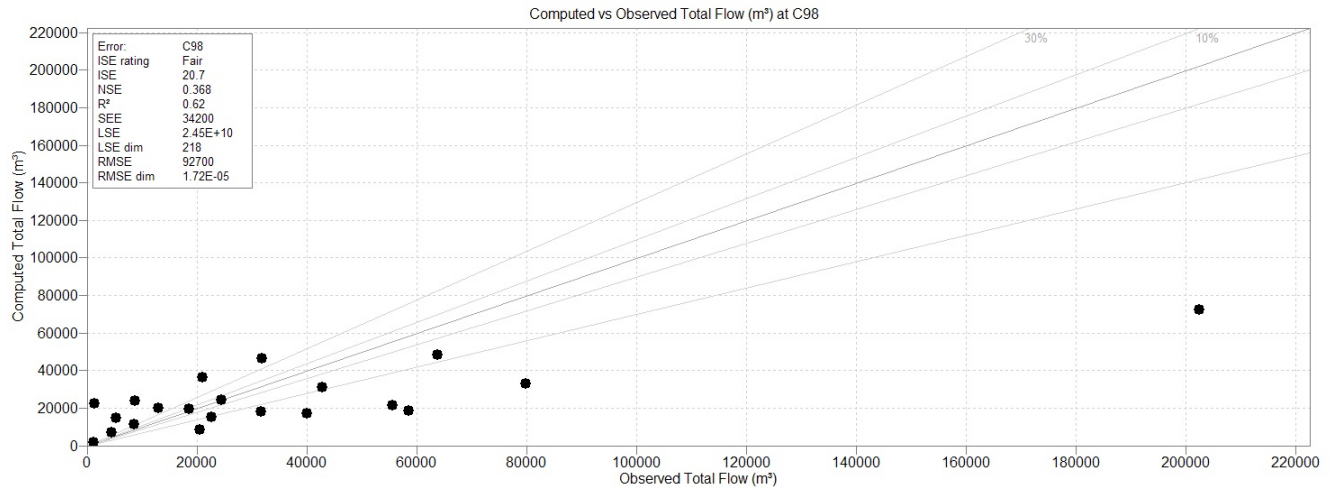


Figure 4.32: Verification error analysis for total flow during single aquifer simulation

No Aquifer Simulation

As expected from this no aquifer configuration model outputs have produced dramatically lower total flow volumes. Figure 4.33 displays this lack of modeling capability clearly. All data points were close to x-axis indicating poor modeling results.

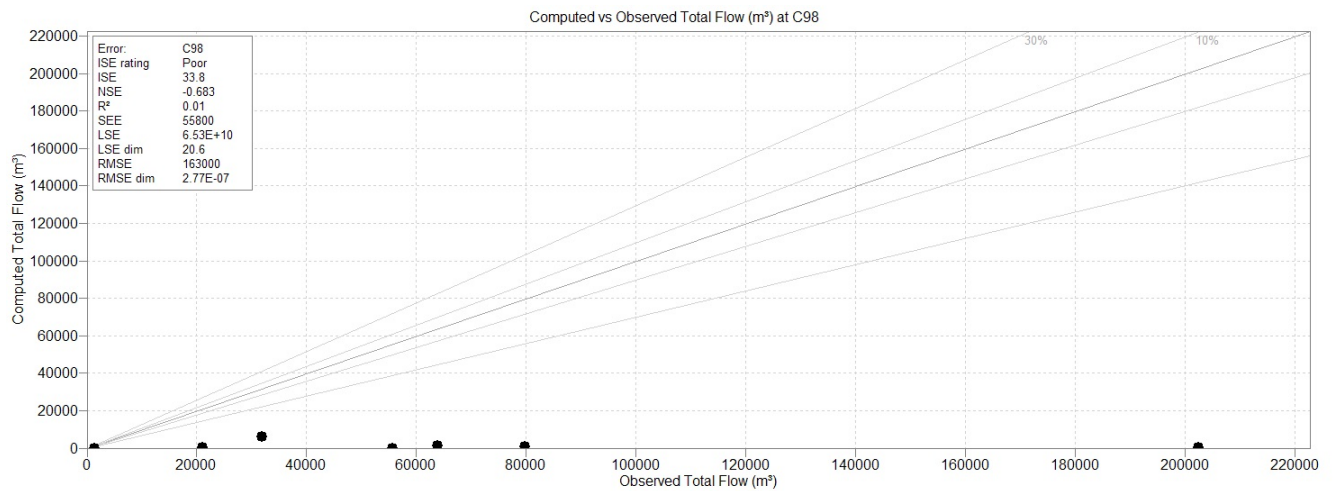


Figure 4.33: Verification error analysis for total flow during no aquifer simulation

4.2.4 Statistical Summary

Following recommendations provided by Moriasi et al. (2007), Krause et al. (2005) and Legates and McCabe (1999), not only should graphical methods be used to evaluate a models performance but also a compilation of statistical parameters. More specifically Legates and McCabe (1999) suggest that at least one dimensionless statistics and one absolute error index statistic should be used in the analysis. For this study the Nash-Sutcliffe efficiency (NSE) and root mean square error ($RMSE$) provided the latter respectively and also included is the coefficient of determination (R^2). Each of the previous were determined between the predicted (P) and observed runoff values (O) over the entire calibration and verification periods. Methods used by PCSWMM to determine each of these statistics are seen in Equations 4.1-4.3.

$$R^2 = \frac{\sum_{i=1}^n (O_i - \bar{O})(P_i - \bar{P})}{\sqrt{\sum_{i=1}^n (O_i - \bar{O})^2} \sqrt{\sum_{i=1}^n (P_i - \bar{P})^2}} \quad (4.1)$$

$$NSE = 1 - \frac{\sum_{i=1}^n (O_i - P_i)^2}{\sum_{i=1}^n (O_i - \bar{O})^2} \quad (4.2)$$

$$RMSE = \sqrt{\sum_{i=1}^n (O_i - P_i)^2} \quad (4.3)$$

Performance ratings, Table 4.12, were also assigned to NSE values based upon a collaboration of studies organized by Moriasi et al. (2007). These rating categories were based upon models run at the monthly time scale but are still assumed to be valid in this sub-hourly simulation.

Table 4.12: Performance ratings for NSE, (Moriassi et al., 2007)

Performance Rating	NSE
Very good	$0.75 < NSE \leq 1.00$
Good	$0.65 < NSE \leq 0.75$
Satisfactory	$0.50 < NSE \leq 0.65$
Unsatisfactory	$NSE \leq 0.50$

Examining Table 4.13 for calibration statistics it can be seen that out of the three configurations created the no aquifer configuration performed the poorest with respect to R^2 values. During maximum and mean flow results, R^2 values have fallen below 0.5 or the minimum value that is considered a satisfactory result, (Moriassi et al., 2007). However, during the total volume the no aquifer configuration did produce a R^2 value of 0.9. This is misleading as it would suggest a good agreement between modeled and observed runoff which was not the case. Now examining the NSE values of the no aquifer configuration, prior observations of a poor modeling effort based on R^2 values is reinforced by NSE values. With ranges between $-\infty$ and 1.0, where 1 is a optimal value, 0 is a neutral value and $-\infty$ is the worst case, this configuration hasn't produced values above 0.07 in all categories. These NSE values indicate a unsatisfactory simulation result even where the R^2 value of total volume indicated a good match. Finally, when examining $RMSE$ values for this configuration only the mean flow has resulted in a value close to 0. According with literature presented by Moriassi et al. (2007), values 0 indicate a perfect fit between modeled and computed data sets. Based on the prior statistics described and present in Table 4.13 the no aquifer configuration has produced unacceptable results during the calibration period.

Table 4.13: Calibration error analysis for all simulations performed

Calibration Error									
Model Configuration	Max Flow (m ³ /s)			Mean Flow (m ³ /s)			Total Volume (m ³)		
	R ²	NSE	RMSE	R ²	NSE	RMSE	R ²	NSE	RMSE
No Aquifer	0.448	0.034	2.500	0.390	-0.333	0.344	0.904	0.070	101000
Multiple Aquifer	0.674	0.292	2.130	0.941	0.532	0.246	0.986	0.699	61700
Single Aquifer	0.523	0.230	2.130	0.934	0.491	0.230	0.986	0.653	66000

Continuing to analyze Table 4.13 it can be seen that the multiple aquifer configuration has exceeded over the single configuration values of R^2 in two of the three categories. Though both configurations produced R^2 above the acceptable 0.5 provided from Moriasi et al. (2007), resulting in each having satisfactory error variance. To distinguish these two configurations further the NSE values must be inspected. NSE values for each of these configurations are relatively close in each category. However, the multiple aquifer model has produced satisfactory results in the mean flow and total volume categories. This fact provides evidence toward the multiple configuration performing the best for all three categories with the exception of an unsatisfactory NSE value during the maximum flow comparison.

Verification errors are presented in Table 4.14 for each model configuration and calculated over the entire duration of this period. Once again the no aquifer configuration has proved to be the worst in each statistic over every category. It has not produced R^2 values above 0.05 and NSE values followed similar trends as not one value was above 0. This outcome was expected as these results were the main reason for the addition of a aquifer compartment of *SWMM*.

Disregarding the no aquifer configuration, details on multiple and single configurations now come into light. During maximum flow comparisons both configurations performed poorly. Each did not achieve an R^2 value greater then 0.5 and NSE values were close to zero or below. Mean flow comparisons provided better results as the multiple aquifer configuration displayed a R^2 value just above 0.5, a NSE value of 0.45 and a $RMSE$ of 0.45. The single aquifer configuration however under-performed in this category producing results in each statistic below recommendations and the multiple aquifer configuration. Lastly, looking into

the total volume category it is seen that both the single and multiple aquifer configurations produced R^2 values above 0.5. The multiple aquifer configuration has produced the higher value once again in this category. Using NSE values to distinguish these two further it is seen that the multiple aquifer configuration has produced an NSE of 0.68 which has fallen into the "Good" performance rating.

Table 4.14: Verification error analysis for all simulations performed

Verification Error									
Model Configuration	Max Flow (m ³ /s)			Mean Flow (m ³ /s)			Total Volume (m ³)		
	R ²	NSE	RMSE	R ²	NSE	RMSE	R ²	NSE	RMSE
No Aquifer	0.056	-0.343	5.710	0.012	-1.370	0.857	0.010	-0.683	163000
Multiple Aquifer	0.123	0.007	3.340	0.505	0.455	0.454	0.753	0.686	82600
Single Aquifer	0.223	-0.023	3.580	0.340	0.201	0.451	0.620	0.368	92700

After examining each configurations outcomes with respect to the statistics described above some conclusions can be made about the best simulation results. During calibration effort the single and multiple aquifer configurations provided the best results in the maximum flow, mean flow and total volume categories which were very comparable. Both configurations provided statistics in the satisfactory to good range with respect to NSE values. R^2 values followed the same path as each configuration had values above 0.5. However, the multiple aquifer configuration was able to simulate all three categories with the best performance during calibration efforts. Continuing to the verification period results from the single and multiple aquifer configurations both performed poorly during the maximum flow category. The mean flow produced similarly poor results for the single aquifer configuration as it was unable to meet minimum R^2 and NSE values. On the other hand the multiple aquifer configuration met minimum R^2 requirements but fell just short of a satisfactory NSE value while exceeding the single aquifer configuration performance. Finally, investigating the total volume category of Table 4.14 the multiple aquifer configuration surpasses in each statistic once again. Combining all of the prior examinations the multiple aquifer configuration has been most consistent in modeling WS-AGC. In summary this *SWMM* configuration models peak flows poorly but is able to simulate total volumes fairly well.

Chapter 5

Summary of Findings and Suggestions for Future Studies

5.1 Summary

The investigations involved the development of field and numerical studies to represent hydrological processes at WS-AGC. During this study the first objective of developing a field monitoring program was met and exceeded. Now within WS-AGC there are three rain gauges, two weirs, four groundwater wells and a Kestrel 4500 weather meter. As construction efforts began each piece of equipment was set online at different time frames due to delays in weather and construction time. The first and longest recording devices installed at WS-AGC were three rain gauges. They have recorded local rainfall since early February 2012 producing a short, year and 6 months, duration of data. Even though data from the field monitoring program has only been collected for this short duration, insights into many dynamic aspects of the local hydrological cycle have been observed.

Early field data collected presented many interesting and significant findings related to the hydrology of WS-AGC. Rainfall runoff events have shown evidences of an alternating transition between losing/gaining stream flow regimes. As wet and dry periods occur over the year this phenomena was seen in recorded hydrographs. Wet period runoff events showed large increases in recession times while dry period runoff events typically displayed short recession times. When comparing similar size rainfall events from dry to wet periods, dramatic differences were seen from one season to the other.

In forested shallow soil watersheds, the vertical hydraulic conductivity of the soil is often high, resulting in rapid conduction of infiltrated water from the near surface of the sub-catchment through the soil matrix to the subsurface boundary below (Axworthy and Karney, 1999). Fast rates of infiltration along with a low permeable subsurface layer are

thought to have caused increased groundwater elevations. These increases in groundwater elevations were mainly seen during the wet period and are hypothesized to have supported extended contributions of flow. On the contrary, dry period events seen during 2012 displayed large peak flows but without the extended recession curve. The groundwater levels were unfortunately not monitored during this time frame but the current hypothesis is that low or none existing levels allowed for excessive infiltration and minimal runoff. Despite the lack of groundwater monitoring, it is also speculated that during this time there existed a disconnection between groundwater and channel water elevations.

Another interesting phenomena seen in the shallow groundwater wells was evapotranspiration (*ET*). During the largest differences in water table elevations observed, an amplitude of 2.8 cm was measured over a 12 hour period. Declines and ascents throughout the record followed specific diurnal patterns. Lowest levels were seen during mid-day to mid-afternoon hours and recovering water table elevations occurred during late-afternoon to late-night hours. Similar observations were seen in undeveloped forested watersheds during studies performed by (Czikowsky and Fitzjarrald, 2004; Gribovszki et al., 2008, 2010). As discovered from Czikowsky and Fitzjarrald (2004), Gribovszki et al. (2008) and Gribovszki et al. (2010), *ET* is responsible for large amounts of losses experienced in the natural watershed. This component of the hydrology must continue to be analyzed in order to better understand its role in the WS-AGC water budget.

Field data including rainfall, runoff, atmospheric pressure and temperature recorded from the 15 month study period were incorporated in a *SWMM* watershed model. Focus during model development was on creating a modeling configuration that represented the local physical features as well as model parameters with reasonable and defensible values. This was achieved with the use of GIS, field surveys, literature studies and engineering judgment.

Through a sound approach during modeling development, this study added a realistic assessment of the model's replication abilities. During calibration efforts the multiple aquifer,

single aquifer and no aquifer configurations were analyzed and compared using graphical and statistical methods. Out of the three configurations the multiple aquifer proved to be the leader in modeling mean flow and total volumes. Statistical values for the multiple aquifer configuration were ($R^2=0.94$ and $NSE=0.53$) and ($R^2=0.98$ and $NSE=0.69$) for both mean flow and total volumes respectively. Maximum flows were not simulated as well with statistical values of ($R^2=0.67$ and $NSE=0.29$) produced from the multiple aquifer configuration.

During the verification stage of the model, results from the multiple aquifer configuration showed the best correlation with observed field data. Maximum flow conditions were poorly simulated with R^2 and NSE values well below minimum requirements. When simulating mean flows the multiple aquifer configuration met minimum R^2 requirements but fell just short of a satisfactory NSE value, ($R^2=0.51$ and $NSE=0.34$). However, the multiple aquifer configuration exceeded in total volumes simulated. This configuration met and exceed minimum requirements for both statistical values, ($R^2=0.75$ and $NSE=0.69$).

Overall, *SWMM* performed well with regards to mean and total flows produced from the multiple and single aquifer configurations. It however was unable to capture peak discharge events observed in the field with any reliable accuracy. Depending on what type of flow category that the user is interested in, *SWMM* could either constitute as a great tool or a misleading one for pre-development watershed studies. Since most pre-development studies do not have the opportunity to perform collection of localized hydrological data, accuracy of outputs from these constructed model may never truly be known. If peak discharges are of concern during any undeveloped study which does not have observed data, then *SWMM* is likely to be a ill-advised alternative. However, during this study total flow volumes were of key interest and such model outputs were deemed satisfactory. The model created for WS-AGC will ultimately be applied to simulate the feasibility of a pond to be sustained. Inflow volumes for the reservoir, representative of a small pond, will be critical in determining its capabilities of supporting water.

5.2 Suggested Future Studies

Work completed has provided an excellent foundation to continue studying WS-AGC's hydrology. One of most important items to be continued is field data collection. Data should be continually collected and installed equipment maintained in order to uphold measurement integrity. This includes maintenance and collection from weirs, rain gauges, groundwater wells and meteorological station. Long term hydrological data will provided more confidence in judgments about the interactions between intrinsic processes at WS-AGC.

SWMM development must also continue as new insights have been produced from soil studies and shallow groundwater well data. Using the four monitoring wells now existing at WS-AGC the groundwater dynamics must be examined in more detail. During soil boring operations, material below the litterfall layer has shown very low permeability of approximately $2.83 \times 10^{-8} \frac{cm}{s}$. These developments could assist in a new approach for implementing the aquifer compartment in *SWMM*.

During this study data was insufficient from the rectangular weir to attempt calibration and verification processes. New model developments should also focus on data from both rectangular and broad crested weirs. This will ensure that upper portions and lower portions of WS-AGC are simulated accurately through numerical models such as *SWMM*.

Bibliography

- Akan, O. A. (1993). *Urban Stormwater Hydrology: A Guide to Engineering Calculations*. Lancaster: Technomic Publishing Co., Inc.
- Amatya, D., Harrison, C., and Trettin, C. (2007). Water quality of two first order forested watersheds in coastal south carolina. *Notes*.
- Axworthy, D. H. and Karney, B. W. (1999). Modeling surface and subsurface runoff in a forested watershed. *Journal of Hydrologic Engineering*, 4(2):165–173.
- Borah, D. K., Weist, J. H., Wall, J. D., Powell, D. N., et al. (2009). Watershed models for storm water management: Comparing hydrologic and hydraulic procedures. ASCE.
- Bormann, H. (2011). Sensitivity analysis of 18 different potential evapotranspiration models to observed climatic change at german climate stations. *Climatic change*, 104(3-4):729–753.
- Brater, E. F., King, H. W., and James E. Lindell (1996). *Handbook of hydraulics*. McGraw-Hill New York.
- Czikowsky, M. J. and Fitzjarrald, D. R. (2004). Evidence of seasonal changes in evapotranspiration in eastern us hydrological records. *Journal of Hydrometeorology*, 5(5):974–988.
- Davis, J., Rohrer, C., and Roesner, L. (2007). Calibration of rural watershed models in the north carolina piedmont ecoregion. In *Proceedings of the 2007 World Environmental and Water Resources Congress: Restoring Our Natural Habitat*. Reston: ASCE, pages 1–10.
- Dodge, R. (2001). *Water measurement manual: A guide to effective water measurement practices for better water management*. Government Printing Office.

- Federer, C. A. and Lash, D. (1978). Brook: A hydrologic simulation model for eastern forests.
- Gribovszki, Z., Kalicz, P., Szilágyi, J., and Kucsara, M. (2008). Riparian zone evapotranspiration estimation from diurnal groundwater level fluctuations. *Journal of Hydrology*, 349(1):6–17.
- Gribovszki, Z., Szilágyi, J., and Kalicz, P. (2010). Diurnal fluctuations in shallow groundwater levels and streamflow rates and their interpretation—a review. *Journal of Hydrology*, 385(1):371–383.
- Hamon, W. R. (1963). Computation of direct runoff amounts from storm rainfall c1).
- Harder, S. V., Amatya, D. M., Callahan, T. J., Trettin, C. C., and Hakkila, J. (2007). Hydrology and water budget for a forested atlantic coastal plain watershed, south carolina1. *JAWRA Journal of the American Water Resources Association*, 43(3):563–575.
- Hargreaves, G. H. and Allen, R. G. (2003). History and evaluation of hargreaves evapotranspiration equation. *Journal of Irrigation and Drainage Engineering*, 129(1):53–63.
- James, W. R. C., Wan, B., and James, W. (2002). Implementation in pcswm using genetic algorithms for auto calibration and design-optimization. In *Proc. 9th Int. Conf. Urban Drainage—Global Solutions for Urban Drainage*.
- Jang, S., Cho, M., Yoon, J., Yoon, Y., Kim, S., Kim, G., Kim, L., and Aksoy, H. (2007). Using swmm as a tool for hydrologic impact assessment. *Desalination*, 212(1):344–356.
- Krause, P., Boyle, D., and Bäse, F. (2005). Comparison of different efficiency criteria for hydrological model assessment. *Advances in Geosciences*, 5(5):89–97.
- La Torre Torres, I. B., Amatya, D. M., Sun, G., and Callahan, T. J. (2011). Seasonal rainfall–runoff relationships in a lowland forested watershed in the southeastern usa. *Hydrological Processes*, 25(13):2032–2045.

- Legates, D. R. and McCabe, G. J. (1999). Evaluating the use of goodness-of-fit measures in hydrologic and hydroclimatic model validation. *Water Resources Research*, 35(1):233–241.
- Lu, J., Sun, G., McNulty, S. G., and Amatya, D. M. (2005). A comparison of six potential evapotranspiration methods for regional use in the southeastern united states1. *JAWRA Journal of the American Water Resources Association*, 41(3):621–633.
- Makkink, G. (1957). Testing the penman formula by means of lysimeters. *J. Inst. Water Eng*, 11(3):277–288.
- McCuen, R. H., Johnson, P. A., and Ragan, R. M. ((1996)). *Highway Hydrology Hydraulic Design Series*, No.2. Rep. no. FHWA-SA-067.
- Moriasi, D., Arnold, J., Van Liew, M., Bingner, R., Harmel, R., and Veith, T. (2007). Model evaluation guidelines for systematic quantification of accuracy in watershed simulations. *Transactions of the ASABE*, 50(3):885–900.
- Onset (2011). *Data Logging Rain Gauge RG3 and RG3-M User's Manual*. Onset Computer Corportaiion.
- Priestley, C. and Taylor, R. (1972). On the assessment of surface heat flux and evaporation using large-scale parameters. *Monthly weather review*, 100(2):81–92.
- Rossman, L. A. and Supply, W. (2005). *Storm water management model user's manual, version 5.0*. National Risk Management Research Laboratory, Office of Research and Development, US Environmental Protection Agency.
- Sun, G., McNulty, S., Amatya, D., Skaggs, R., Swift Jr, L., Shepard, J., and Riekerk, H. (2002). A comparison of the watershed hydrology of coastal forested wetlands and the mountainous uplands in the southern us. *Journal of Hydrology*, 263(1):92–104.

- Sun, G., Noormets, A., Gavazzi, M., McNulty, S., Chen, J., Domec, J.-C., King, J., Amatya, D., and Skaggs, R. (2010). Energy and water balance of two contrasting loblolly pine plantations on the lower coastal plain of north carolina, usa. *Forest Ecology and Management*, 259(7):1299–1310.
- Thornthwaite, C. and Mather, J. (1955). The water balance. *Climatology*, 8:1–104.
- Thornthwaite, C. and Mather, J. (1957). Instructions and tables for computing potential evapotranspiration and the water balance. *Climatology*, 10.
- Thornthwaite, C. W. (1948). An approach toward a rational classification of climate. *Geographical review*, 38(1):55–94.
- Trajkovic, S. (2005). Temperature-based approaches for estimating reference evapotranspiration. *Journal of irrigation and drainage engineering*, 131(4):316–323.
- Turc, L. (1961). Evaluation des besoins en eau d'irrigation, évapotranspiration potentielle. *Ann. agron*, 12(1):13–49.
- Viessman, W., Lewis, G. L., Knapp, J. W., and Harbaugh, T. E. (2003). *Introduction to hydrology*. Prentice Hall NJ.
- Vörösmarty, C. J., Federer, C. A., and Schloss, A. L. (1998). Potential evaporation functions compared on us watersheds: Possible implications for global-scale water balance and terrestrial ecosystem modeling. *Journal of Hydrology*, 207(3):147–169.
- Wear, D. N. and Greis, J. G. (2002). Southern forest resource assessment: summary of findings. *Journal of Forestry*, 100(7):6–14.
- Winter, T. C. (2007). The role of ground water in generating streamflow in headwater areas and in maintaining base flow¹. *JAWRA Journal of the American Water Resources Association*, 43(1):15–25.

Appendices

Appendix A
Soil Analysis

September 4, 2013



Alabama AGC
5000 Grantswood Road
Irondale, Alabama 35210

Attn: Mr. Jeff Rogers
E: jeffr@alagc.org

Re: Geotechnical Engineering Report
AGC - Auburn University Dam Site
Russell County, Alabama
Terracon Project No. E1135088

Dear Mr. Rogers:

Terracon has completed the geotechnical engineering services for the above referenced project. This study was performed in general accordance with our Proposal PE1130324, dated May 15, 2013.

Subsurface conditions encountered at each boring location are indicated on the accompanying individual boring logs. The approximate location of each boring is indicated on the accompanying Figure A-2, Boring Location Plan. Selected samples were tested in our laboratories to determine physical engineering characteristics of the onsite soils. These tests included: Atterberg limits, grain-size analyses, moisture contents, standard Proctors, Triaxial Shear and permeability tests. The results of the laboratory analysis are included in Appendix B.

We appreciate the opportunity to be of service to you on this project. If you have any questions concerning this report, or if we may be of further service, please contact us.

Sincerely,
Terracon Consultants, Inc.

Charlie L. Bragg
Field Project Manager

Jerome A. Smith, P.E.
Manager, Geotechnical Services
Alabama P.E. No. 20478



Terracon Consultants, Inc. 110 12TH Street North Birmingham, Alabama 35203
P [205] 942-1289 F [205] 443- 5302 terracon.com

Geotechnical



Environmental



Construction Materials



Facilities

APPENDIX A – FIELD EXPLORATION

Exhibit A-1	Site Location Map
Exhibit A-2	Boring Location Plan
Exhibit A-3	Field Exploration Description
Exhibits A-4 to A-9	Boring Logs, Borings B-1 through B-6

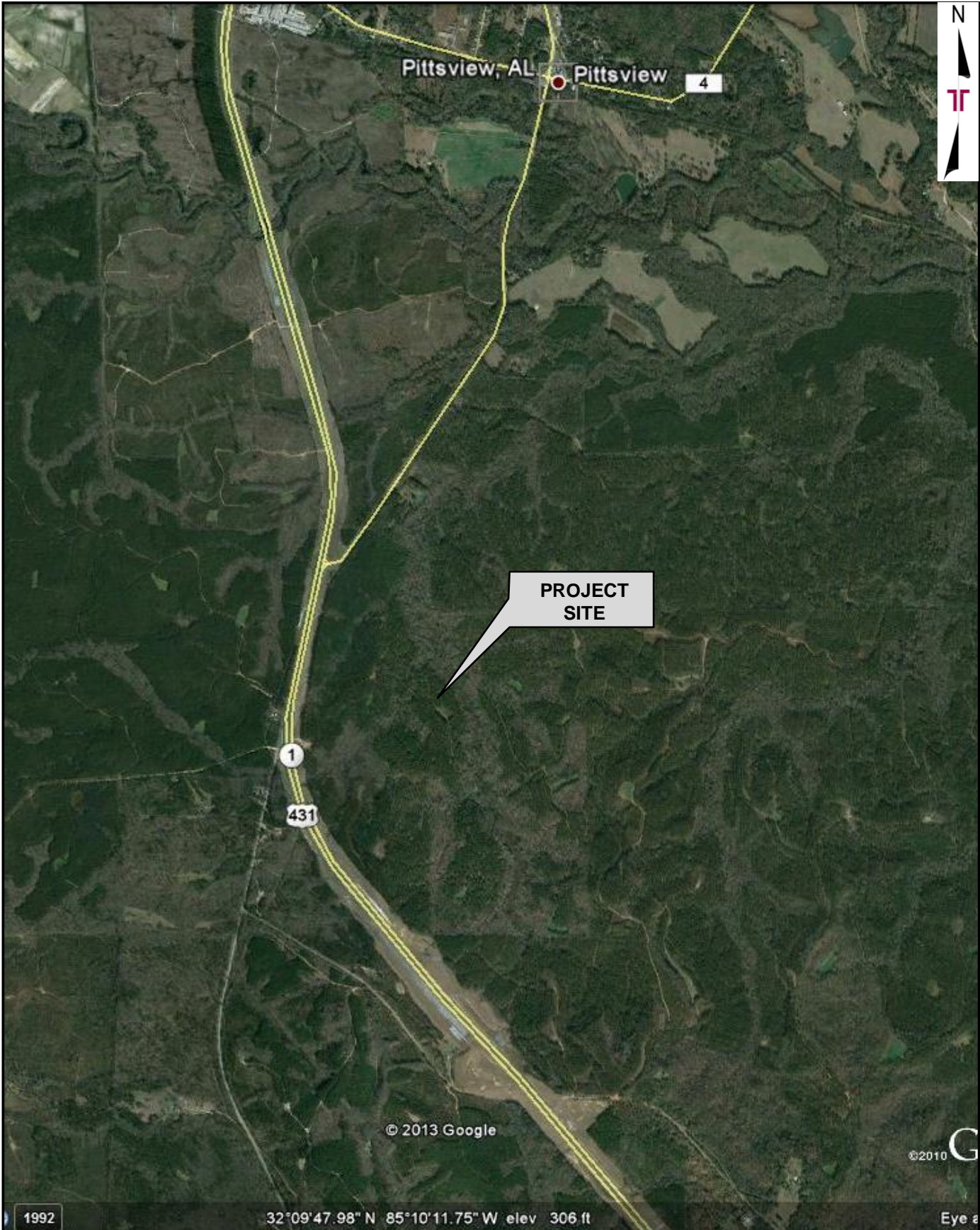
APPENDIX B – LABORATORY TESTING

Exhibit B-1	Laboratory Testing
-------------	--------------------

APPENDIX C – SUPPORTING DOCUMENTS

Exhibit C-1	General Notes
Exhibit C-2	Unified Soil Classification System

APPENDIX A
FIELD EXPLORATION



Project Manager:	CLB
Drawn By:	CLB
Checked By:	JAS
Approved By:	JAS
Proposal No.:	E1135088
Scale:	NTS
File Name:	E1135088.1.pdf
Date:	07-10-2013

Terracon

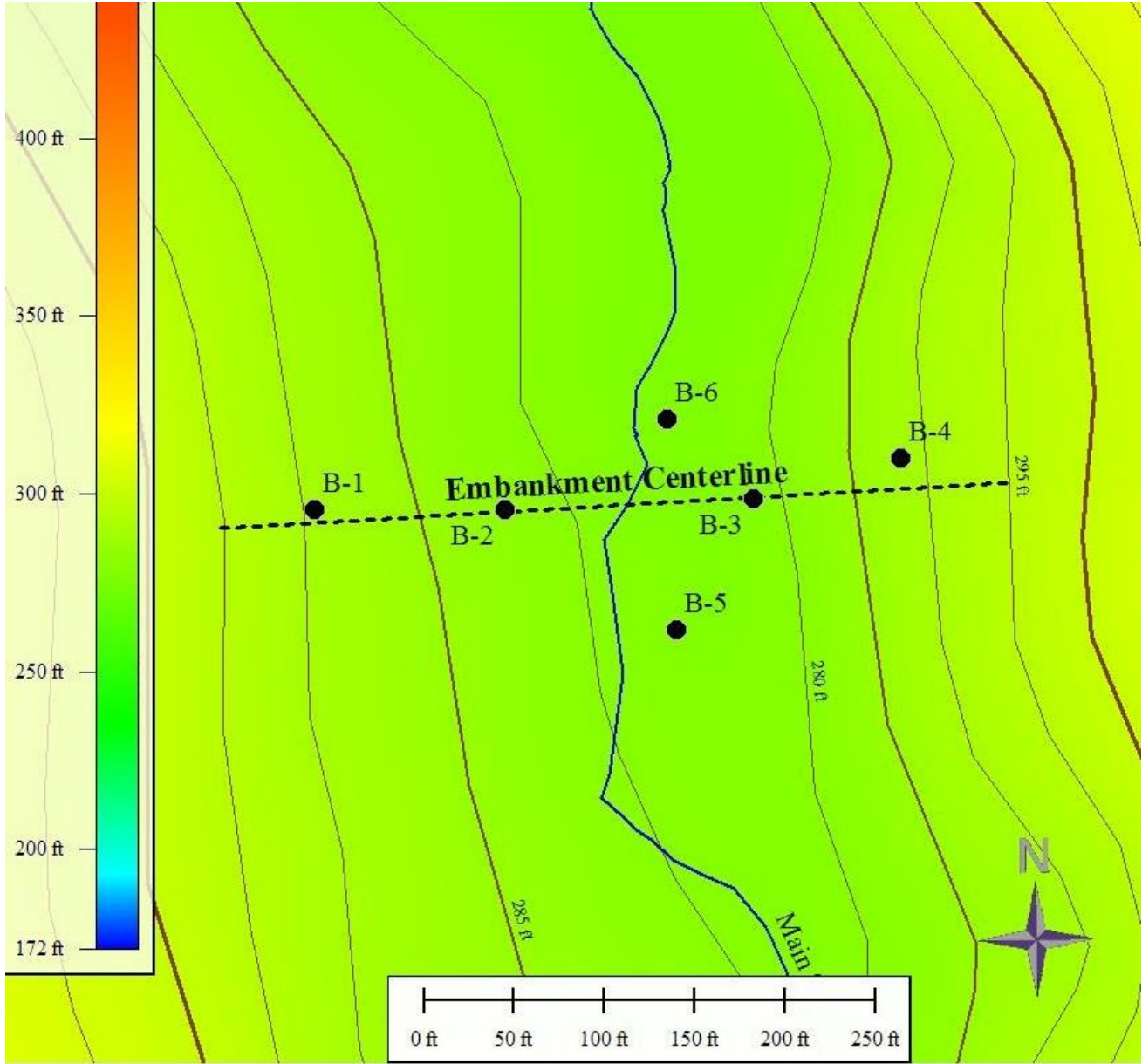
110 12th Street North Birmingham, Alabama 35203
 PH. (205) 942-1289 FAX. (205) 443-5302

SITE LOCATION MAP

AGC – AUBURN UNIVERSITY DAM SITE
 RUSSELL COUNTY, ALABAMA

Exhibit

A-1



● **BORING LOCATION**

DIAGRAM IS FOR GENERAL LOCATION ONLY, AND IS NOT INTENDED FOR CONSTRUCTION PURPOSES

DIAGRAM PROVIDED BY KYLE MOYNIHAN

Project Manager:	CLB
Drawn By:	CLB
Checked By:	JAS
Approved By:	JAS
Proposal No.:	E1135088
Scale:	As Shown
File Name:	E1135088.2.pdf
Date:	07-10-2013

Terracon

110 12th Street North
 PH. (205) 942-1289
 Birmingham, Alabama 35203
 FAX. (205) 443-5302

BORING LOCATION PLAN

AGC – AUBURN UNIVERSITY DAM SITE
 RUSSELL COUNTY, ALABAMA

Exhibit

A-2

Geotechnical Engineering Report

AGC- Auburn University Dam Site ■ Russell County, Alabama
September 4, 2013 ■ Terracon Project No. E1135088

Field Exploration Description

A total of six (6) test borings were performed across the site. These borings were extended to a depth of approximately 20 feet below the existing surface grade. The boring locations were marked in the field by measuring from the dam abutment stakes set by Auburn University representatives. The location of each boring was then recorded by Auburn University representatives utilizing a GPS receiver and plotted on the provided Boring Location Plan included in Appendix A.

The borings were drilled with an ATV-mounted CME-550 rotary drill rig with an automatic hammer using hollow-stem augers and rock coring equipment to advance the borehole. Samples of the soil encountered in the boring were obtained using the split-barrel sampling procedures (general accordance with ASTM D1586.

In the split-barrel sampling procedure, the number of blows required to advance a standard 2-inch O.D. split-barrel sampler the last 12 inches of the typical total 18-inch penetration by means of a 140-pound hammer with a free fall of 30 inches, is the Standard Penetration Test N-value (SPT-N). This value is used to estimate the in situ relative density of cohesionless soils and consistency of cohesive soils.

Following the completion of the SPT borings, boring B-2 was offset minimally and the drill rigs were utilized to push a total of three (3) thin-walled Shelby tubes. The Shelby tubes recovered relatively undisturbed samples of the in-situ soils. Additionally, two (2) bulk samples were collected at boring location B-1, at depths of 0 -5 feet and 5-10 feet.

The soil samples were placed in containers to reduce moisture loss, tagged for identification, and taken to our laboratory (general accordance with ASTM D4220) for further examination, testing, and classification. Information provided on the boring logs attached to this report includes soil descriptions, consistency evaluations, boring depths, sampling intervals, and groundwater conditions.

A field log of the boring was prepared by the Terracon engineer. The log included visual classifications (general accordance with ASTM D5434) of the materials encountered during drilling as well as the engineer's interpretation of the subsurface conditions between samples. Final boring log included with this report represent the engineer's interpretation of the field log and include modifications based on laboratory observation and tests of the samples.

BORING LOG NO. B-1

PROJECT: AGC Auburn University Dam Site

CLIENT: Alabama AGC Irondale, Alabama

SITE: Auburn University Auburn, Alabama

GRAPHIC LOG	LOCATION See Exhibit A-2	DEPTH (Ft.)	WATER LEVEL OBSERVATIONS	SAMPLE TYPE	FIELD TEST RESULTS	WATER CONTENT (%)	ATTERBERG LIMITS		PERCENT FINES
	DEPTH						LL-PL-PI		
5.0	SANDY CLAY (CL) , brown and yellowish red mottled, soft becomes medium stiff	5		X	1-1-2 N=3	20			
5.0				X	3-3-3 N=6		45-25-20	67	
18.5	FAT CLAY (CH) , trace fine sand, light gray and brownish yellow mottled, stiff, micaceous	5		X	2-4-6 N=10	43	59-30-29	88	
18.5				X	3-6-7 N=13				
18.5				X	4-5-8 N=13	32			
20.0	SANDY CLAY (CL) , dark gray, hard, micaceous	20		X	7-13-19 N=32				
Boring Terminated at 20 Feet									

Stratification lines are approximate. In-situ, the transition may be gradual.

Advancement Method:
Hollow-stem auger

See Exhibit A-3 for description of field procedures.
See Appendix B for description of laboratory procedures and additional data (if any).

Notes:

Abandonment Method:
Borings backfilled with soil cuttings upon completion.

See Appendix C for explanation of symbols and abbreviations.

WATER LEVEL OBSERVATIONS

No free water observed during boring



110 12th Street North
Birmingham, Alabama

Boring Started: 7/10/2013

Boring Completed: 7/10/2013

Drill Rig: CME-550

Driller: B.C.

Project No.: E1135088

Exhibit: A-4

THIS BORING LOG IS NOT VALID IF SEPARATED FROM ORIGINAL REPORT.

BORING LOG NO. B-2

PROJECT: AGC Auburn University Dam Site

CLIENT: Alabama AGC Irondale, Alabama

SITE: Auburn University Auburn, Alabama

GRAPHIC LOG	LOCATION See Exhibit A-2	DEPTH (Ft.)	WATER LEVEL OBSERVATIONS	SAMPLE TYPE	FIELD TEST RESULTS	WATER CONTENT (%)	ATTERBERG LIMITS		PERCENT FINES
	DEPTH						LL-PL-PI		
4.0	SANDY CLAY (CL) , brown and yellowish red mottled, medium stiff			X	2-2-3 N=5				
8.0	FAT CLAY (CH) , trace fine sand, light gray and brownish yellow mottled, soft	5		X	2-2-3 N=5	36			
8.0				X	1-1-3 N=4	37			
13.5	SILTY SAND (SM) , brown and gray, loose		▽	X	1-3-5 N=8				
20.0	SANDY CLAY (CL) , dark gray, very stiff, micaceous becomes hard	15		X	4-10-14 N=24	29			
20.0	Boring Terminated at 20 Feet	20		X	6-13-22 N=35				

Stratification lines are approximate. In-situ, the transition may be gradual.

Advancement Method:
Hollow-stem auger

See Exhibit A-3 for description of field procedures.
See Appendix B for description of laboratory procedures and additional data (if any).

Notes:

Abandonment Method:
Borings backfilled with soil cuttings upon completion.

See Appendix C for explanation of symbols and abbreviations.

WATER LEVEL OBSERVATIONS

▽ Water observed at 9 feet during boring



Boring Started: 7/10/2013

Boring Completed: 7/10/2013

Drill Rig: CME-550

Driller: B.C.

Project No.: E1135088

Exhibit: A-5

THIS BORING LOG IS NOT VALID IF SEPARATED FROM ORIGINAL REPORT.

BORING LOG NO. B-3

PROJECT: AGC Auburn University Dam Site

CLIENT: Alabama AGC Irondale, Alabama

SITE: Auburn University Auburn, Alabama

GRAPHIC LOG	LOCATION See Exhibit A-2	DEPTH (Ft.)	WATER LEVEL OBSERVATIONS	SAMPLE TYPE	FIELD TEST RESULTS	WATER CONTENT (%)	ATTERBERG LIMITS		PERCENT FINES
							LL-PL-PI		
	DEPTH								
0.5	6 inches TOPSOIL			X	3-3-5 N=8	22			
	SANDY CLAY (CL) , brown and yellowish red mottled, stiff			X	2-3-5 N=8				
		5.0		X	3-6-5 N=11	25			
	SANDY CLAY (CL) , light gray and brownish yellow mottled, stiff			X	17 N=50/3"				
		8.5	▽	X	4-11-15 N=26	25			
	SANDY SILT (ML) , dark gray, hard, micaceous			X	24-19-27 N=46				
		13.5		X					
	SANDY CLAY (CL) , dark gray, very stiff, micaceous			X					
		20.0		X					
	becomes hard			X					
	Boring Terminated at 20 Feet								

Stratification lines are approximate. In-situ, the transition may be gradual.

Advancement Method:
Hollow-stem auger

See Exhibit A-3 for description of field procedures.
See Appendix B for description of laboratory procedures and additional data (if any).

Notes:

Abandonment Method:
Borings backfilled with soil cuttings upon completion.

See Appendix C for explanation of symbols and abbreviations.

WATER LEVEL OBSERVATIONS

▽ Water observed at 9 feet during boring



110 12th Street North
Birmingham, Alabama

Boring Started: 7/10/2013

Boring Completed: 7/10/2013

Drill Rig: CME-550

Driller: B.C.

Project No.: E1135088

Exhibit: A-6

THIS BORING LOG IS NOT VALID IF SEPARATED FROM ORIGINAL REPORT.

BORING LOG NO. B-4

PROJECT: AGC Auburn University Dam Site

CLIENT: Alabama AGC Irondale, Alabama

SITE: Auburn University Auburn, Alabama

GRAPHIC LOG	LOCATION See Exhibit A-2	DEPTH (Ft.)	WATER LEVEL OBSERVATIONS	SAMPLE TYPE	FIELD TEST RESULTS	WATER CONTENT (%)	ATTERBERG LIMITS		PERCENT FINES
							LL-PL-PI		
	DEPTH								
0.3	4 inches TOPSOIL			X	WOH				
2.5	SANDY CLAY (CL) , yellowish red, very soft			X					
8.5	SANDY CLAY (CL) , light gray and yellowish red mottled, medium stiff	5		X	3-3-4 N=7	21			
13.5	SILTY SAND (SM) , light gray and light brown, medium dense	10		X	3-4-6 N=10				
20.0	SANDY SILT (ML) , dark gray and brown, hard, micaceous	15		X	3-5-8 N=13	31			
20.0	SANDY SILT (ML) , dark gray and brown, hard, micaceous	20		X	8-13-24 N=37	22			
20.0	Boring Terminated at 20 Feet	20		X	12-17-20 N=37				

Stratification lines are approximate. In-situ, the transition may be gradual.

Advancement Method:
Hollow-stem auger

See Exhibit A-3 for description of field procedures.
See Appendix B for description of laboratory procedures and additional data (if any).

Notes:

Abandonment Method:
Borings backfilled with soil cuttings upon completion.

See Appendix C for explanation of symbols and abbreviations.

WATER LEVEL OBSERVATIONS

No free water observed during boring



110 12th Street North
Birmingham, Alabama

Boring Started: 7/10/2013

Boring Completed: 7/10/2013

Drill Rig: CME-550

Driller: B.C.

Project No.: E1135088

Exhibit: A-7

THIS BORING LOG IS NOT VALID IF SEPARATED FROM ORIGINAL REPORT.

BORING LOG NO. B-5

PROJECT: AGC Auburn University Dam Site

CLIENT: Alabama AGC Irondale, Alabama

SITE: Auburn University Auburn, Alabama

GRAPHIC LOG	LOCATION See Exhibit A-2	DEPTH (Ft.)	WATER LEVEL OBSERVATIONS	SAMPLE TYPE	FIELD TEST RESULTS	WATER CONTENT (%)	ATTERBERG LIMITS		PERCENT FINES
							LL-PL-PI		
	DEPTH								
2.5	SANDY CLAY (CL) , brown and yellowish red, mottled, stiff			X	3-4-5 N=9				
5.0	CLAY (CL) , with fine sand, gray, brown and yellowish red mottled, medium stiff	5		X	2-3-3 N=6	42			
8.5	SANDY CLAY (CL) , brown, stiff		▽	X	3-5-5 N=10	23			
13.5	SILTY SAND (SM) , brown and gray, loose	10		X	2-3-3 N=6				
20.0	SANDY CLAY (CL) , dark gray, very stiff, micaceous	15		X	5-10-14 N=24	31			
	Boring Terminated at 20 Feet	20		X	6-11-15 N=26				

Stratification lines are approximate. In-situ, the transition may be gradual.

Advancement Method:
Hollow-stem auger

See Exhibit A-3 for description of field procedures.
See Appendix B for description of laboratory procedures and additional data (if any).
See Appendix C for explanation of symbols and abbreviations.

Notes:

Abandonment Method:
Borings backfilled with soil cuttings upon completion.

WATER LEVEL OBSERVATIONS

▽ Water observed at 8 feet during boring



Boring Started: 7/10/2013

Boring Completed: 7/10/2013

Drill Rig: CME-550

Driller: B.C.

Project No.: E1135088

Exhibit: A-8

THIS BORING LOG IS NOT VALID IF SEPARATED FROM ORIGINAL REPORT.

BORING LOG NO. B-6

PROJECT: AGC Auburn University Dam Site

CLIENT: Alabama AGC Irondale, Alabama

SITE: Auburn University Auburn, Alabama

GRAPHIC LOG	LOCATION See Exhibit A-2	DEPTH (Ft.)	WATER LEVEL OBSERVATIONS	SAMPLE TYPE	FIELD TEST RESULTS	WATER CONTENT (%)	ATTERBERG LIMITS		PERCENT FINES
							LL-PL-PI		
DEPTH									
0.3	TOPSOIL SANDY CLAY (CL) , brown and yellowish red mottled, medium stiff			X	2-3-3 N=6	38			
5.0	CLAYEY SAND (SC) , brown, loose	5		X	3-3-4 N=7				
8.5	SILTY SAND (SM) , gray, very loose			X	3-4-3 N=7	21			
10.0			▽	X	0-0-3 N=3				
13.5	SANDY CLAY (CL) , dark gray, hard			X	15-16-20 N=36	21			
18.5	SANDY SILT (ML) , dary gray, hard			X	N=50+				
20.0	Boring Terminated at 20 Feet								

Stratification lines are approximate. In-situ, the transition may be gradual.

Advancement Method:
Hollow-stem auger

See Exhibit A-3 for description of field procedures.
See Appendix B for description of laboratory procedures and additional data (if any).

Notes:

Abandonment Method:
Borings backfilled with soil cuttings upon completion.

See Appendix C for explanation of symbols and abbreviations.

WATER LEVEL OBSERVATIONS

▽ Water observed at 10 feet during boring



Boring Started: 7/10/2013

Boring Completed: 7/10/2013

Drill Rig: CME-550

Driller: B.C.

Project No.: E1135088

Exhibit: A-9

THIS BORING LOG IS NOT VALID IF SEPARATED FROM ORIGINAL REPORT.

APPENDIX B
LABORATORY TESTING

Geotechnical Engineering Report

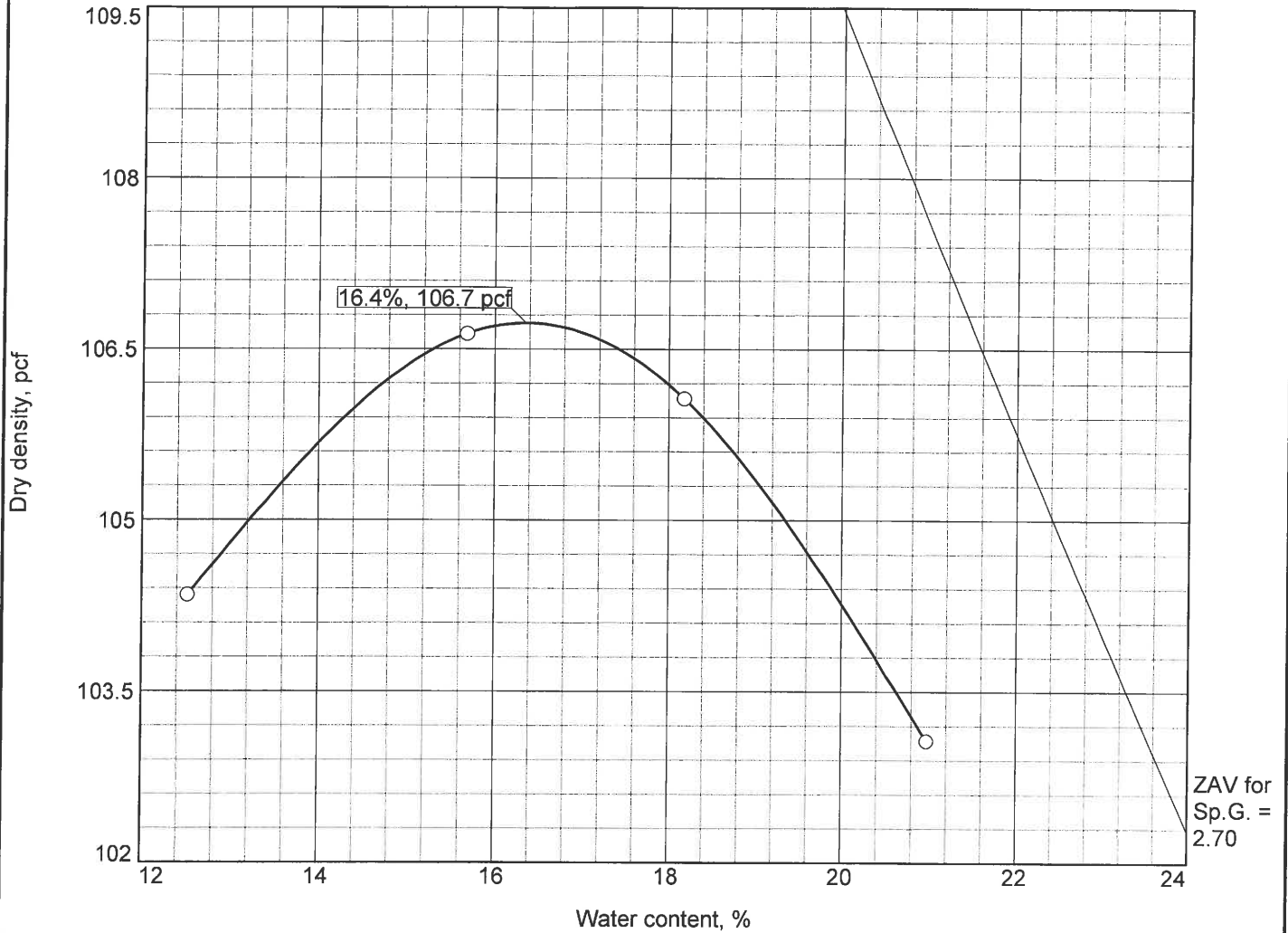
AGC- Auburn University Dam Site ■ Russell County, Alabama
September 4, 2013 ■ Terracon Project No. E1135088

Laboratory Testing

Selected soil samples were tested for properties such as Atterberg limits, grain-size analyses, moisture contents, standard Proctors, Triaxial Shear and permeability tests. The results of the laboratory analysis are included in Appendix B and/or on the boring logs included in Appendix A.

Descriptive classifications of the soils indicated on the boring logs are in accordance with the enclosed General Notes and the Unified Soil Classification System. Also shown are estimated Unified Soil Classification Symbols. A brief description of this classification system is attached to this report. All classification was by visual manual procedures.

COMPACTION TEST REPORT



Test specification: ASTM D 698-07 Method B Standard

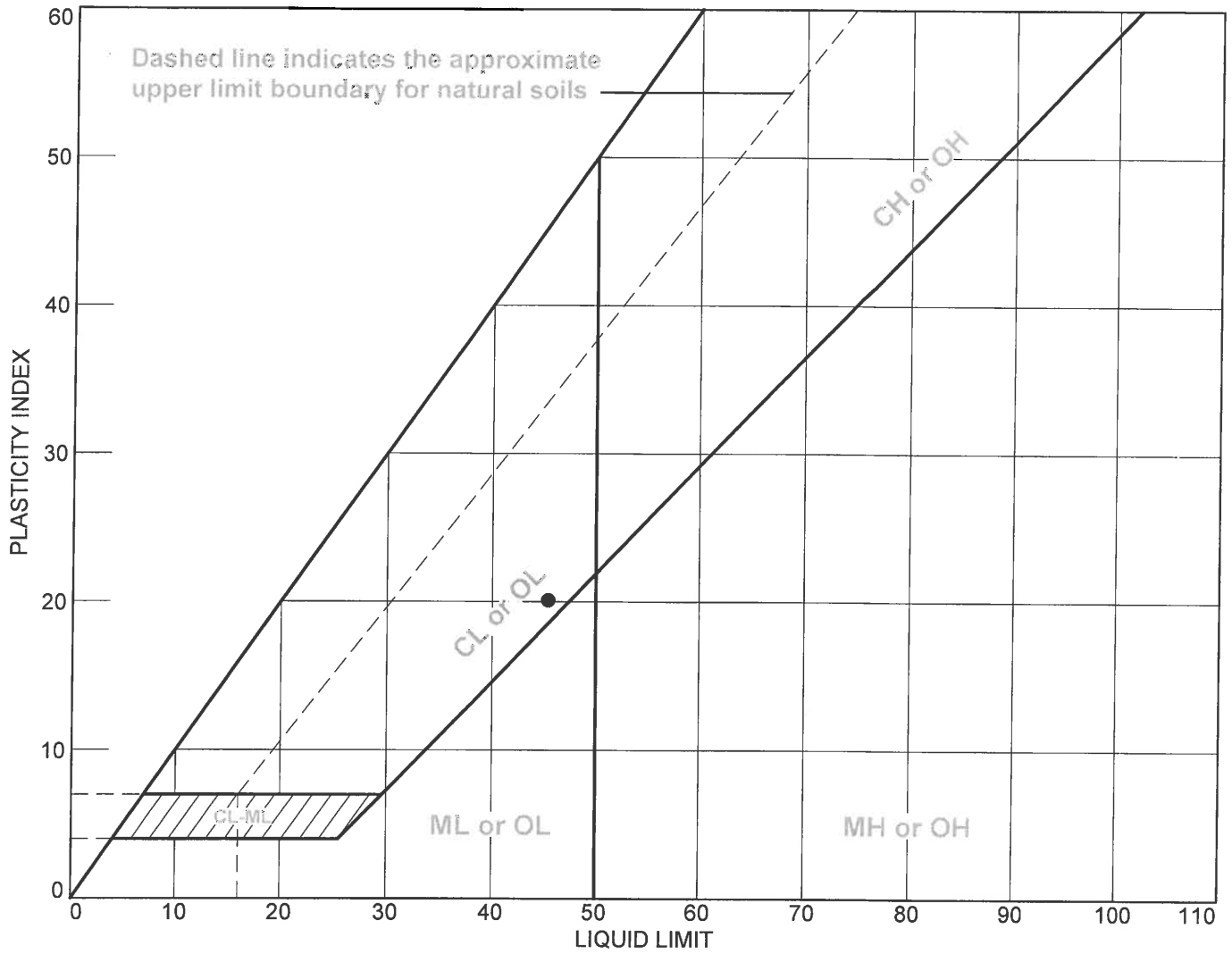
Elev/ Depth	Classification		Nat. Moist.	Sp.G.	LL	PI	% > 3/8 in.	% < No.200
	USCS	AASHTO						
0-5'	CL	A-7-6(12)		2.7	45.4	20.1	0.0	67.0

TEST RESULTS	MATERIAL DESCRIPTION
Maximum dry density = 106.7 pcf Optimum moisture = 16.4 %	light brown sandy lean clay
Project No. E1135088 Client: Project: AGC Dam Site <div style="text-align: right;">Date: 7/23/13</div> ○ Source of Sample: Bulk Sample Number: 13-125	Remarks:
Terracon Consultants, Inc. Birmingham, Alabama	

Figure

Tested By: LW

LIQUID AND PLASTIC LIMITS TEST REPORT



SOIL DATA								
SYMBOL	SOURCE	SAMPLE NO.	DEPTH	NATURAL WATER CONTENT (%)	PLASTIC LIMIT (%)	LIQUID LIMIT (%)	PLASTICITY INDEX (%)	USCS
●	Bulk	13-125	0-5'		25.3	45.4	20.1	CL

Terracon Consultants, Inc.

Birmingham, Alabama

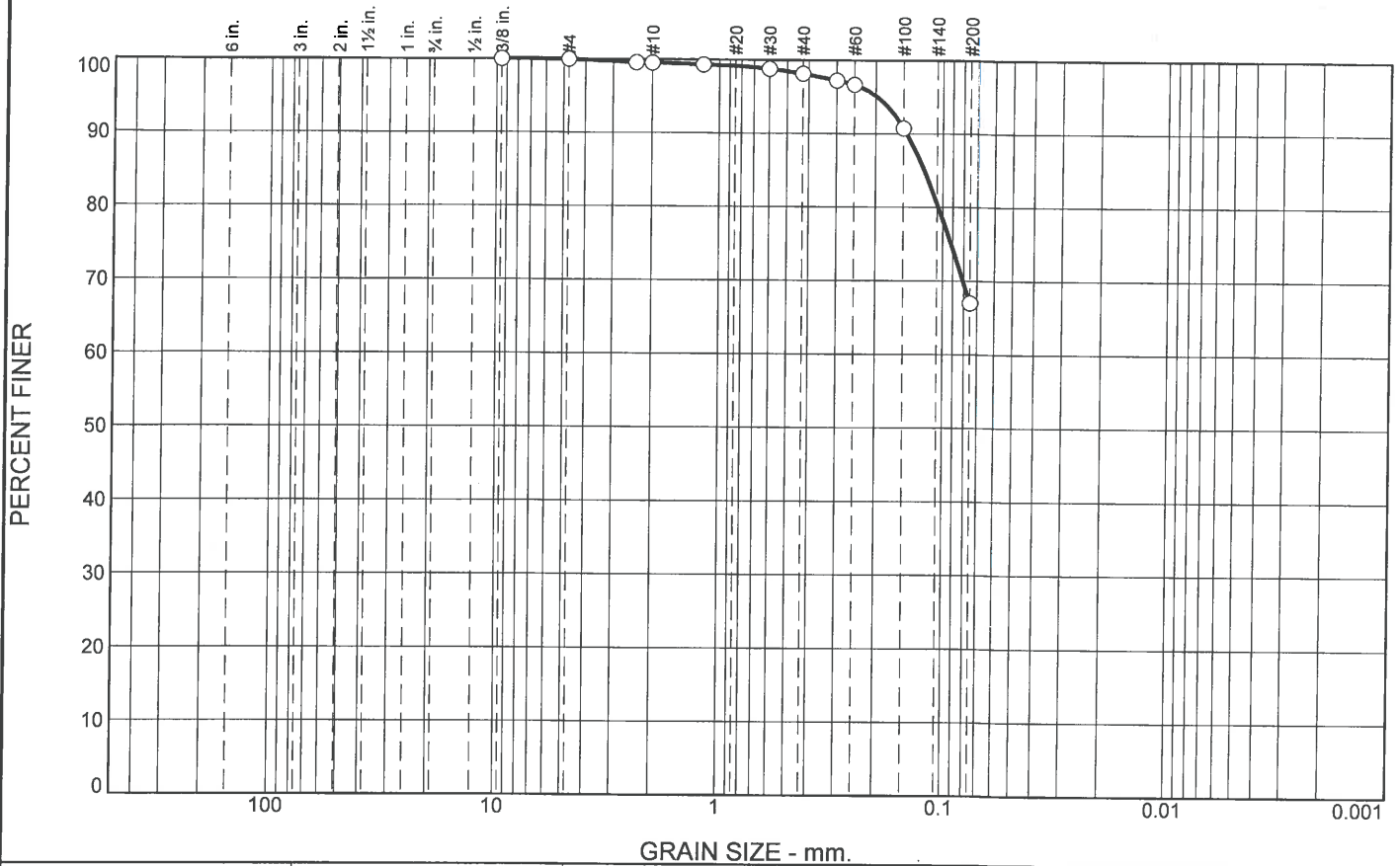
Client:
Project: AGC Dam Site

Project No.: E1135088

Figure

Tested By: LW

Particle Size Distribution Report



% +3"	% Gravel		% Sand			% Fines	
	Coarse	Fine	Coarse	Medium	Fine	Silt	Clay
0.0	0.0	0.0	0.5	1.4	31.1	67.0	

SIEVE SIZE	PERCENT FINER	SPEC.* PERCENT	PASS? (X=NO)
.375"	100.0		
#4	100.0		
#8	99.6		
#10	99.5		
#16	99.3		
#30	98.8		
#40	98.1		
#50	97.3		
#60	96.7		
#100	90.7		
#200	67.0		

Material Description

light brown sandy lean clay

PL= 25.3 **Atterberg Limits** LL= 45.4 PI= 20.1

Coefficients

D₉₀= 0.1452 D₈₅= 0.1213 D₆₀=
D₅₀= D₃₀= D₁₅=
D₁₀= C_u= C_c=

Classification

USCS= CL AASHTO= A-7-6(12)

Remarks

* (no specification provided)

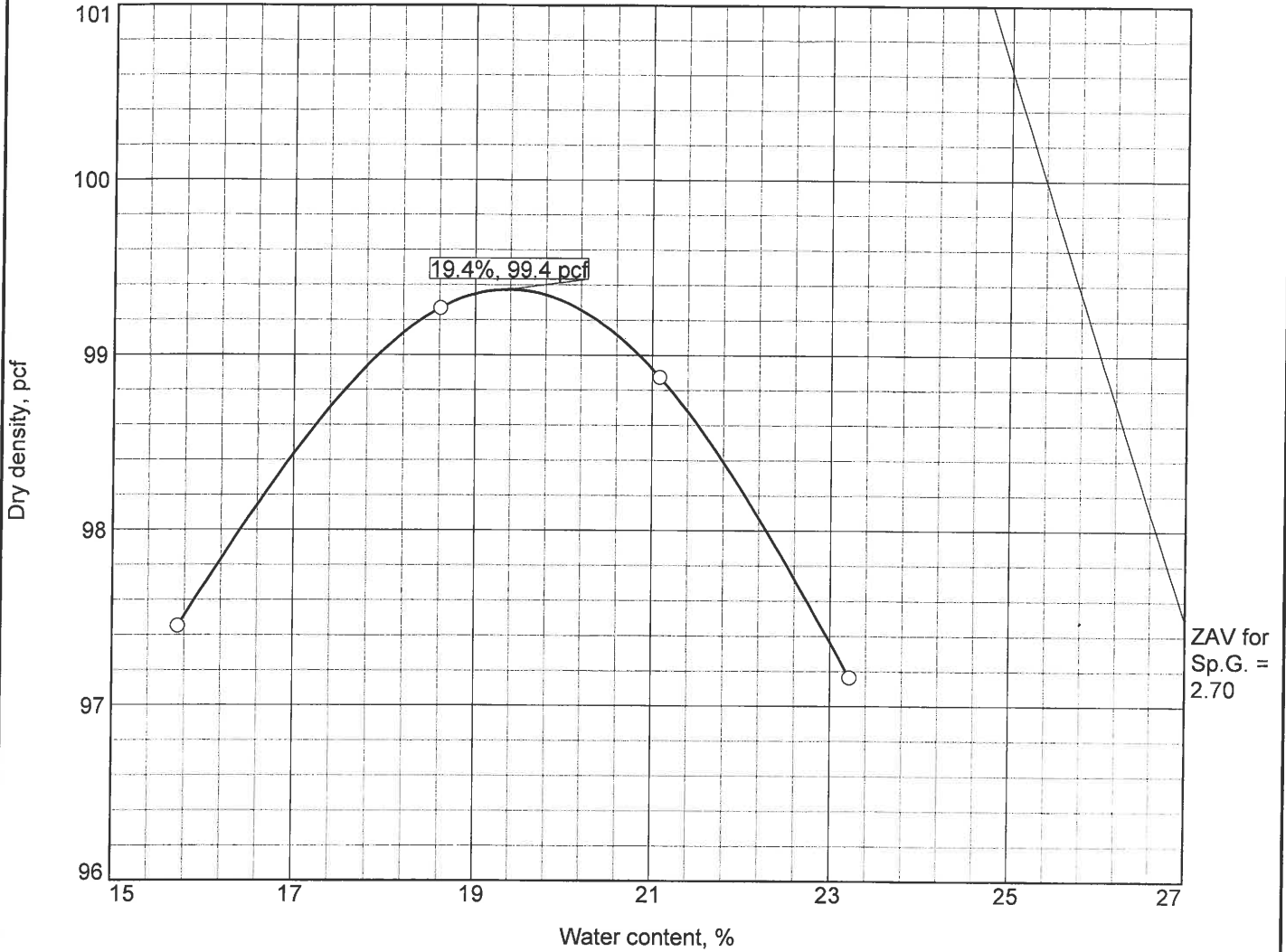
Source of Sample: Bulk Depth: 0-5'
Sample Number: 13-125

Date: 7/23/13

Terracon Consultants, Inc. Birmingham, Alabama	Client: Project: AGC Dam Site Project No: E1135088
Figure	

Tested By: LW

COMPACTION TEST REPORT



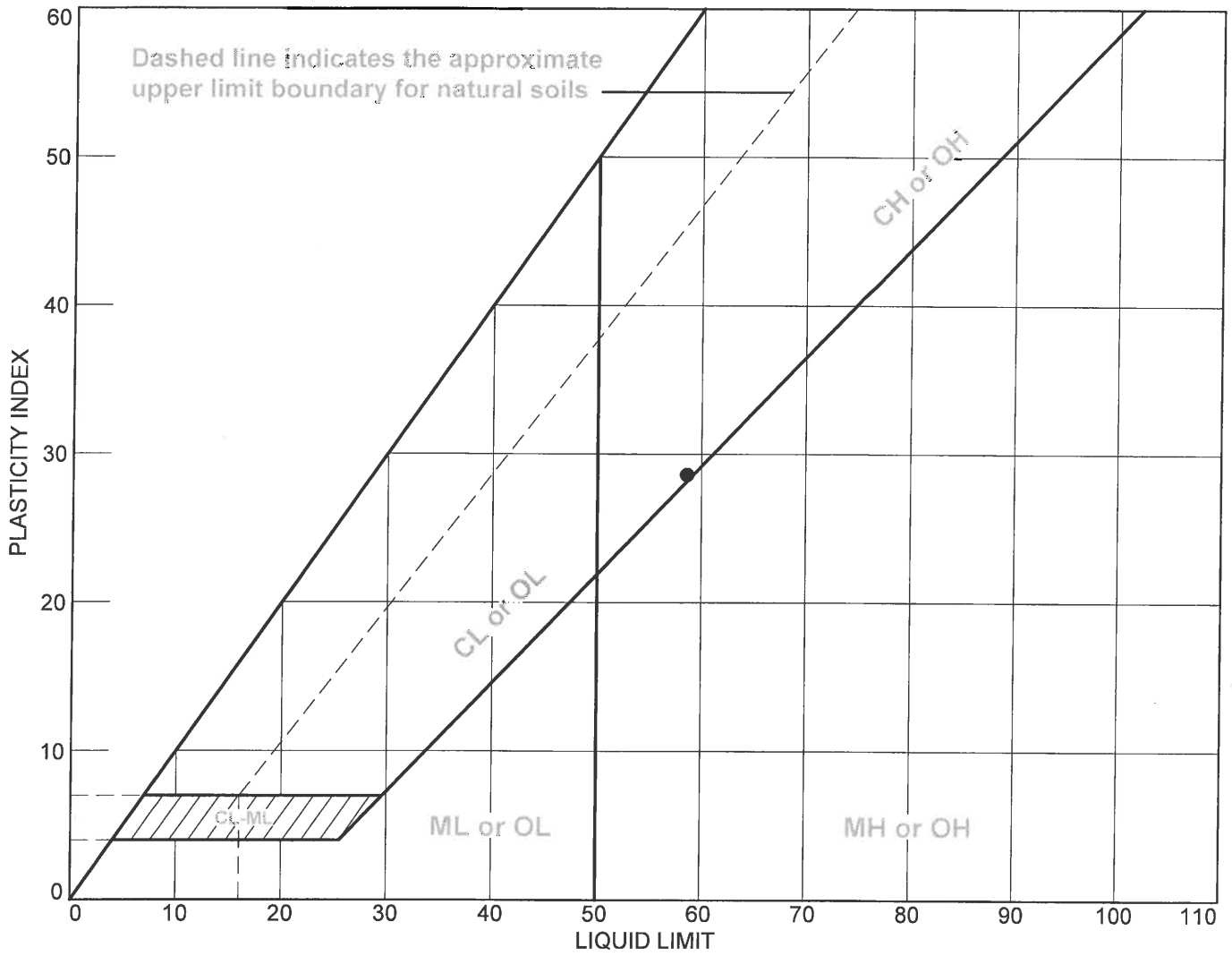
Test specification: ASTM D 698-07 Method B Standard

Elev/ Depth	Classification		Nat. Moist.	Sp.G.	LL	PI	% > 3/8 in.	% < No.200
	USCS	AASHTO						
5-10'	CH	A-7-5(30)		2.7	58.6	28.6	0.0	87.6

TEST RESULTS	MATERIAL DESCRIPTION
Maximum dry density = 99.4 pcf Optimum moisture = 19.4 %	Tan fat clay
Project No. E1135088 Client: Project: AGC Dam Site <div style="text-align: right;">Date: 7/23/13</div> ○ Source of Sample: Bulk Sample Number: 13-126 Terracon Consultants, Inc. Birmingham, Alabama	Remarks:
	Figure

Tested By: LW

LIQUID AND PLASTIC LIMITS TEST REPORT



SOIL DATA								
SYMBOL	SOURCE	SAMPLE NO.	DEPTH	NATURAL WATER CONTENT (%)	PLASTIC LIMIT (%)	LIQUID LIMIT (%)	PLASTICITY INDEX (%)	USCS
●	Bulk	13-126	5-10'		30.0	58.6	28.6	CH

Terracon Consultants, Inc.

Birmingham, Alabama

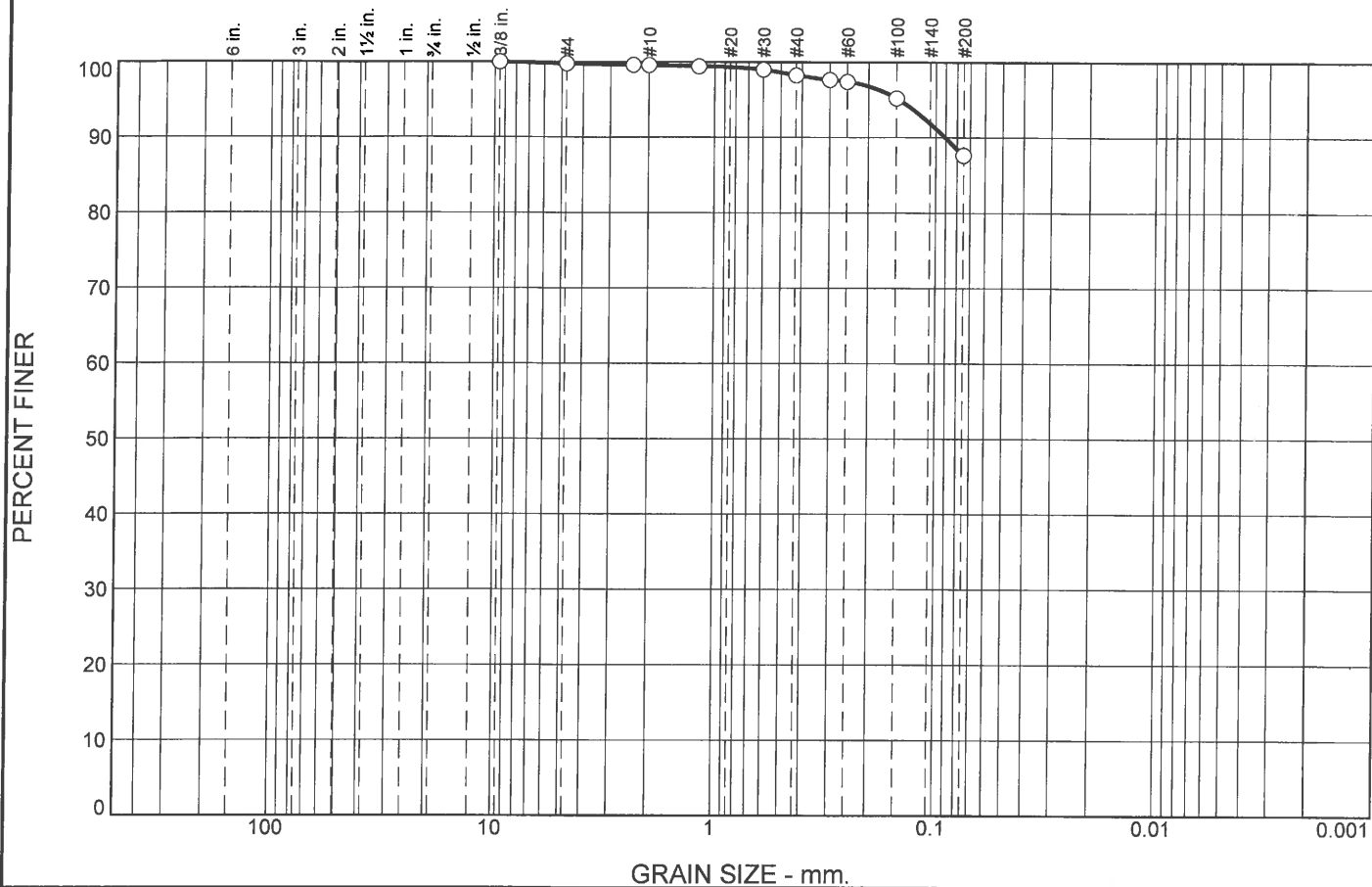
Client:
Project: AGC Dam Site

Project No.: E1135088

Figure

Tested By: LW

Particle Size Distribution Report



% +3"	% Gravel		% Sand			% Fines	
	Coarse	Fine	Coarse	Medium	Fine	Silt	Clay
0.0	0.0	0.2	0.2	1.3	10.7	87.6	

SIEVE SIZE	PERCENT FINER	SPEC.* PERCENT	PASS? (X=NO)
.375"	100.0		
#4	99.8		
#8	99.6		
#10	99.6		
#16	99.4		
#30	99.0		
#40	98.3		
#50	97.7		
#60	97.4		
#100	95.2		
#200	87.6		

Material Description

Tan fat clay

Atterberg Limits
 PL= 30.0 LL= 58.6 PI= 28.6

Coefficients
 D₉₀= 0.0906 D₈₅= D₆₀=
 D₅₀= D₃₀= D₁₅=
 D₁₀= C_u= C_c=

Classification
 USCS= CH AASHTO= A-7-5(30)

Remarks

* (no specification provided)

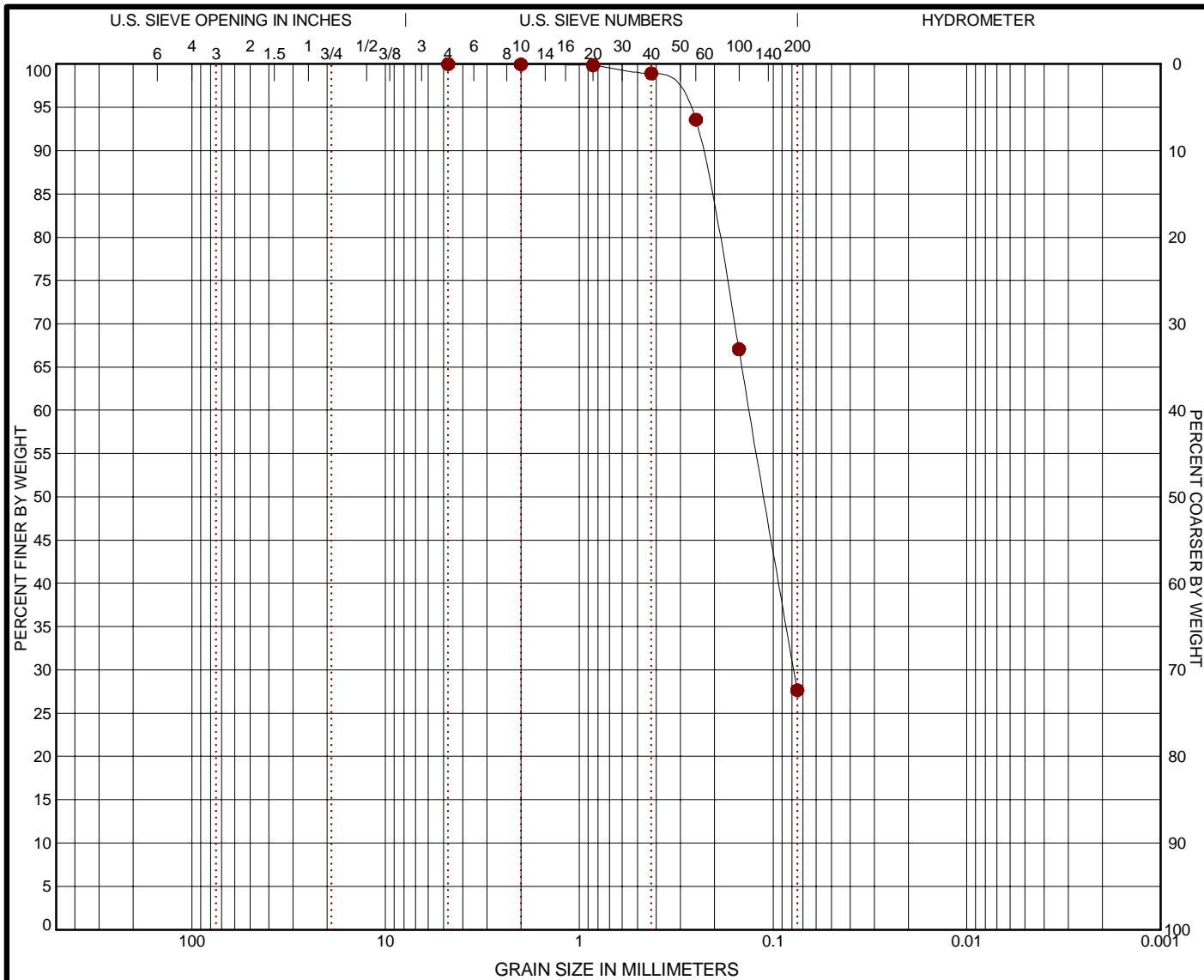
Source of Sample: Bulk Depth: 5-10'
 Sample Number: 13-126

Date:

Terracon Consultants, Inc. Birmingham, Alabama	Client: Project: AGC Dam Site Project No: E1135088
Figure	

GRAIN SIZE DISTRIBUTION

ASTM D422



COBBLES	GRAVEL		SAND			SILT OR CLAY
	coarse	fine	coarse	medium	fine	

BORING ID	DEPTH	% COBBLES	% GRAVEL	% SAND	% SILT	% FINES	% CLAY	USCS
B2	8 - 10	0.0	0.0	72.3		27.7		

GRAIN SIZE	
D ₆₀	0.132
D ₃₀	0.078
D ₁₀	
COEFFICIENTS	
C _c	
C _u	

SIEVE (size)	PERCENT FINER	
1 1/2"		
1"		
3/4"		
1/2"		
3/8"		
#4	100.0	
#10	99.96	
#20	99.87	
#40	98.92	
#60	93.58	
#100	67.06	
#200	27.66	

SOIL DESCRIPTION
 ● Brownish Gray Silty Sand with Clay

REMARKS
 ●

LABORATORY TESTS ARE NOT VALID IF SEPARATED FROM ORIGINAL REPORT. GRAIN SIZE: USCS 1 E1135088 AGC DAM SITE.GPJ TERRACON2012.GDT 8/21/13

PROJECT: AGC Dam Site

SITE: AGC Dam

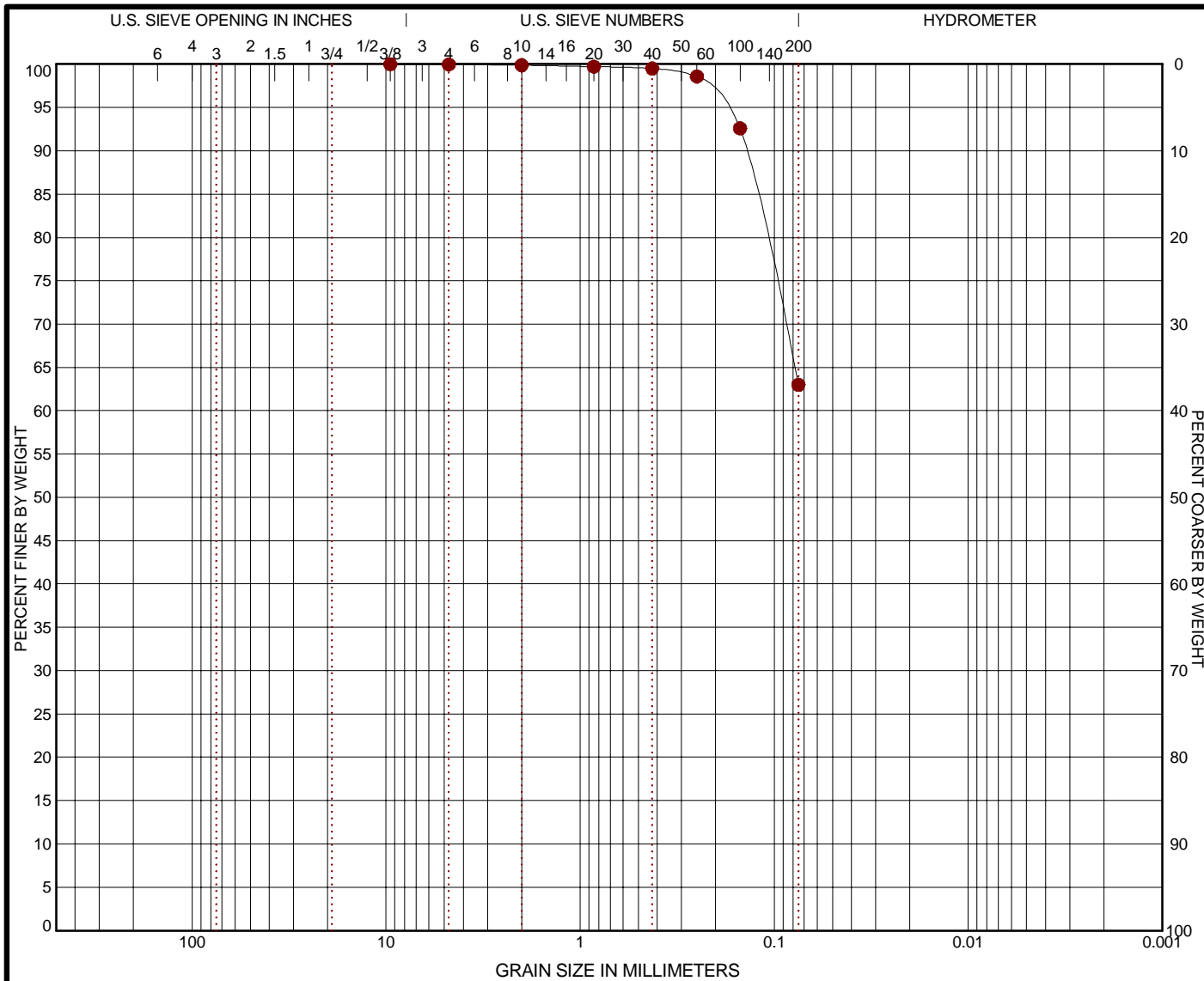


PROJECT NUMBER: E1135088

CLIENT:

GRAIN SIZE DISTRIBUTION

ASTM D422



COBBLES	GRAVEL		SAND			SILT OR CLAY
	coarse	fine	coarse	medium	fine	

BORING ID	DEPTH	% COBBLES	% GRAVEL	% SAND	% SILT	% FINES	% CLAY	USCS
B2	13 - 15	0.0	0.0	37.0		63.0		

GRAIN SIZE	
D ₆₀ D ₃₀ D ₁₀	●
COEFFICIENTS	
C _c C _u	●

SIEVE (size)	PERCENT FINER	
1 1/2"	●	
1"		
3/4"		
1/2"		
3/8"		100.0
#4		99.97
#10		99.89
#20		99.72
#40		99.51
#60		98.58
#100		92.6
#200		62.99

SOIL DESCRIPTION
● Greenish Gray Silty Sandy Clay

REMARKS
●

LABORATORY TESTS ARE NOT VALID IF SEPARATED FROM ORIGINAL REPORT. GRAIN SIZE: USCS 1 E1135088 AGC DAM SITE.GPJ TERRACON2012.GDT 8/21/13

PROJECT: AGC Dam Site

SITE: AGC Dam

Terracon

51 Lost Mound Drive, Suite 135
Chattanooga, Tennessee

PROJECT NUMBER: E1135088

CLIENT:



**HYDRAULIC CONDUCTIVITY DETERMINATION
FLEXIBLE WALL PERMEAMETER - CONSTANT VOLUME
(Mercury Permmeter Test)**

Project :	AGC Dam Site				
Date:	8/21/2013	Panel Number : P-1			
Project No. :	E1135088	Permmeter Data			
Boring No.:	B2	$a_p = 0.031416 \text{ cm}^2$	Set Mercury to Pipet Rp at beginning	Equilibrium	1.6 cm^3
Sample:		$a_a = 0.767120 \text{ cm}^2$		Pipet Rp	16.8 cm^3
Depth (ft):	8.0-10.0	$M_1 = 0.030180$	$C = 0.0017912$	Annulus Ra	1.0 cm^3
Other Location:	Tube	$M_2 = 1.040953$	$T = 0.0658646$		
Material Description :	Brownish Gray Silty Sand with Clay				

SAMPLE DATA

Wet Wt. sample + ring or tare :	124.70 g		
Tare or ring Wt. :	0.0 g	Before Test	After Test
Wet Wt. of Sample :	124.70 g	Tare No.:	348 Tare No.:
Diameter :	1.37 in	3.48 cm^2	Wet Wt.+tare: 127.67 Wet Wt.+tare: 132.69
Length :	2.80 in	7.11 cm	Dry Wt.+tare: 100.31 Dry Wt.+tare: 106.08
Area:	1.47 in^2	9.51 cm^2	Tare Wt: 21.00 Tare Wt: 31.26
Volume :	4.13 in^3	67.64 cm^3	Dry Wt.: 79.31 Dry Wt.: 74.82
Unit Wt.(wet):	115.04 pcf	1.84 g/cm^3	Water Wt.: 27.36 Water Wt.: 26.61
Unit Wt.(dry):	85.54 pcf	1.37 g/cm^3	% moist.: 34.5 % moist.: 35.6

Assumed Specific Gravity: **2.70** Max Dry Density(pcf) = _____ OMC = _____
 % of max = _____ +/- OMC = _____
 Calculated % saturation: **98.93** Void ratio (e) = **0.97** Porosity (n)= **0.49**

Test Pressures During Hydraulic Conductivity Test

Cell Pressure (psi) = 55.00 Back Pressure (psi) = 50.00 Confining Pressure = 5.00 psi

Note: The above value is Effective Confining Pressure

TEST READINGS

Z_1 (Mercury Height Difference @ t_1):	15.8 cm	Hydraulic Gradient =	28.00					
Date	elapsed t (seconds)	Z (pipet @ t)	ΔZ_p (cm)	temp (deg C)	α (temp corr)	k (cm/sec)	k (ft./day)	Reset = *
8/20/2013	300	16.4	0.382666	21	0.977	1.49E-07	4.22E-04	
8/20/2013	600	16	0.782666	21	0.977	1.54E-07	4.37E-04	
8/20/2013	900	15.6	1.182666	21	0.977	1.58E-07	4.47E-04	
8/20/2013	1200	15.2	1.582666	21	0.977	1.61E-07	4.55E-04	

SUMMARY

$k_a = 1.55E-07 \text{ cm/sec}$	Acceptance criteria =	50 %
k_i	V_m	
$k_1 = 1.49E-07 \text{ cm/sec}$	4.2 %	$V_m = \frac{ k_a - k_i }{k_a} \times 100$
$k_2 = 1.54E-07 \text{ cm/sec}$	0.6 %	
$k_3 = 1.58E-07 \text{ cm/sec}$	1.5 %	
$k_4 = 1.61E-07 \text{ cm/sec}$	3.3 %	

Hydraulic conductivity	$k = 1.55E-07 \text{ cm/sec}$	4.40E-04 ft/day
Void Ratio	$e = 0.97$	
Porosity	$n = 0.49$	
Bulk Density	$\gamma = 1.84 \text{ g/cm}^3$	115.0 pcf
Water Content	$W = 0.47 \text{ cm}^3/\text{cm}^3$	(at 20 deg C)
Intrinsic Permeability	$k_{int} = 1.59E-12 \text{ cm}^2$	(at 20 deg C)



**HYDRAULIC CONDUCTIVITY DETERMINATION
FLEXIBLE WALL PERMEAMETER - CONSTANT VOLUME
(Mercury Permometer Test)**

Project :	AGC Dam Site				
Date:	8/21/2013	Panel Number : P-1			
Project No. :	E1135088	Permometer Data			
Boring No.:	B2	$a_p = 0.031416 \text{ cm}^2$	Set Mercury to Pipet Rp at beginning	Equilibrium	1.6 cm^3
Sample:		$a_a = 0.767120 \text{ cm}^2$		Pipet Rp	13.7 cm^3
Depth (ft):	13.0-15.0	$M_1 = 0.030180$	$C = 0.0003415$	Annulus Ra	1.1 cm^3
Other Location:	Tube	$M_2 = 1.040953$	$T = 0.0826999$		
Material Description :	Greenish Gray Silty Sandy Clay				

SAMPLE DATA

Wet Wt. sample + ring or tare :	429.70 g				
Tare or ring Wt. :	0.0 g	Before Test			
Wet Wt. of Sample :	429.70 g	Tare No.:	207		
Diameter :	2.80 in	7.11 cm ²	Wet Wt.+tare:	89.45	
Length :	2.23 in	5.66 cm	Dry Wt.+tare:	72.77	
Area:	6.16 in ²	39.73 cm ²	Tare Wt.:	20.87	
Volume :	13.73 in ³	225.02 cm ³	Dry Wt.:	51.9	
Unit Wt.(wet):	119.16 pcf	1.91 g/cm ³	Water Wt.:	16.68	
Unit Wt.(dry):	90.18 pcf	1.45 g/cm ³	% moist.:	32.1	
Assumed Specific Gravity:	2.70	Max Dry Density(pcf) =	_____	OMC =	_____
Calculated % saturation:	97.02	% of max =	_____	+/- OMC =	_____
		Void ratio (e) =	0.87	Porosity (n)=	0.47

Test Pressures During Hydraulic Conductivity Test

Cell Pressure (psi) = 55.00 Back Pressure (psi) = 50.00 Confining Pressure = 5.00 psi

Note: The above value is Effective Confining Pressure

TEST READINGS

Z_1 (Mercury Height Difference @ t_1):	12.6 cm	Hydraulic Gradient =	28.00					
Date	elapsed t (seconds)	Z (pipet @ t)	ΔZ_p (cm)	temp (deg C)	α (temp corr)	k (cm/sec)	k (ft./day)	Reset = *
8/20/2013	60	9.8	3.891909	21	0.977	2.16E-06	6.12E-03	
8/20/2013	120	7.5	6.191909	21	0.977	1.99E-06	5.65E-03	
8/20/2013	180	5.8	7.891909	21	0.977	1.96E-06	5.56E-03	
8/20/2013	240	4.5	9.191909	21	0.977	1.98E-06	5.63E-03	

SUMMARY

$k_a = 2.02E-06 \text{ cm/sec}$	Acceptance criteria =	50 %
k_i	V_m	
$k_1 = 2.16E-06 \text{ cm/sec}$	6.7 %	$V_m = \frac{ k_a - k_i }{k_a} \times 100$
$k_2 = 1.99E-06 \text{ cm/sec}$	1.5 %	
$k_3 = 1.96E-06 \text{ cm/sec}$	3.2 %	
$k_4 = 1.98E-06 \text{ cm/sec}$	2.0 %	

Hydraulic conductivity	$k = 2.02E-06 \text{ cm/sec}$	$5.74E-03 \text{ ft/day}$
Void Ratio	$e = 0.87$	
Porosity	$n = 0.47$	
Bulk Density	$\gamma = 1.91 \text{ g/cm}^3$	119.2 pcf
Water Content	$W = 0.47 \text{ cm}^3/\text{cm}^3$	(at 20 deg C)
Intrinsic Permeability	$k_{int} = 2.07E-11 \text{ cm}^2$	(at 20 deg C)



**HYDRAULIC CONDUCTIVITY DETERMINATION
FLEXIBLE WALL PERMEAMETER - CONSTANT VOLUME
(Mercury Permometer Test)**

Project :	AGC Dam Site				
Date:	8/21/2013	Panel Number : P-1			
Project No. :	E1135088	Permometer Data			
Boring No.:	Bulk	$a_p = 0.031416 \text{ cm}^2$	Set Mercury to Pipet Rp at beginning	Equilibrium	1.6 cm^3
Sample:		$a_a = 0.767120 \text{ cm}^2$		Pipet Rp	16.8 cm^3
Depth (ft):	0.0-5.0	$M_1 = 0.030180$	$C = 0.0004288$	Annulus Ra	1.0 cm^3
Other Location:	Remolded	$M_2 = 1.040953$	$T = 0.0658646$		
Material Description :	Light Brown Sandy Lean Clay				

SAMPLE DATA

Wet Wt. sample + ring or tare :	543.40 g					
Tare or ring Wt. :	0.0 g					
Wet Wt. of Sample :	543.40 g					
Diameter :	2.80 in	7.11 cm^2	Before Test	After Test		
Length :	2.80 in	7.11 cm	Tare No.:	123	Tare No.:	318
Area:	6.16 in^2	39.73 cm^2	Wet Wt.+tare:	89.45	Wet Wt.+tare:	118.56
Volume :	17.24 in^3	282.53 cm^3	Dry Wt.+tare:	78.90	Dry Wt.+tare:	99.87
Unit Wt.(wet):	120.02 pcf	1.92 g/cm^3	Tare Wt.:	21.55	Tare Wt.:	21.26
Unit Wt.(dry):	101.37 pcf	1.62 g/cm^3	Dry Wt.:	57.35	Dry Wt.:	78.61
			Water Wt.:	10.55	Water Wt.:	18.69
			% moist.:	18.4	% moist.:	23.8
Assumed Specific Gravity:	2.70	Max Dry Density(pcf) =	106.7	OMC =	16.4	
		% of max =	95.0	+/- OMC =	2.00	
Calculated % saturation:	96.84	Void ratio (e) =	0.66	Porosity (n)=	0.40	

Test Pressures During Hydraulic Conductivity Test

Cell Pressure (psi) = 55.00 Back Pressure (psi) = 50.00 Confining Pressure = 5.00 psi

Note: The above value is Effective Confining Pressure

TEST READINGS

Z_1 (Mercury Height Difference @ t_1):	15.8 cm	Hydraulic Gradient =	28.00					
Date	elapsed t (seconds)	Z (pipet @ t)	ΔZ_p (cm)	temp (deg C)	α (temp corr)	k (cm/sec)	k (ft./day)	Reset = *
8/20/2013	600	16.2	0.582666	21	0.977	2.73E-08	7.74E-05	
8/20/2013	1200	15.6	1.182666	21	0.977	2.83E-08	8.02E-05	
8/20/2013	1800	15	1.782666	21	0.977	2.91E-08	8.24E-05	
8/20/2013	2400	14.5	2.282666	21	0.977	2.84E-08	8.06E-05	

SUMMARY

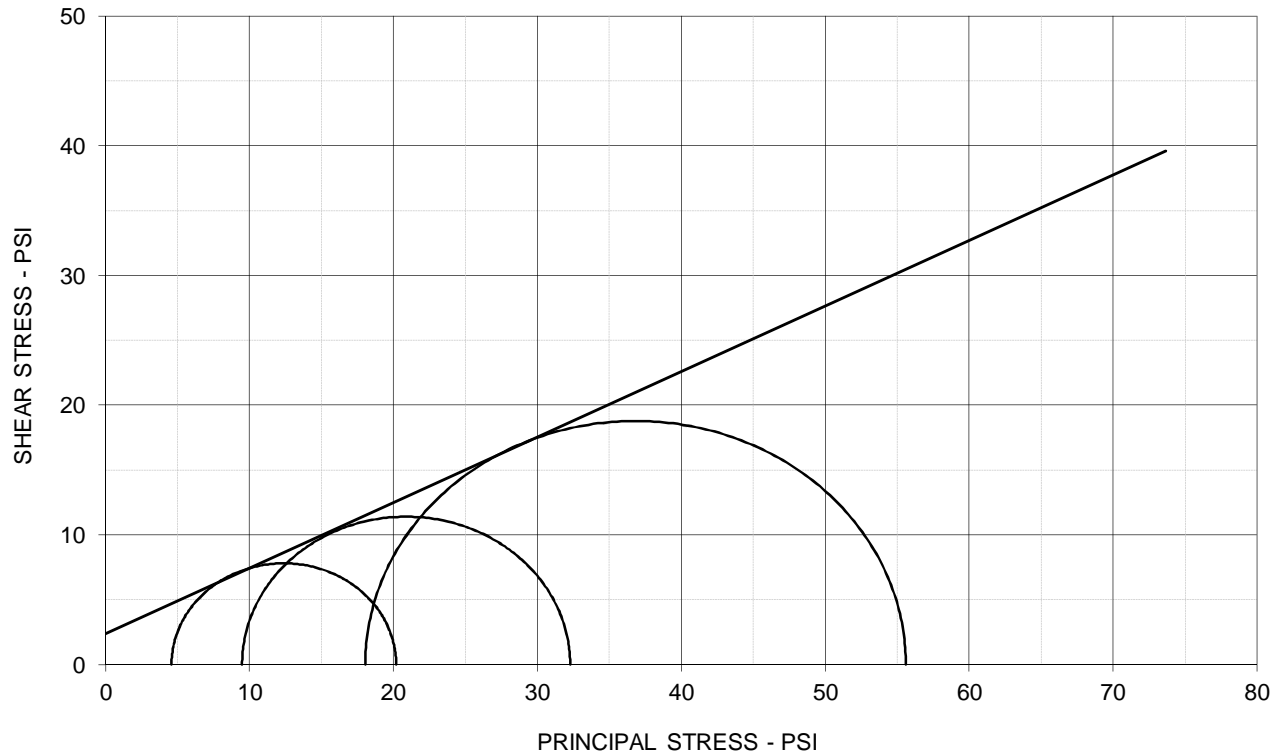
$k_a =$	2.83E-08 cm/sec	Acceptance criteria =	50 %
k_i		V_m	
$k_1 =$	2.73E-08 cm/sec	3.4 %	$V_m = \frac{ k_a - k_i }{k_a} \times 100$
$k_2 =$	2.83E-08 cm/sec	0.1 %	
$k_3 =$	2.91E-08 cm/sec	2.8 %	
$k_4 =$	2.84E-08 cm/sec	0.5 %	

Hydraulic conductivity	$k =$	2.83E-08 cm/sec	8.02E-05 ft/day
Void Ratio	$e =$	0.66	
Porosity	$n =$	0.40	
Bulk Density	$\gamma =$	1.92 g/cm^3	120.0 pcf
Water Content	$W =$	0.30 cm^3/cm^3	(at 20 deg C)
Intrinsic Permeability	$k_{int} =$	2.90E-13 cm^2	(at 20 deg C)

TRIAXIAL SHEAR TEST REPORT



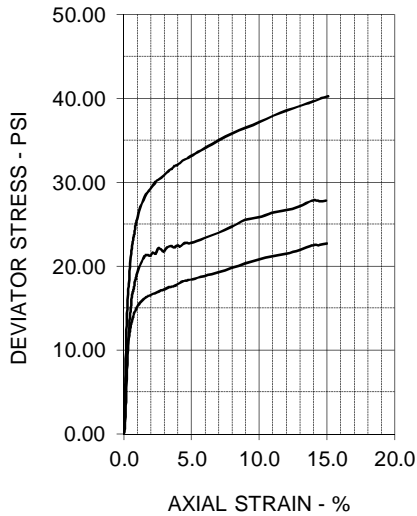
P.O. Box 5010, 51 Lost Mound Drive, Suite 135 Chattanooga, TN 37406



EFFECTIVE STRESS PARAMETERS

$\phi' = 26.8 \text{ deg}$

$c' = 2.4 \text{ psi}$



SPECIMEN NO.	1	2	3	4
INITIAL				
Moisture Content - %	18.4	18.4	18.4	
Dry Density - pcf	101.4	101.4	101.4	
Diameter - inches	2.80	2.80	2.80	
Height - inches	5.60	5.60	5.60	
AT TEST				
Final Moisture - %				
Dry Density - pcf	101.9	102.9	105.1	
Calculated Diameter (in.)	2.81	2.80	2.78	
Height - inches	5.62	5.59	5.54	
Effect. Cell Pressure - psi	10.0	20.0	40.0	
Failure Stress - psi	15.60	22.79	37.55	
Total Pore Pressure - psi	55.4	60.5	72.0	
Strain Rate - inches/min.	0.00060	0.00060	0.00060	
Failure Strain - %	1.2	4.6	10.5	
σ_1' Failure - psi	20.19	32.28	55.60	
σ_3' Failure - psi	4.59	9.49	18.05	

TEST DESCRIPTION

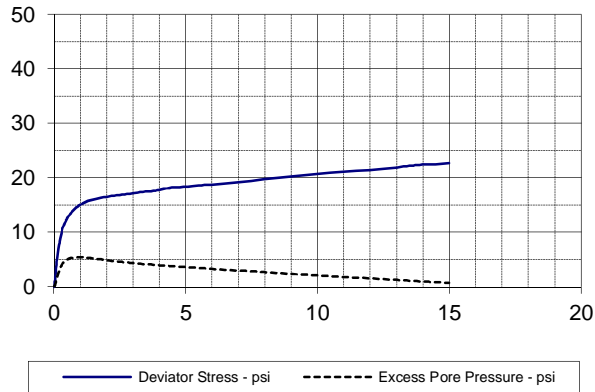
TYPE OF TEST & NO: CU with Pore Pressure
 SAMPLE TYPE: Remolded
 DESCRIPTION: Light Brown Sandy Lean Clay (CL)
 SAMPLE LOCATION: Bulk 0.0-5.0 ft
 ASSUMED SPECIFIC GRAVITY: 2.7
 LL: 45.4 PL: 25.3 PI: 20.1 Percent -200: 67
 REMARKS: Specimens remolded to 95% +2 opt.

PROJECT INFORMATION

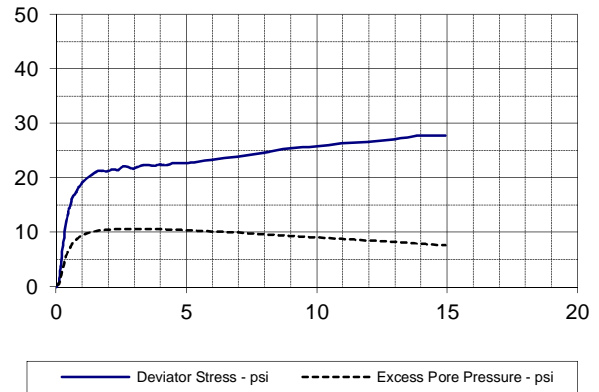
PROJECT: AGC Dam Site
 LOCATION: AGC Dam
 PROJECT NO: E1135088
 CLIENT:
 DATE: 8/21/13

TERRACON

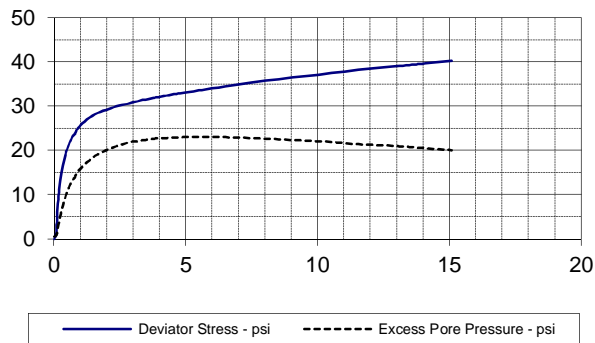
SPECIMEN NO. 1



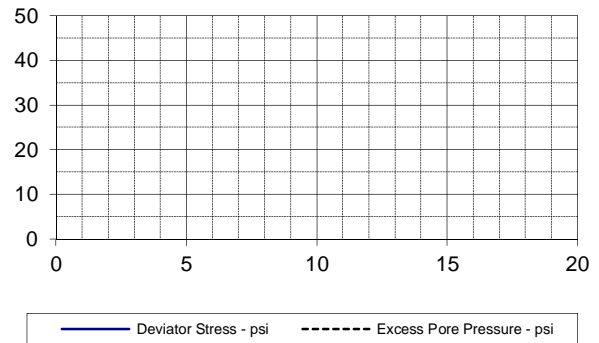
SPECIMEN NO. 2



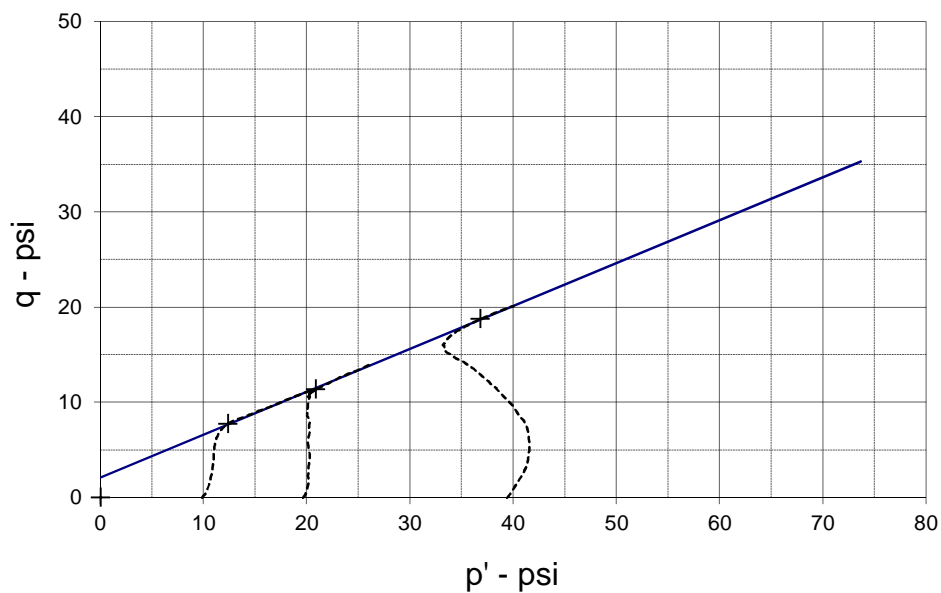
SPECIMEN NO. 3



SPECIMEN NO. 4



p - q DIAGRAM

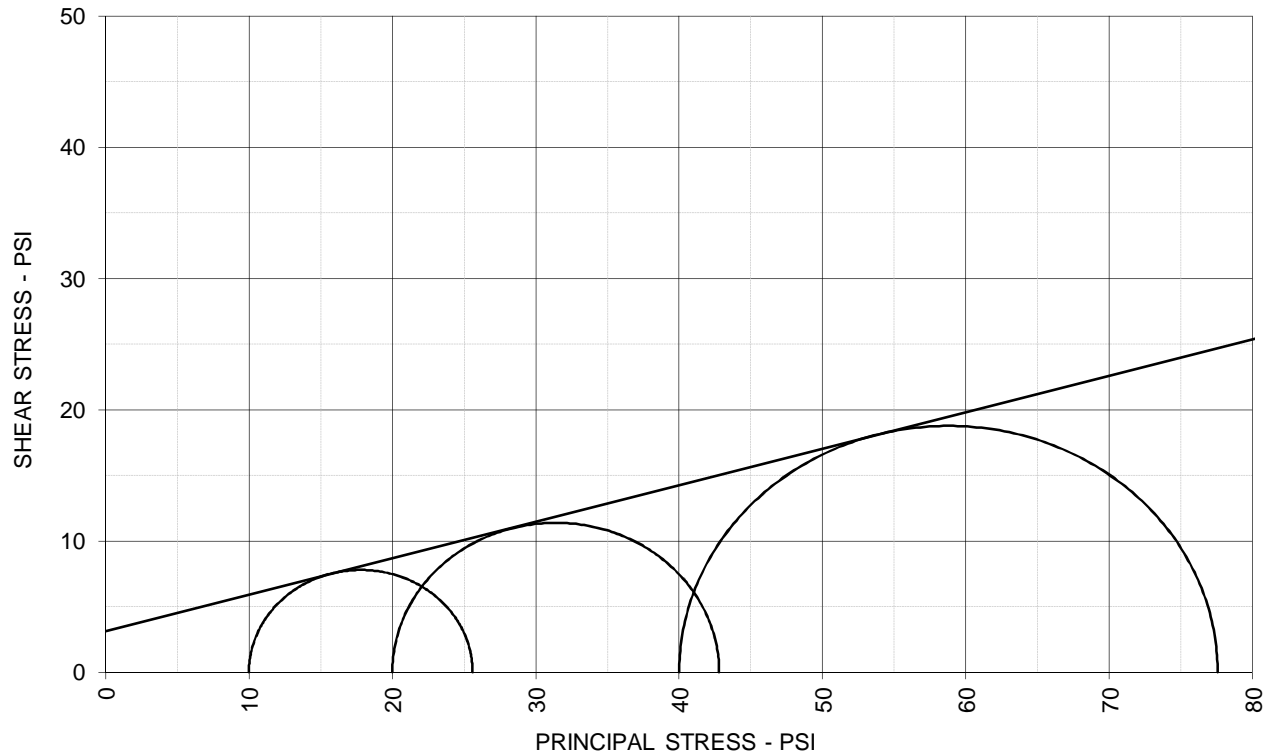


EFFECTIVE STRESS PARAMETERS	$R^2 = 1.00$	α (deg) = 24.3	a (psi) = 2.1
PROJECT: AGC Dam Site	TYPE OF TEST & NO: CU with Pore Pressure		
PROJECT NO: E1135088	TERRACON		
DESCRIPTION: Light Brown Sandy Lean Clay (CL)			

TRIAXIAL SHEAR TEST REPORT



P.O. Box 5010, 51 Lost Mound Drive, Suite 135 Chattanooga, TN 37406














TOTAL STRESS PARAMETERS		$\phi = 15.6 \text{ deg}$		$c = 3.1 \text{ psi}$		
	SPECIMEN NO.	1	2	3	4	
	INITIAL					
	Moisture Content - %	18.4	18.4	18.4		
	Dry Density - pcf	101.4	101.4	101.4		
	Diameter - inches	2.80	2.80	2.80		
	Height - inches	5.60	5.60	5.60		
	AT TEST					
	Final Moisture - %					
	Dry Density - pcf	101.9	102.9	105.1		
	Calculated Diameter (in.)	2.81	2.80	2.78		
Height - inches	5.62	5.59	5.54			
Effect. Cell Pressure - psi	10.0	20.0	40.0			
Failure Stress - psi	15.60	22.79	37.55			
Total Pore Pressure - psi	55.4	60.5	72.0			
Strain Rate - inches/min.	0.00060	0.00060	0.00060			
Failure Strain - %	1.2	4.6	10.5			
σ_1 Failure - psi	25.60	42.79	77.55			
σ_3 Failure - psi	10.00	20.00	40.00			
TEST DESCRIPTION			PROJECT INFORMATION			
TYPE OF TEST & NO: CU with Pore Pressure SAMPLE TYPE: Remolded DESCRIPTION: Light Brown Sandy Lean Clay (CL) SAMPLE LOCATION: Bulk 0.0-5.0 ft ASSUMED SPECIFIC GRAVITY: 2.7 LL: 45.4 PL: 25.3 PI: 20.1 Percent -200: 67 REMARKS: Specimens remolded to 95% +2 opt.			PROJECT: AGC Dam Site LOCATION: AGC Dam PROJECT NO: E1135088 CLIENT: DATE: 8/21/13			
			TERRACON			

APPENDIX C
SUPPORTING DOCUMENTS

GENERAL NOTES

DESCRIPTION OF SYMBOLS AND ABBREVIATIONS

SAMPLING			WATER LEVEL		Water Initially Encountered	FIELD TESTS	(HP) Hand Penetrometer	
	Auger	Split Spoon			Water Level After a Specified Period of Time		(T) Torvane	
					Water Level After a Specified Period of Time		(b/f) Standard Penetration Test (blows per foot)	
	Shelby Tube	Macro Core		Water levels indicated on the soil boring logs are the levels measured in the borehole at the times indicated. Groundwater level variations will occur over time. In low permeability soils, accurate determination of groundwater levels is not possible with short term water level observations.			(PID) Photo-Ionization Detector	
							(OVA) Organic Vapor Analyzer	
Ring Sampler	Rock Core							
								
Grab Sample	No Recovery							

DESCRIPTIVE SOIL CLASSIFICATION

Soil classification is based on the Unified Soil Classification System. Coarse Grained Soils have more than 50% of their dry weight retained on a #200 sieve; their principal descriptors are: boulders, cobbles, gravel or sand. Fine Grained Soils have less than 50% of their dry weight retained on a #200 sieve; they are principally described as clays if they are plastic, and silts if they are slightly plastic or non-plastic. Major constituents may be added as modifiers and minor constituents may be added according to the relative proportions based on grain size. In addition to gradation, coarse-grained soils are defined on the basis of their in-place relative density and fine-grained soils on the basis of their consistency.

LOCATION AND ELEVATION NOTES

Unless otherwise noted, Latitude and Longitude are approximately determined using a hand-held GPS device. The accuracy of such devices is variable. Surface elevation data annotated with +/- indicates that no actual topographical survey was conducted to confirm the surface elevation. Instead, the surface elevation was approximately determined from topographic maps of the area.

STRENGTH TERMS	RELATIVE DENSITY OF COARSE-GRAINED SOILS (More than 50% retained on No. 200 sieve.) Density determined by Standard Penetration Resistance Includes gravels, sands and silts.			CONSISTENCY OF FINE-GRAINED SOILS (50% or more passing the No. 200 sieve.) Consistency determined by laboratory shear strength testing, field visual-manual procedures or standard penetration resistance		
	Descriptive Term (Density)	Standard Penetration or N-Value Blows/Ft.	Ring Sampler Blows/Ft.	Descriptive Term (Consistency)	Unconfined Compressive Strength, Qu, psf	Standard Penetration or N-Value Blows/Ft.
Very Loose	0 - 3	0 - 6	Very Soft	less than 500	0 - 1	< 3
Loose	4 - 9	7 - 18	Soft	500 to 1,000	2 - 4	3 - 4
Medium Dense	10 - 29	19 - 58	Medium-Stiff	1,000 to 2,000	4 - 8	5 - 9
Dense	30 - 50	59 - 98	Stiff	2,000 to 4,000	8 - 15	10 - 18
Very Dense	> 50	≥ 99	Very Stiff	4,000 to 8,000	15 - 30	19 - 42
			Hard	> 8,000	> 30	> 42

RELATIVE PROPORTIONS OF SAND AND GRAVEL

<u>Descriptive Term(s) of other constituents</u>	<u>Percent of Dry Weight</u>
Trace	< 15
With	15 - 29
Modifier	> 30

GRAIN SIZE TERMINOLOGY

<u>Major Component of Sample</u>	<u>Particle Size</u>
Boulders	Over 12 in. (300 mm)
Cobbles	12 in. to 3 in. (300mm to 75mm)
Gravel	3 in. to #4 sieve (75mm to 4.75 mm)
Sand	#4 to #200 sieve (4.75mm to 0.075mm)
Silt or Clay	Passing #200 sieve (0.075mm)

RELATIVE PROPORTIONS OF FINES

<u>Descriptive Term(s) of other constituents</u>	<u>Percent of Dry Weight</u>
Trace	< 5
With	5 - 12
Modifier	> 12

PLASTICITY DESCRIPTION

<u>Term</u>	<u>Plasticity Index</u>
Non-plastic	0
Low	1 - 10
Medium	11 - 30
High	> 30

UNIFIED SOIL CLASSIFICATION SYSTEM

Criteria for Assigning Group Symbols and Group Names Using Laboratory Tests ^A				Soil Classification			
				Group Symbol	Group Name ^B		
Coarse Grained Soils: More than 50% retained on No. 200 sieve	Gravels: More than 50% of coarse fraction retained on No. 4 sieve	Clean Gravels: Less than 5% fines ^C	$Cu \geq 4$ and $1 \leq Cc \leq 3$ ^E	GW	Well-graded gravel ^F		
			$Cu < 4$ and/or $1 > Cc > 3$ ^E	GP	Poorly graded gravel ^F		
		Gravels with Fines: More than 12% fines ^C	Fines classify as ML or MH	GM	Silty gravel ^{F,G,H}		
			Fines classify as CL or CH	GC	Clayey gravel ^{F,G,H}		
	Sands: 50% or more of coarse fraction passes No. 4 sieve	Clean Sands: Less than 5% fines ^D	$Cu \geq 6$ and $1 \leq Cc \leq 3$ ^E	SW	Well-graded sand ^I		
			$Cu < 6$ and/or $1 > Cc > 3$ ^E	SP	Poorly graded sand ^I		
		Sands with Fines: More than 12% fines ^D	Fines classify as ML or MH	SM	Silty sand ^{G,H,I}		
			Fines classify as CL or CH	SC	Clayey sand ^{G,H,I}		
		Fine-Grained Soils: 50% or more passes the No. 200 sieve	Silts and Clays: Liquid limit less than 50	Inorganic:	$PI > 7$ and plots on or above "A" line ^J	CL	Lean clay ^{K,L,M}
					$PI < 4$ or plots below "A" line ^J	ML	Silt ^{K,L,M}
Organic:	Liquid limit - oven dried			< 0.75	OL	Organic clay ^{K,L,M,N}	
	Liquid limit - not dried				OH	Organic silt ^{K,L,M,O}	
Silts and Clays: Liquid limit 50 or more	Inorganic:		PI plots on or above "A" line	CH	Fat clay ^{K,L,M}		
			PI plots below "A" line	MH	Elastic Silt ^{K,L,M}		
Organic:	Liquid limit - oven dried	< 0.75	OH	Organic clay ^{K,L,M,P}			
	Liquid limit - not dried		OH	Organic silt ^{K,L,M,Q}			
Highly organic soils:	Primarily organic matter, dark in color, and organic odor			PT	Peat		

^A Based on the material passing the 3-inch (75-mm) sieve

^B If field sample contained cobbles or boulders, or both, add "with cobbles or boulders, or both" to group name.

^C Gravels with 5 to 12% fines require dual symbols: GW-GM well-graded gravel with silt, GW-GC well-graded gravel with clay, GP-GM poorly graded gravel with silt, GP-GC poorly graded gravel with clay.

^D Sands with 5 to 12% fines require dual symbols: SW-SM well-graded sand with silt, SW-SC well-graded sand with clay, SP-SM poorly graded sand with silt, SP-SC poorly graded sand with clay

$$E \quad Cu = D_{60}/D_{10} \quad Cc = \frac{(D_{30})^2}{D_{10} \times D_{60}}$$

^F If soil contains $\geq 15\%$ sand, add "with sand" to group name.

^G If fines classify as CL-ML, use dual symbol GC-GM, or SC-SM.

^H If fines are organic, add "with organic fines" to group name.

^I If soil contains $\geq 15\%$ gravel, add "with gravel" to group name.

^J If Atterberg limits plot in shaded area, soil is a CL-ML, silty clay.

^K If soil contains 15 to 29% plus No. 200, add "with sand" or "with gravel," whichever is predominant.

^L If soil contains $\geq 30\%$ plus No. 200 predominantly sand, add "sandy" to group name.

^M If soil contains $\geq 30\%$ plus No. 200, predominantly gravel, add "gravelly" to group name.

^N $PI \geq 4$ and plots on or above "A" line.

^O $PI < 4$ or plots below "A" line.

^P PI plots on or above "A" line.

^Q PI plots below "A" line.

